Aus der Klinik für Zahnerhaltung, Parodontologie und Präventive Zahnheilkunde,

Universitätsklinikum des Saarlandes, Homburg/Saar

Direktor: Prof. Dr. M. Hannig

Hydroxyapatite based mouthrinses against oral biofilm formation in situ

Dissertation zur Erlangung des Grades eines Doktors der Medizin und der Naturwissenschaften (MD-PhD)

der UNIVERSITÄT DES SAARLANDES

2021

vorgelegt von:

Cíntia Mirela Guimarães Nobre

geb. am: 17.10.1988 in Mossoró/Brasilien

Tag der Promotion: 09.06.2021

Dekan: Prof. Dr. M.D. Menger

Berichterstatter:

Prof. Dr. M. Hoth

Prof. Dr. M. Hannig

Prof. Dr. M. Madry

To my husband and family who strongly supported me.

Abbreviations

AAID	American Academy of Implant Dentistry
c.	*circa*
°C	Celsius scale
CHX	Chlorhexidine
DGI	German Society for Implant Dentistry
EDX	Energy-dispersive X-ray spectroscopy
HAP	Hydroxyapatite
FM	Fluorescence microscope
h	Hour
Kv	Kilovolts
M	Molar
min	Minutes
ml	Milliliter
mm	Millimeter
n°	Number
NP	Non-polished
P	Polished
p	p-value/probability value
PI	Peri-implantitis
PM	Peri-implant mucositis
PMMA	Poly(methyl methacrylate)
Ra	Arithmetic mean roughness
s	Seconds
SLA	Sandblasted and acid-etched

SRP	Scaling and root planing
SEM	Scanning electron microscope
TEM	Transmission electron microscope
Ti	Titanium
µm	Micrometer
µl	Microliter
v/v	Volume concentration / percentage volume per volume
w/v	Percent weight per volume

Content

1 Abstract

1.1 English

Introduction: Nowadays, various artificial dental materials are applied for oral rehabilitation with high rates of success. However, there is still the risk of bacterial colonization, which can affect their clinical performance and lead to failures. Recent reports have shown that hydroxyapatite particles (HAP) may have preventive properties against bacterial adhesion.

Objectives: This *in situ* study aims to investigate the effect of different sizes and shapes of HAP on the acquired pellicle and on the biofilm formed on enamel, titanium (Ti), ceramic, and polymethyl methacrylate (PMMA).

Material and Methods: This study was performed according to three different protocols. In all of them, the volunteers carried an upper jaw splint with attached samples. Three minutes after the splint placement, the volunteers rinsed with 10 ml of the selected solution for 30 seconds. The tested solutions included three 5% HAP watery solutions, as well as chlorhexidine (CHX) and water, as controls. The HAP solutions were prepared from three powders containing nanoparticles with different shapes and medium sizes: HAP I (needle, 40 nm), HAP II (needle, 100 nm), HAP III (spherical, 200 nm).

In Protocol 1, two volunteers used the selected rinsing solution after 3 min of pellicle formation. Scanning Electron Microscopy (SEM) was used to evaluate the samples immediately after rinsing, 30 min and 2 h after rinsing to assess the capacity of HAP particles to adhere to the pellicle formed on enamel, Ti, ceramic, and PMMA. Protocol 1 also evaluated the influence of the size and shape of the different HAP particles on their adhesion to the pellicle' surface.

In Protocol 2, the splints remained in the oral cavity for 24 h after pellicle formation and the five volunteers made the rinsing at two different time points. The first rinsing was performed after 3 min of pellicle formation and a second rinsing after a 12 h interval. Protocol 2 evaluated the effects of three different HAP solutions on the biofilm formed on the applied materials.

Protocol 3 evaluated the effects of HAP II on the biofilm adhesion on polished and non-polished titanium discs. The objective was to access the influence of Ti surface topography. The five volunteers rinsed at 4-time points on a 48-h interval. The first rinsing was performed after 3 min of pellicle formation, and three followings rinsing were made each 12 h.

The biofilm coverage and viability in protocols 2 and 3 were assessed by SEM, Fluorescence Microscope (FM) and Transmission Electron Microscope (TEM).

Results: In Protocol 1, descriptive results showed that HAP might interact with the salivary proteins from acquired pellicle despite the particles' size or shape or the material applied. Protocols 2 and 3 presented similar results: the three HAP solutions did not alter the bacterial viability, but successfully reduced the biofilm adhered to all surfaces tested on protocol 2 and on polished titanium surfaces from protocol 3. The HAP size and shape had no significant

influence on its anti-adhesive effects on enamel, titanium, ceramics, or PMMA. Additionally, protocol 3 indicated that the Ti surface topography influences biofilm adhesion and accumulation. SEM figures also suggest that HAP may interact with the oral bacteria from the biofilm.

Conclusions: The anti-adhesive effect of the bioinspired HAP solutions yielded a significant impact on the *in situ* oral biofilm formation on polished enamel, titanium, ceramics, and PMMA surfaces, representing a promising adjunct solution for biofilm management.

1.2   Deutsche Zusammenfassung

Effect von Hydroxylapatit basierten Mundspülungen auf die orale Biofilmbildung in situ

Einleitung: Heutzutage werden verschiedene künstliche Zahnmaterialien mit hohen Erfolgsraten für orale Rehabilitationsbehandlungen eingesetzt. Es besteht jedoch weiterhin das Risiko einer Besiedlung mit Bakterien, die deren klinische Erfolg beeinträchtigen und zum Versagen führen können. Jüngste Berichte haben gezeigt, dass Hydroxylapatit-Partikel (HAP) präventive Eigenschaften gegen die Anhaftung von Bakterien haben können.

Zielsetzung: Ziel dieser in situ-Studie ist es, die Auswirkung unterschiedlicher Größen und Formen von HAP auf die erworbene Pellikel und den auf Zahnschmelz, Titan (Ti), Keramik und Polymethylmethacrylat (PMMA) gebildeten Biofilm zu untersuchen.

Material und Methoden: In dieser Studie wurden drei verschiedene Protokolle durchgeführt. Bei allen versuchen trugen die Probanden eine mit Proben bestückte Oberkieferschiene. Drei Minuten nach der Platzierung der Schiene spülten die Probanden 30 Sekunden lang mit 10 ml der ausgewählten Lösung. Die getesteten Lösungen waren drei wässrige, 5%ige HAP-Lösungen sowie Chlorhexidin (CHX) und Wasser als Kontrollen. Die drei HAP-Lösungen wurden aus unterschiedlichen Pulvern hergestellt, welche Nanopartikel mit unterschiedlichen Formen und mittleren Größen enthielten: HAP I (nadelförmig, 40 nm), HAP II (nadelförmig, 100 nm), HAP III (sphärisch, 200 nm).

Gemäß Protokoll 1 verwendeten zwei Probanden die ausgewählte Spüllösung nach 3 Minuten Pellikelbildung. Die Analyse der Proben erfolgte mittels Rasterelektronenmikroskopie (REM) unmittelbar nach dem Spülen sowie 30 Minuten und 2 Stunden nach dem Spülen, um die Fähigkeit von HAP-Partikeln an die auf Zahnschmelz, Ti, Keramik und PMMA gebildete Pellikel anzuhaften. Protokoll 1 bewertete auch den Einfluss der Größe und Form der HAP-partikel auf das Adhärenzverhalten au des Pellikeloberfläche.

Gemäß Protokoll 2 blieben die Oberkieferschienen nach der Pellikelbildung für 24 Stunden in der Mundhöhle, und die 5 Probanden führten die Spülungen zu zwei verschiedenen Zeitpunkten durch. Die erste Spülung erfolgte nach 3 Minuten Pellikelbildung und eine zweite Spülung nach 12 Stunden. Protokoll 2 bewertete die Auswirkungen dreier verschiedener HAP-Lösungen auf dem Biofilm, der auf den untersuchten Materialien innerhalb von 24 h gebildet wurde.

Protokoll 3 bewertete die Auswirkungen von HAP II auf die Biofilmhaftung an polierten und nicht polierten Titanscheiben. Ziel war es, den Einfluss der Ti-Oberflächentopographie zu erfassen. Die 5 Probanden spülten zu vier Zeitpunkten im Zeitraum von 48 Stunden. Die erste Spülung wurde erfolgter 3 Minuten nach der Pellikelbildung durchgeführt und die drei nachfolgenden Spülungen wurden alle 12 Stunden.

In den Protokollen 2 und 3 wurde die Biofilmbedeckung und Vitalität mittels REM, Fluoreszenzmikroskopie (FM) und Transmissionselektronenmikroskopie (TEM) analysiert.

Ergebnisse: Die Ergebnisse aus Protokoll 1 zeigen, dass HAP unabhängig von der Größe oder Form der Partikel mit den Speichelproteinen der Pellikel interagieren kann. Protokoll 2 und 3 zeigen ähnliche Ergebnisse: Die drei HAP-Lösungen änderten die Vitalität der Bakterien nicht,

3

reduzierten jedoch erfolgreich den Biofilm, der auf allen nach Protokoll 2 getesteten Oberflächen und auch auf den polierten Titanoberflächen nach Protokoll 3 haftete. Die Größe und Form des HAP Partikel hatte keinen signifikanten Einfluss auf die Antihaftwirkung auf Zahnschmelz, Titan, Keramik oder PMMA. Zusätzlich zeigt Protokoll 3, dass die Ti-Oberflächentopographie die Biofilmadhäsion und -akkumulation beeinflusst. Die REM-Analysen zeigen außerdem, dass HAP mit den Bakterien des Biofilms interagieren kann.

Schlussfolgerungen: Die antiadhäsive Wirkung der bioinspirierten HAP-Lösungen hat einen signifikanten Einfluss auf die in situ Biofilmbildung auf polierten Zahnschmelz-, Titan-, Keramik- und PMMA- Oberflächen. Dies stellt einen vielversprechenden neuen Ausatz für das bioinspirierte Biofilm-Management.

2 Introduction

The smile plays an essential role in interpersonal relationships. Currently, more and more patients demand an aesthetic and healthy smile. Tooth loss causes significant functional and emotional negative effects, reducing the quality of life. Reasons are the consequent reduced masticatory efficiency, disability, changes in nutritional habits, pain, trouble speaking, and the aesthetic discontent (ALLEN et al., 2001; LOCKER et al., 2002; OH et al., 2016; RICHMOND et al., 2007; SARGOZAIE et al., 2017).

Nowadays, there are different options for oral rehabilitation based on the patient condition, such as single and partial prostheses, complete dentures, fixed bridges, fixed and removable implant-supported prostheses. A recent systematic review and meta-analysis showed that patient's satisfaction was higher for implant-supported prostheses (WITTNEBEN et al., 2018). In the past few years, implantology has presented as highly predictable with high rates of success for oral rehabilitation (BUSENLECHNER et al., 2014). Different materials are used to produce each part of the prostheses. For example, acrylic resin is usually used to build the device framework. Feldspathic ceramics are well known as a pioneer material for tooth replacement. Due to its biocompatibility and mechanical properties, titanium (Ti) is the main material for dental implants (GONÇALVES, BRESCIANI, 2017; MUDDUGANGADHAR et al., 2015; VALLITTU, SHINYA, 2017).

However, there are still multiple factors that can affect the clinical success of implant-supported prostheses, including the risk of bacterial colonization around the devices (VEERACHAMY et al., 2014). Biofilm is a microbial community with various bacterial species adhering to each other and usually also to a surface. Biofilms are ubiquitous and can develop on various surfaces, such as on enamel, dental implants and dental prostheses. (COSTERTON et al., 2005; HAO et al., 2018). The bacteria from the biofilm are embedded within a self-produced matrix, allowing further adhesion and proliferation of microorganisms (BLANC et al., 2014; FILOCHE et al., 2010; KOLENBRANDER et al., 2006). Biofilms are usually benign, but a dysbiosis within the biofilm can lead to common oral diseases such as caries, dental plaque-induced gingivitis, periodontitis and peri-implantitis (ARWEILER, NETUSCHIL, 2016; BELIBASAKIS et al., 2015; CHAPPLE et al., 2018; HANNIG, HANNIG, 2009).

Periimplantitis is an inflammatory disease that affects the soft and hard tissue around an implant. It starts with bacteria adhesion to the titanium surface, leading to biofilm formation

and accumulation. Once a mature multi-layered biofilm is formed, it is extremely resistant to conventional antimicrobial therapies and immune system lines of defence and may lead to an inflammatory response (SCHWARZ et al., 2018; SMEETS et al., 2014).

Until the present date, chlorhexidine 0.2% (CHX) is still the first-choice adjunct solution for prevention of dental biofilm accumulation. It is widely used as a broad-spectrum antiseptic, being the gold standard in dentistry (JAMES et al., 2017). However, despite its antimicrobial effect, CHX is not recommended for long-term use, due to various adverse effects such as teeth staining, oral mucosal erosion, and transient taste disturbance (JAMES et al., 2017). Therefore, to achieve reasonable biofilm control and less adverse effects as possible, the search for new biomimetic materials is of utmost importance.

Synthetic hydroxyapatite is a calcium phosphate ceramic that has structural and functional similarities to the main mineral component in teeth. It can mimic the natural enamel crystallites, which are the smallest structure of dental enamel (KENSCHE et al., 2017; SAKAE et al., 2011). As a bioinspired material, hydroxyapatite (HAP) particles are non-toxic and non-immunogenic (EPPLE, 2018). According to the literature, the size and shape of the particles and aggregates affect the HAP properties and, consequently, its applications, playing an important role in HAP effects. Recent publications indicate that smaller particles are related to better remineralizing effects (ELIAZ, METOKI, 2017; HU et al., 2007; HUANG et al., 2011; JIN et al., 2013). Kensche et al. observed that a pure hydroxyapatite containing mouthwash could reduce the number of bacteria adhered to the enamel surface exposed to the intraoral environment, having comparable effects to chlorhexidine (KENSCHE et al., 2017). Thus, HAP may have preventive properties against bacterial adhesion.

Additionally, many studies use *in vitro* models to mimic the biofilm formation, however, it is well known that the biofilm formation is a dynamic and a multifactorial process (DUCKWORTH, 2006; HANNIG, HANNIG, 2009). For that reason, *in vitro* studies are not reliable, because they do not mirror the real intraoral condition. Thus, an *in situ* experimental model will be applied in this study due to its better capacity to reproduce the intraoral conditions and to better understand the oral bioadhesion process (HANNIG, HANNIG, 2009; HANNIG et al., 2007; VAN DER MEI et al., 2008; YAO et al., 2001).

Hence, the objective of the present *in situ* study is to investigate the properties and effects of various sizes and shapes of three different hydroxyapatite powders as a mouthwash. Their effects will be tested on enamel and on the following dental materials commonly used for oral rehabilitation: titanium, ceramics and polymethyl methacrylate resin (Figure 1). The

hypothesis is that this bioinspired HAP solution would reduce biofilm formation, and the size of the particles does matter.
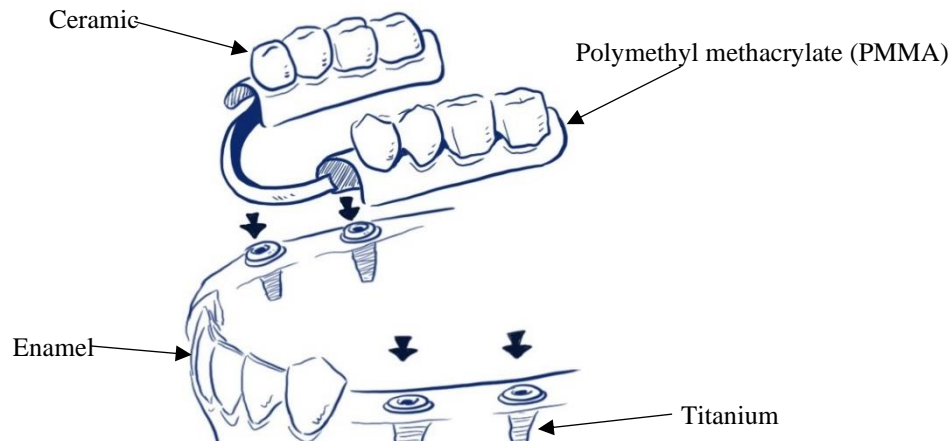

Figure 1 Illustration of implant-supported prostheses' materials

2.1 Enamel, dental materials and biofilm

2.1.1 Enamel

The human tooth structure comprehends four major tissues: enamel, dentin, and cementum as hard tissues, and dental pulp as soft tissue (Figure 2). Dental enamel is an avascular, acellular, and translucid hard tissue present on the outer layer of the tooth. The enamel is in contact with the oral cavity and is responsible for protecting the crown (SAKAGUCHI, POWERS, 2012; STAINES et al., 1981).
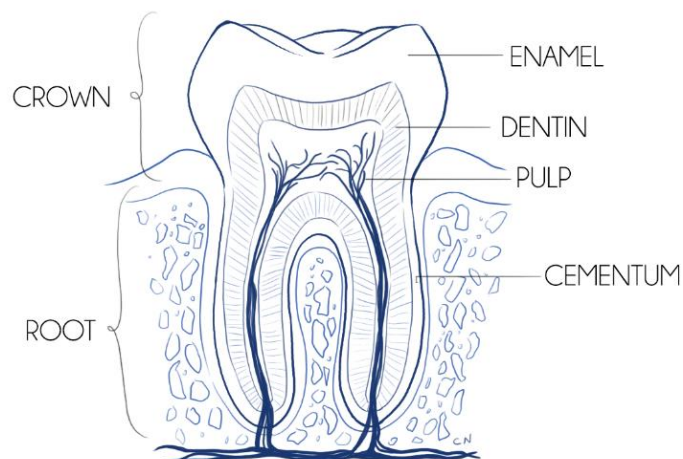
Figure 2 Illustration of tooth' structure

Dental enamel is considered a hard and mineralized tissue, due to its highly dense mineral composition (*c.* 97%) and a few percentages of proteins. On the micromorphological level, enamel is organized in small units (4-8 μm in diameter), called enamel prisms, which follows an oriented fish-scale or key-hole like pattern in the cross-sectional view (BERKOVITZ et al., 2017; FABRITIUS-VILPOUX et al., 2019). A calcium phosphate named hydroxyapatite ($Ca_{10}(PO_4)_6(OH)_2$) is the main mineral component of the enamel prisms (KOBLISCHKA-VENEVA et al., 2018). The apatite grain presents a thin (c. 50 nm) and elongated (up to 1000 µm) needle-like ultrastructure and was recently described as a densely packed and highly-oriented chain-like arrangement (ENAX, EPPLE, 2018; KOBLISCHKA-VENEVA et al., 2018). Other inorganic components such as sodium, magnesium, chlorine, carbonate, potassium, and fluoride are also present in minor quantities (SHAHMORADI et al., 2014).

2.1.2 Titanium

Restoring the patient's smile has always been a big challenge for modern dentistry. Several techniques aim not only to recover the function of the normal and healthy dentition, but also to maintain the aesthetics. Over the last 20 years, oral implants have emerged as the treatment of choice for most edentulous patients, being the standard treatment to replace missing teeth. Therefore, the application of oral implants became a successful and well-established technique in the actual oral rehabilitation treatment (RUPP et al., 2018).

A dental implant is a component that fuses with the jawbone or skull to support a dental prosthesis or to act as an orthodontic anchor (Figure 3). Nowadays, most dental implants are cylindrical screw-like devices that can mimic the dental root's appearance. The implants are connected to an abutment, which is the structure that supports the artificial prosthodontic restoration (MISCH, 2007). They are manufactured in various sizes to match different and individual situations (NOROWSKI, BUMGARDNER, 2009).
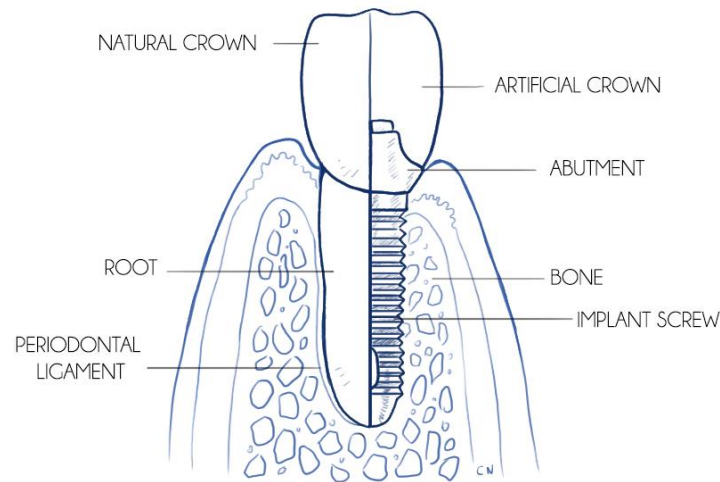
Figure 3 Illustration of the implant components

Titanium (Ti) and its alloys are the most widely used materials in dental implantology (BRANEMARK, 1983; MUDDUGANGADHAR et al., 2015; RUPP et al., 2018). This fact is due to the specific Ti properties, such as biological, mechanical and morphological biocompatibility to surrounding tissues, resistance to corrosion, high strength/weight ratio, and low modulus of elasticity (MISCH, 2007; NOROWSKI, BUMGARDNER, 2009; OSHIDA et al., 2010; WILLIAMS, 1977). Ti also has a natural oxide layer, usually titanium dioxide (TiO_2), which is responsible for a direct bonding to the jawbone, providing the osseointegration (BRANEMARK, 1983).

Brånemark first described osseointegration as "a direct connection between living bone and a load-carrying endosseous implant at the light microscopic level" (BRÅNEMARK, CHIEN, 2005). He performed an *in vivo* experiment with rabbits and observed that the titanium chambers could not be removed from bone tissue, being inseparately incorporated to the bone (BRANEMARK et al., 1977). Nowadays, the term osseointegration is widely used in implantology, and it is well-known that this integration between the Ti surface and the surrounding bone is essential for treatment success (JAYESH, DHINAKARSAMY, 2015).

According to the German Society for Implant Dentistry (DGI), about one million implants are placed every year in Germany. Additionally, the American Academy of Implant Dentistry (AAID) states that around 500.000 implants are placed per year in the United States of America. Finally, in 2005, Klinge et al. estimated that two million implants are inserted each year around the world (KLINGE et al., 2005). This data shows how important implantology is in contemporary dentistry. However, despite high long-term survival rates

being reported greater than 89% after 10 years, complications can occur, and implants do fail (JEMT, 2016; PJETURSSON et al., 2007).

The present study uses SLA grade 2 implants, which are among the most used types of dental implants and are very well documented. SLA is a term introduced by Buser *et al.* in 1991 and stands for sand-blasted, large grit, and acid-etched (BUSER et al., 1991). Grade 2 means that it is considered as commercially pure titanium; however, minor quantities of other compounds are present in its composition (CAMILO et al., 2011). The implant surfaces are produced with a large-grit (250-500 µm) sandblasting technique, succeeded by an acid-etching bath with HCl/H_2SO_4 at high temperature. As a result, a surface with micro-roughness (2-4 µm micro pits) is created, which is ideal for cell attachment (BALLO et al., 2011). Albrektsson et al. (1981) and Westas et al. (2014) reported that an implant surface is an important characteristic that determines the osseointegration success (ALBREKTSSON et al., 1981; WESTAS et al., 2014). According to the literature, rough surfaces provide better implant-bone interface interaction. For this reason, an average micro pits height deviation of 0.5 µm to 2 µm is present in most available implants (ALBREKTSSON, WENNERBERG, 2004). On the other hand, various articles relate an increased surface roughness to higher bacterial adherence (BHARDWAJ et al., 2015; PUCKETT et al., 2010).

Implant failure can be caused by many reasons, such as mechanical problems, poor osseointegration, and infection (MOY et al., 2005; VEERACHAMY et al., 2014). However, biofilm accumulation with consequent bacterial infection is the leading cause of implant failures (BHARDWAJ et al., 2015; FURST et al., 2007; RUPP et al., 2018; VEERACHAMY et al., 2014; WESTAS et al., 2014).

2.1.3 Feldspathic ceramic

Dental ceramic is one of the most common materials used for teeth reconstruction and teeth replacement in oral prostheses. They have been used since the 1960s in a metal-ceramic system, which is considered to have a high performance until nowadays (BABU et al., 2015; RASHID, 2014). Dental ceramics are used in both removable and fixed prostheses, for instance as crowns, bridges, denture teeth, abutments, and teeth structure over dental implants (BABU et al., 2015).

Ceramics are mainly used due to their strength, biocompatibility, intraoral stability, color stability, and well-accepted aesthetics (KIM et al., 2017; RAGHAVAN, 2012). These characteristics are closely linked to their structural architecture. Ceramics have a crystal phase,

responsible for the mechanical properties and a glassy phase, giving ceramics the tooth-like color (RUSE, SADOUN, 2014; SHENOY, SHENOY, 2010).

In the past few years, the research in the ceramics field increased and evolved substantially. There are different kinds of ceramic systems, and they are classified in different ways, such as based on the composition, type, firing temperature, and microstructure. In this study, feldspathic ceramic was chosen because it is the most common used material for metal-ceramic restorations and provides aesthetic on alumina-based ceramics (RAGHAVAN, 2012).

Ceramics, like any other surface exposed to the intraoral environment, is prone to bacterial colonization (PADOVANI et al., 2015). However, there isn't much in the literature about this matter. Studies from Auschill et al. and Eick et al. showed that bacteria could accumulate on ceramics surface. They observed a thin and non-homogeneous biofilm layer with viable bacteria (AUSCHILL et al., 2002; EICK et al., 2004). They explained that the flat and smooth surface of this material would prevent the bacterial adhesion. However, the ceramic surface may present microscopic irregularities, allowing bacteria to adhere to and colonize the surface (KIM et al., 2017). In the present research, it will be assessed the behavior of feldspathic ceramic regarding biofilm accumulation after mouthrinsing with a hydroxyapatite-based watery test solution.

2.1.4 Poly(methyl methacrylate) resin

Poly(methyl methacrylate) (PMMA) is an acrylic resin polymer composed of an extended carbon chain matrix (Figure 4). It is considered a bioinert and rigid material (FRAZER et al., 2005).
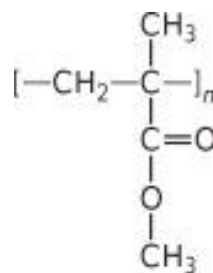
Figure 4 Illustration of the chemical structure of PMMA

Walter Wright introduced this acrylic material in 1937 (JOHN et al., 2001). The first use of PMMA in dentistry was as a base for complete dentures (FRAZER et al., 2005). Since then, PMMA is commonly used for full denture bases, gum design for removable prostheses,

removable partial dentures, provisional prostheses, maxillary expansion appliances, artificial teeth, and orthodontic appliances (DARVELL, 2018; FANG et al., 2016).

The widespread use of PMMA in the dental field is related with its good qualities, such as biocompatibility, reliability, shape and color stability, good aesthetics, durability, low cost, easy handling and processing and easy repair (BERTOLINI et al., 2014; FANG et al., 2016). However, despite these qualities, PMMA has low mechanical properties, such as susceptibility to distortion, reduced strength and insufficient surface hardness, limiting the use of this material in dentistry (AJAJ-ALKORDY, ALSAADI, 2014; CHEN et al., 2017). Furthermore, PMMA is associated with bacterial adhesion mainly due to its capacity of water absorption and its intrinsic porous structure, which creates retention sites (CHEN et al., 2017; SPASOJEVIC et al., 2015).

The biofilm accumulated on PMMA surfaces may lead to gingivitis, stomatitis, and halitosis. Thus, the search for new bioinspired materials with the potential to inhibit bacterial adherence and growth around these devices is a goal to be achieved in preventive dentistry. Therefore, this study will evaluate the effects of a hydroxyapatite-based watery mouthrinse test solution on biofilm formation on poly(methyl methacrylate) resin.

2.1.5 Biofilm

As mentioned before, the oral biofilm is composed by a heterogeneous group of microorganisms surrounded by a polysaccharide-based matrix. As it is the primary etiologic agent for common oral diseases, it is essential to understand its formation process and how to prevent it.

Biofilm formation

The oral biofilm formation is a dynamic process divided into several stages: salivary pellicle formation, bacterial attachment by single organisms, growth and multiplication and, finally, sequential bacterial adhesion to form a complex and mature biofilm (HANNIG, HANNIG, 2009). This microbial community is embedded in a polymeric extracellular matrix (EPS), which provides protection, stabilization, and the necessary nutrients within the biofilm (BERGER et al., 2018).

Biofilm formation on a solid surface starts immediately after the exposure to the oral environment, when proteins from saliva adsorb onto the material's surface, forming a conditioning film: the acquired pellicle (HANNIG, 1999a). The acquired pellicle is a proteinaceous, acellular and bacteria-free layer composed of salivary molecules, such as

proteins, glycoproteins, mucins, immunoglobulins, lipids, bacterial components, and other macromolecules (HANNIG, HANNIG, 2009; HANNIG, 1999a; HANNIG, JOINER, 2006). The pellicle ultrastructure is organized into two layers. An electron-dense basal layer is in contact with the material surface and usually has a thickness ranging between 10 – 20 nm; and an outer layer that has a granular and loose appearance with a thickness ranging between 1000-1300 nm after 24 h (HANNIG, 1999a; HANNIG, JOINER, 2006). Salivary protein adsorption reaches a plateau after 90-120 minutes (HANNIG, JOINER, 2006; SKJORLAND et al., 1995). Concerning the functions of the pellicle, it has lubricating function and can act as a protective barrier. The presence of the pellicle around a surface also changes the surface free energy and charge. Additionally, there are pellicle proteins, which serve as specific receptors for bacterial adhesins, providing sites for bacterial attachment (HANNIG, JOINER, 2006).

In the next stage of biofilm formation, bacteria adhere to the pellicle layer. First, a reversible adhesion takes place via a weak and long-range physicochemical interaction (van der Waals force). Next, an irreversible attachment is created by short-range specific forces (receptor-adhesins interactions) that are present during the bacterial approach to the pellicle's surface (HANNIG, JOINER, 2006; MARSH, 2006). Initial colonizers are mainly gram-positive Streptococci (*S. sanguis*, *S. oralis*, *S. mitis*) (MARSH, 2006; XIMENEZ-FYVIE et al., 2000). After the formation of this initial bacterial layer, co-aggregation of other colonizers starts. If left undisturbed, diverse bacteria continue to attach, forming micro-colonies. The growth continues, and the complexity and heterogeneity of the bacterial community increase over time, with more gram-negative and strictly anaerobic species, which contribute to the biofilm pathogenicity (MARSH, 2006).

Biofilm formation on implant-supported prostheses

Biofilms can form on any surface exposed to the oral cavity. This way, implant-supported prostheses' and restorative materials surfaces are also prone to biofilm attachment. Bacterial adhesion and accumulation depend not only on the prosthetic design but also on the physical and chemical characteristics of each material (HAO et al., 2018; SOUZA et al., 2016; TEUGHELS et al., 2006).

Biofilm formation is mainly influenced by the surface topography and morphology of each material. An increased roughness is directly associated with a higher bacterial attachment rate (AL-AHMAD et al., 2010; DO NASCIMENTO et al., 2008; SOUZA et al., 2016; TEUGHELS et al., 2006). Rimondini et al., in a scanning electron microscopy in vitro study, showed that a rough titanium surface had more bacterial attachment than grooved or smooth

surfaces (RIMONDINI et al., 1997). In accordance, Quirynen et al. also reported a positive relationship between biofilm development and roughness on implants (QUIRYNEN et al., 1990). The same relationship has been observed by Auschill et al. and Eick et al. for ceramics, and by Chen et al. and Spasojevic et al. for PMMA resin (AUSCHILL et al., 2002; CHEN et al., 2017; EICK et al., 2004; SPASOJEVIC et al., 2015). Thus, surface morphology contributes to biofilm formation and growth. This factor is related to bacteria accumulation in valleys, being then protected from mechanical shear forces and serving as a reservoir to the following colonizers (DHIR, 2013).

Bacterial attachment on implant-supported prostheses follows the similar colonization sequence as on teeth (KALYKAKIS et al., 1998; SOUZA et al., 2016). Concerning the implant, Furst et al. stated that the colonization of bacteria occurred within 30 minutes after the implant installation surgery (FURST et al., 2007). The initial colonizers are mostly the same as on the natural dentition, composed of gram-positive cocci, rods and actinomyces bacteria (DHIR, 2013). The later periopathogenic colonizers can vary in number and in species present, but are mostly also the same when compared to teeth and includes the gram-negative *P. gingivalis*, *P. intermedia*, *Fusobacterium spp., T. denticola, T. forsythia*, etc. (MOMBELLI, 1993; MOMBELLI, LANG, 1994; PELGRIFT, FRIEDMAN, 2013; SILVERSTEIN et al., 1994; TANNER et al., 1997). Some studies state that Staphylococcus aureus has a higher affinity to the titanium surface, being a common colonizer around implants, which does not happen on teeth (DHIR, 2013; MOMBELLI et al., 1987). Besides, the opportunistic yeast *Candida albicans* is a common finding in association with biofilm formation on denture bases made of the acryl resin PMMA (KOSEKI et al., 2018). Yeasts may cause stomatitis and oral candidiasis. The gram-negative bacteria mentioned above are part of the red and orange Socransky's microbial complexes (SOCRANSKY et al., 1998). They are responsible for triggering an inflammatory response, resulting in periodontal and peri-implant infections.

Peri-implant disease is defined as an inflammatory biofilm-associated process occurring in the tissues surrounding the implant (BERGLUNDH et al., 2018; SCHWARZ et al., 2018). Figure 5 shows the progression of peri-implant infections. It starts as peri-implant mucositis (PM) and can evolve to peri-implantitis. PM is a reversible inflammatory disease that affects the soft tissue around the dental implant, whereas in peri-implantitis, besides soft tissue inflammation, progressive loss of supporting bone is also visible, which can lead to implant mobility and consequently failure (BERGLUNDH et al., 2018; SCHWARZ et al., 2018).
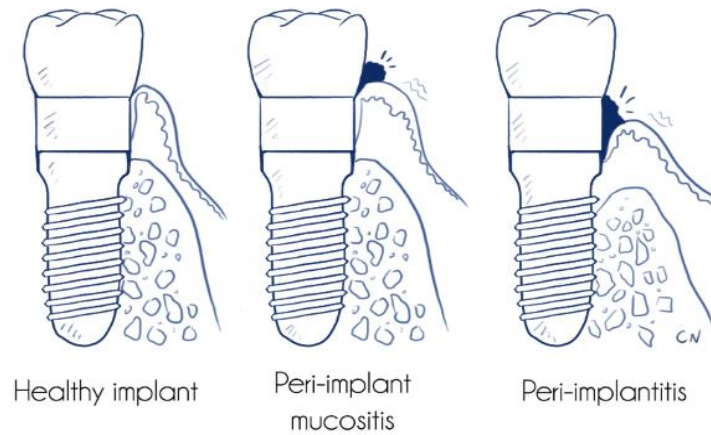
Figure 5 Illustration of peri-implant disease progression.

Therefore, bacterial adhesion plays a critical role in the periodontal infection pathogenesis and on implant-supported prostheses failure. Prevention of this step is essential to achieve good oral health and patient satisfaction.

Prevention of biofilm formation

Mechanical treatment is the standard intervention to control biofilm formation. It involves not only toothbrushing and interdental cleaning performed by the patient, but also professional disruption and removal of biofilm by scaling and root planing (SRP) (INVERNICI et al., 2018).

However, sometimes, the mechanical cleaning alone is not enough to provide oral health. During professional cleaning, for example, there are cases of limited access to the surface, which are hard to reach with instrumentation. Furthermore, the recolonization in treated sites is common (INVERNICI et al., 2018; MOMBELLI, 2018; NICOLINI et al., 2019). Additionally, some patients are unable to reach an acceptable level of oral hygiene alone, either because of personal limitations and impaired dexterity or even due to a lack of motivation (JAMES et al., 2017; VARONI et al., 2012).

Therefore, adjunct therapies are essential to improve mechanical procedures' outcomes. Many different adjuvant strategies to prevent biofilm formation have been proposed in the past few years (JAMES et al., 2017). In this study, three different hydroxyapatite watery solutions will be introduced and compared with the well-established chlorhexidine 0.2% solution.

2.2 Chlorhexidine

Digluconate chlorhexidine, also known as chlorhexidine (CHX) is on the World Health Organization's List of Essential Medicines. It is considered the gold standard mouthrinse in dentistry. Nowadays, it is the most used solution for oral biofilm control, and it has been used since the 1950s (JAMES et al., 2017; LANG, LINDHE, 2015). Besides controlling the formation of the biofilm, it can also reduce gingival inflammation, and gingival bleeding indexes (JAMES et al., 2017; VARONI et al., 2012).

CHX is a cationic bisbiguanide base with a broad-spectrum antibacterial power, proved to be efficient against Gram-positive and Gram-negative bacteria (Figure 6) (JAMES et al., 2017; VARONI et al., 2012).
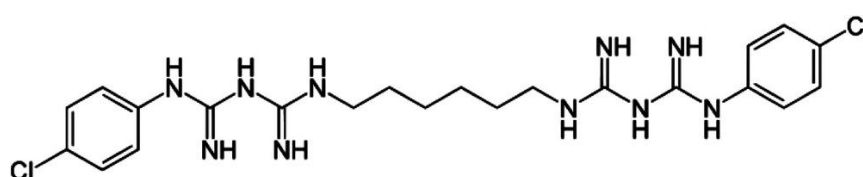
Figure 6 Chlorhexidine molecule from https://en.wikipedia.org/wiki/Chlorhexidine

Chlorhexidine can act either as bacteriostatic or bactericidal agent depending on the dosage: at high concentrations (0.12–0.2%) it has a bactericidal effect, whereas at low concentrations (0.02-0.06%) a bacteriostatic effect is present (VARONI et al., 2012). This event occurs because, at low concentrations, the binding between the positively charged CHX and the negatively charged bacterial cell walls results in disruption of the cell membrane, changing the osmotic balance and increasing the permeability inside the cell membrane, therefore causing the loss of low molecular-weight components. On the other hand, higher concentrations trigger a cascade of cellular events that lead to irreversible cell damage and cell death by cytolysis (JAMES et al., 2017; JONES, 1997; LANG, LINDHE, 2015; VARONI et al., 2012).

Good substantivity is another advantage of this bisbiguanide. According to Bonesvoll, approximately 30% of the CHX active substances remains on the oral mucosa, because the molecules can bind to mucins, which are proteins present in the salivary film that covers the soft and hard intraoral tissues surfaces (BONESVOLL, 1977). Furthermore, CHX absorption through the mucosa is minimal, due to its cationic properties. Those factors contribute to a prolonged activity up to 12 h after application. Moreover, it is stated that the long-term use of CHX does not lead to bacterial resistance or high proliferation of opportunistic strains from the oral flora (SOLDERER et al., 2019; VARONI et al., 2012).

Due to these qualities, CHX is used in dentistry mainly as an antibacterial mouthrinse, being an adjunct to the mechanical cleaning treatment. However, despite its benefits, the long-term use of this substance is associated with several side effects that must be considered. The most common adverse effect is a brownish pigmentation of teeth, mucosa, tongue, and restorative materials, giving the patient a not-aesthetic smile. Other pervasive side effects faced by CHX users are transitory taste alterations, temporary burning sensations, and increasing of supragingival calculus formation. Uncommon cases like facial paresthesia, sialadenitis, hypersensitivity, erythema, and desquamative lesions of gum and oral mucosa have also been reported (JAMES et al., 2017; SOLDERER et al., 2019; VARONI et al., 2012).

Nowadays, the treatment of periodontal related diseases comprehends on removing the biofilm by professional scaling and root planning in association with good oral health habits by the patient (ARWEILER et al., 2018). However, mechanical therapy alone can fail, especially when the subject is not able to maintain proper oral hygiene, either because a lack of motivation, systemic associated disease or compromised ability (ARWEILER et al., 2018). An adjuvant therapy plays a significant role to help those patients to control the biofilm in the oral cavity. Until now, chlorhexidine is the first-choice antiseptic for complementary treatment. But, due to the adverse effects of chlorhexidine, the search for new biomimetic materials is an important task in preventive dentistry.

2.3 Hydroxyapatite

Hydroxyapatite is a calcium-phosphate ceramic with the formula $Ca_{10}(PO_4)_6(OH)_2$ (Figure 7), representing the main mineral component of teeth, representing more than 90% of the mineral composition of dental enamel (ENAX, EPPLE, 2018). Synthetic HAP has morphological and structural similarities to enamel apatite crystals (EPPLE, 2018). Nano-sized hydroxyapatite particles present crystals ranging from 20 to 1000 nm that can be non-aggregated or clustered in bigger particles. Hydroxyapatite nanoparticles have higher surface energy, higher solubility and optimal bioactivity (osteoconductivity), resulting in an intense chemical bond with the tissue (ELIAZ, METOKI, 2017; ELKASSAS, ARAFA, 2017; EPPLE, 2018; PEPLA et al., 2014).
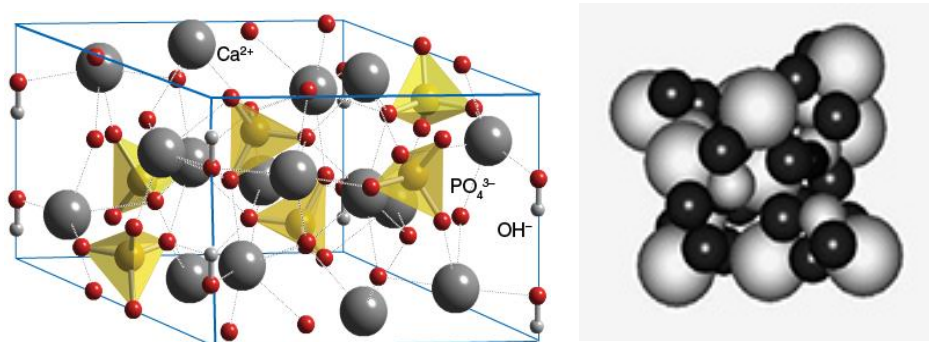
Figure 7 Representative illustrations of HAP molecule from
http://www.chemtube3d.com/solidstate/SShydroxyapatite.htm and
http://www.fluidinova.com/hydroxyapatite-properties-uses-and-applications.

Due to structural and functional similarities to teeth and bone, HAP has not only outstanding biocompatibility and bioactivity properties, but is also a non-toxic and non-immunogenic material, making it an interesting bioinspired material for medical use (ELIAZ, METOKI, 2017; ELKASSAS, ARAFA, 2017; EPPLE, 2018; RAMESH et al., 2018). In a recent literature review, Epple observed that the hydroxyapatite particles present no adverse health effects to the human organism when applied in adequate doses. Additionally, if accidentally ingested, it presents no harm because it is rapidly dissolved by the acids in the stomach (EPPLE, 2018).

In recent years, the use of HAP has increased in dentistry for many different applications. As granules, HAP is being applied as a filling in periodontal bone defects reconstruction with great results (OKADA, FURUZONO, 2012). HAP blocks are used for various cases in maxillofacial surgery, such as facial reconstruction and bone replacement. Prosthetic operations also take advantage of both, HAP granules and blocks, in alveolar ridge reconstruction and augmentation before implant/prosthesis placement (FIGUEIREDO et al., 2010; OKADA, FURUZONO, 2012; PEPLA et al., 2014). The hydroxyapatite particles can be also used in the domain of restorative and preventive dentistry, for example, to promote the remineralization of initial lesions of caries on enamel (ENAX, EPPLE, 2018; PEPLA et al., 2014). HAP has also been used for drug, protein and gene delivery, as coating agent on dental implants, as reparative materials for damaged enamel, and in toothpastes as a polishing agent (ELIAZ, METOKI, 2017; OKADA, FURUZONO, 2012).

Despite all knowledge around hydroxyapatite nanoparticles and their benefits, there are only very few HAP based types of mouthwash on the market. Kensche et al. showed that an experimental 5% hydroxyapatite nanoparticle solution could reduce the initial bacterial adhesion to enamel in situ. They also confirmed the adsorption of HAP microclusters at the tooth surface (KENSCHE et al., 2017). Pepla et al. reported that HAP nanoparticles can bind with proteins, biofilm, and bacteria due to their nano size and consequently increased surface area (PEPLA et al., 2014). Moreover, according to Grenho et al., these nanoparticles could inhibit Gram-negative and Gram-positive bacteria growth (GRENHO et al., 2012). Biofilm formation is not restricted to the enamel surface. Thus, it is essential to evaluate the effects of the HAP solution on biofilm formation on other materials commonly used in dentistry for oral rehabilitation, such as titanium, ceramics and polymethyl methacrylate resin.

2.4   Objectives

Currently, there are several strategies to prevent or delay the formation and accumulation of oral biofilms, mainly focused on substances with antibacterial properties. However, anti-adhesive substances are also an interesting alternative, since they would have no impact on the viability of oral microflora and wouldn't promote bacterial resistance.

Kensche et al. (2017), previously observed the anti-adhesive effect of an experimental, bioinspired HAP solution. In their experiments, decreased bacterial accumulation was visible after application of a 5% watery HAP solution on enamel surfaces (KENSCHE et al., 2017). Thus, continuing research on hydroxyapatite is important, to better understand its behavior on enamel and different dental materials, as well as its effects on biofilm formation on the materials surfaces.

Therefore, this *in situ* study has the objective to assess:

- The behavior of three different HAP watery solutions on enamel and also on 3 artificial dental materials (titanium, ceramic, and PMMA) regarding:
  - o The efficacy of the HAP mouthwash to adhere to the pellicle formed on the tested materials surfaces immediately after rinsing, 30 min and 2 h after rinsing
  - o The effectiveness of the HAP mouthwash against oral biofilm adhesion on the tested materials during 24 h and 48 h
- The size and shape effects of the different applied HAP particles in a watery solution
- The differences between biofilm formation on polished and non-polished titanium surfaces under the influence of HAP solution rinsing.

3   Material and Methods

3.1   Subjects

The present *in situ* experiment was performed with healthy volunteers aged between 28 and 35 years, members of the laboratory staff of the Clinic of Operative Dentistry, Periodontology and Preventive Dentistry, Saarland University. The number of volunteers varied according to the protocol applied (Table 2 Protocol's description). The subjects had to fulfill the following inclusion criteria: good oral health without gingivitis, caries or unphysiologically salivary flow rate; no systemic diseases; no use of antibiotics or any periodontal treatment within the past six months; non-smoker; not pregnant or breastfeeding and absence of orthodontic appliances. The Medical Ethics Committee of the Medical Association of Saarland/Germany approved the study protocol (n° 283/03–2016). Informed written consent concerning the participation in the study was obtained from all subjects.

3.2   Samples

In addition to enamel, the natural component of the tooth, other common materials used for oral rehabilitation and the preparation of implant-supported prostheses were addressed: titanium (main composition of dental implants), feldspathic ceramics (used as dental rehabilitation material), and polymethyl methacrylate resin (common material to make the base of the implant-supported prosthesis).

3.2.1 Enamel samples
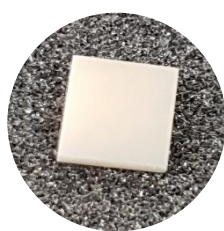
Square enamel slabs measuring approximately 5x5 mm and 1 mm thick were prepared from bovine incisor teeth. Later, they were polished with wet grinding sandpapers (from 240 to 2500 grit for SEM and until 4000 grit for TEM). To remove the smear layer, the samples were washed with 3% NaOCl for 3 min, followed by ultrasonication with distilled water for 5 minutes. Afterward, disinfection in 70% ethanol for 15 minutes took place. Finally, samples were washed with sterile water and stored at 4 °C in sterile water during 24 h before use.

3.2.2 Titanium samples

Titanium discs with a microstructured surface (SLA) Ra = 2 µm, grade 2, were obtained from Dentsply Implant Systems (Firma Friadent, Bensheim, Germany), with 5 mm diameter and 1 mm height. Half of the samples remained unpolished, while the other half was polished by wet grinding with abrasive paper (800 to 4000 grit). Right after, Ti discs were immersed in isopropanol (70%) for 10 min, followed by a wash in distilled water in order to remove the resulting smear layer and for disinfection purpose.

3.2.3 Ceramic samples
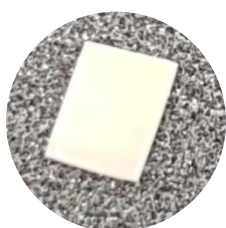
Ceramic slabs with square/rectangular shape with approximately 5x5 mm and 1 mm in height were cut from feldspathic ceramic blocks (VITABLOCS Mark II from VITA Zahnfabrik, Germany). The slabs were polished with wet grinding sandpapers (from 240 to 4000 grit). For cleaning and disinfection purpose, the ceramics samples were immersed in isopropanol (70%) for 15 min, followed by a wash in distilled water and finally dried before use.

3.2.4 PMMA resin samples

Polymethyl methacrylate (PMMA) resin samples measuring approximately 5 mm diameter and 1 mm in height were prepared with an autopolymerising prosthetic resin kit (powder and monomer) from Pala® (Kulzer, Germany) following the manufacturer's instructions. PMMA samples were polished with grid sandpapers (1200 to 4000 grit). For cleaning purpose, samples were first placed three times (10 min each) in the ultrasonicator, two times with isopropanol 70%, and one time with sterile water. Finally, the samples were dried before attachment to the splints.

3.3 Tested solutions

Different sizes of hydroxyapatite nanoparticles were used to prepare three test solutions presented at Table 1. The shape and size from the hydroxyapatite particles were verified by scanning electron microscopy (SEM) and transmission electron microscopy (TEM). The test solutions containing HAP particles were prepared by mixing 0.5 g of the selected HAP powder in 10 ml bidistilled water. Chlorhexidine mouthwash [0.2% (w/v) chlorhexidine-digluconate in 7% (v/v) ethanol - Saarland University Pharmacy, Homburg, Germany] and distilled water rinse, served as positive and negative controls, respectively.

The different rinsing solutions were used by the volunteers in different weeks to avoid interferences between tests and controls solutions, preventing a possible cross-over effect. To standardize our protocol, the rinsing procedure followed a specific order: the water control was the first solution used by each volunteer. After a one-week interval, the HAP test solutions were introduced respecting the following order: HAP I, HAP II and HAP III; and respecting also a two weeks clearance period between each of them. Finally, after two more weeks, the volunteers performed the final rinse with the CHX control solution.

Table 1 Specification of hydroxyapatite particles powders according to manufacturer's information.

	COMPANY	COUNTRY	MEDIUM SIZE	CONFIGURATION SHAPE
HAP I	Eprui	China	40 nm	Needle
HAP II	Kalichem	Italy	100 nm	Needle
HAP III	Sigma Aldrich	Germany	< 200 nm	Globular

3.4   Oral exposure

A customized maxillary splint was prepared containing the mounted samples to evaluate the *in situ* biofilm formation (Figure 8). Methacrylate foils with 1.5 mm thickness were used to prepare the acrylic appliance, which extended from the premolar to the second molar (HANNIG, 1999a). Perforations in the buccal aspects of the splints were prepared to fix the polyvinyl siloxane impression material, in which the samples were placed. The samples were placed in the area from the first premolar to the first molar.

Figure 8 Example of a splint with mounted specimens according to Protocol 2.

Before using their splints, volunteers brushed their teeth without toothpaste and rinsed with tap water only to avoid possible interferences from the compounds of the toothpaste. After the intraoral use of the splints for 3 min to allow the formation of the acquired pellicle (HANNIG, 1999a), 30 s rinsing with 10 ml of the tested solutions described above were carried out according to the protocol detailed in Table 2 and in Figure 9, Figure 10 and Figure 11.

During the experiment, the participants did not use toothpaste or any other kind of mouthwash. They should take off their splints during meals, brush their teeth without toothpaste after each meal, and place the splints again after 10 minutes (HANNIG, 1997). During the mealtime, the splints were placed in a closed humidity environment (HANNIG, 1999a).

After the established time of use for each protocol (Table 2), the splint was removed, and the samples were detached from the polyvinyl siloxane and immediately rinsed with distilled running water to remove non-adsorbed salivary particles. According to the protocol, the samples were prepared for fluorescence microscopy (FM), scanning electron microscopy (SEM) and/or for transmission electron microscopy (TEM).

Table 2 Protocol's description

	Protocol 01	**Protocol 02**	**Protocol 03**
Objective	Evaluate how the size and shape of HAP particles influence their adhesion to the initial pellicle	Evaluate how the size and shape of HAP particles influence the biofilm formation	Evaluate the effects of the HAP II solution on biofilm formation on titanium
Number of Volunteers	2	5	5
Tested samples	Enamel Titanium Ceramic PMMA	Enamel Titanium Ceramic PMMA	Titanium (polished and non-polished surfaces)
Test solutions	HAP I, HAP II, HAP III	HAP I, HAP II, HAP III	HAP II
Negative control solution	Water	Water	Water
Positive control solution	-	0.2% CHX	0.2% CHX
Duration of the *in situ* experiment	2 h	24 h	48 h
Number of rinses	1 time after 3 min pellicle formation	2 times each 12 h (1st rinsing: 3 min after pellicle formation)	4 times each 12 h (1st rinsing: 3 min after pellicle formation)
Samples take off	Immediately after rinse 30 min after rinse 2 h after rinse	After 24 h	After 48 h
Analysis	SEM	SEM, FM, TEM	SEM, FM, TEM

Protocol 1

(a)   (b)
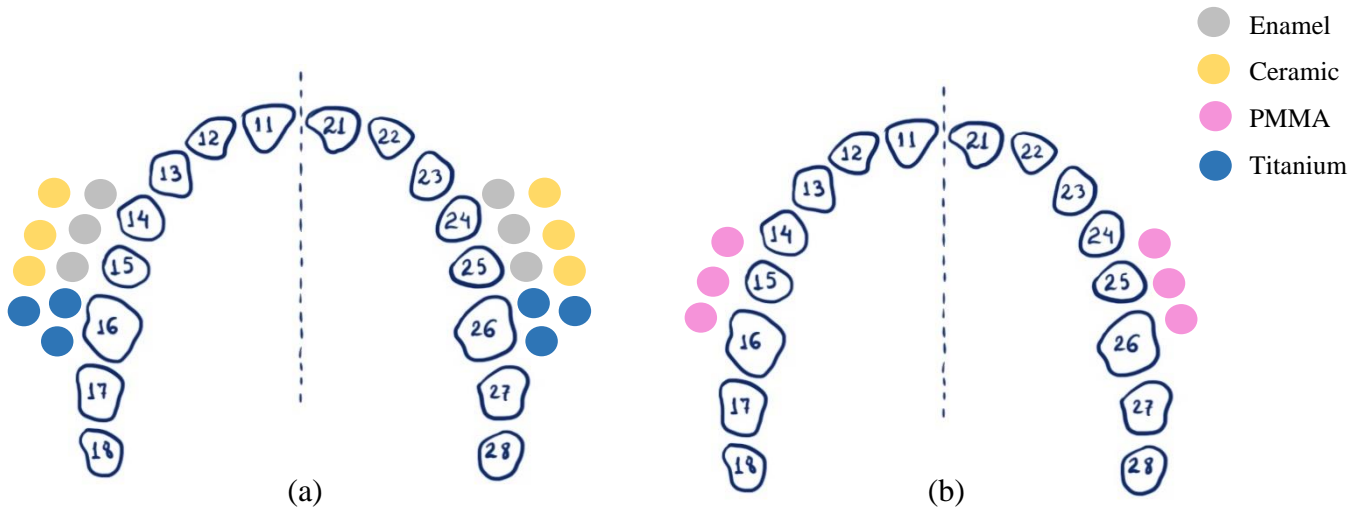
Figure 9 Illustration of Protocol 1. (a) Each volunteer used first the intraoral splint with enamel, ceramic and titanium samples attached. There were three samples from each material on each side. The volunteer placed the splint intraorally, and, after 3 minutes, the 30 seconds selected rinse was performed. One sample from each material from each side was removed immediately, 30 minutes and 120 minutes after rinsing, respectively. The procedure was repeated for all tested solutions (water, HAP I, HAP II, HAP III). Thus, each volunteer used the intraoral appliance four times. (b) Later, it was decided to include PMMA as a material of interest. Therefore, the same subjects repeated the same protocol for PMMA samples for all the solutions. All samples were analyzed with SEM.

Protocol 2

(a)   (b)
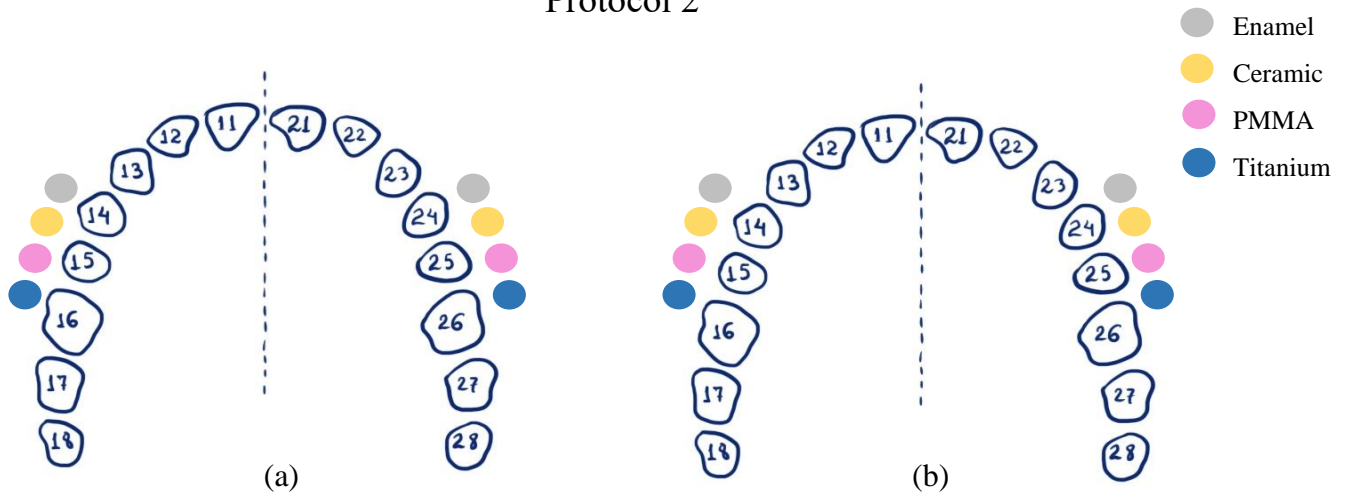
Figure 10 Illustration of Protocol 2. (a) The volunteers used the intraoral splints with one sample of enamel, ceramic, titanium and PMMA attached on each side. Here, five rinsing solutions were tested: water, HAP I, HAP II. HAP III and CHX. All samples were removed from the acrylic appliance after 24 h of intraoral exposure. The right side was analyzed with FM and the left side with SEM. (b) Later was decided to perform a TEM analysis, therefore, two volunteers repeated the protocol 2 for this evaluation.

Protocol 3
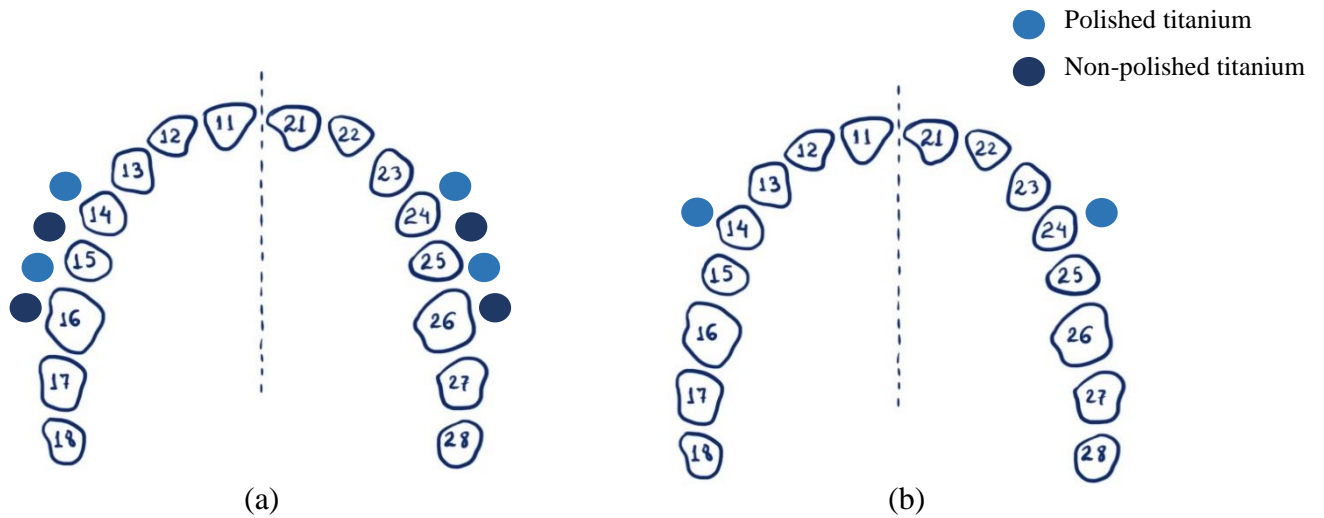
Figure 11 Illustration of Protocol 3. (a) The intraoral splint was mounted with four titanium samples: 2 polished and 2 non-polished discs. In this protocol, the volunteers rinsed with water, HAP II and CHX. After 48h, the samples were removed and analyzed with SEM (one polished and one non-polished sample from each side) and with FM (one polished and one non-polished sample from each side). (b) Two volunteers repeated the protocol for TEM evaluation (one polished sample from each side).

3.5   BacLight viability assay

This assay differentiates living from dead bacteria based on two nucleic acid stains: SYTO 9 and propidium iodide. While the first one will stain all bacteria green (with intact or damaged membranes), the last one will stain cells with compromised membranes in red. When mixed, propidium iodide reduces SYTO 9 fluorescence, enabling a viability evaluation between live and dead bacteria (Figure 12) (STIEFEL et al., 2015).

27
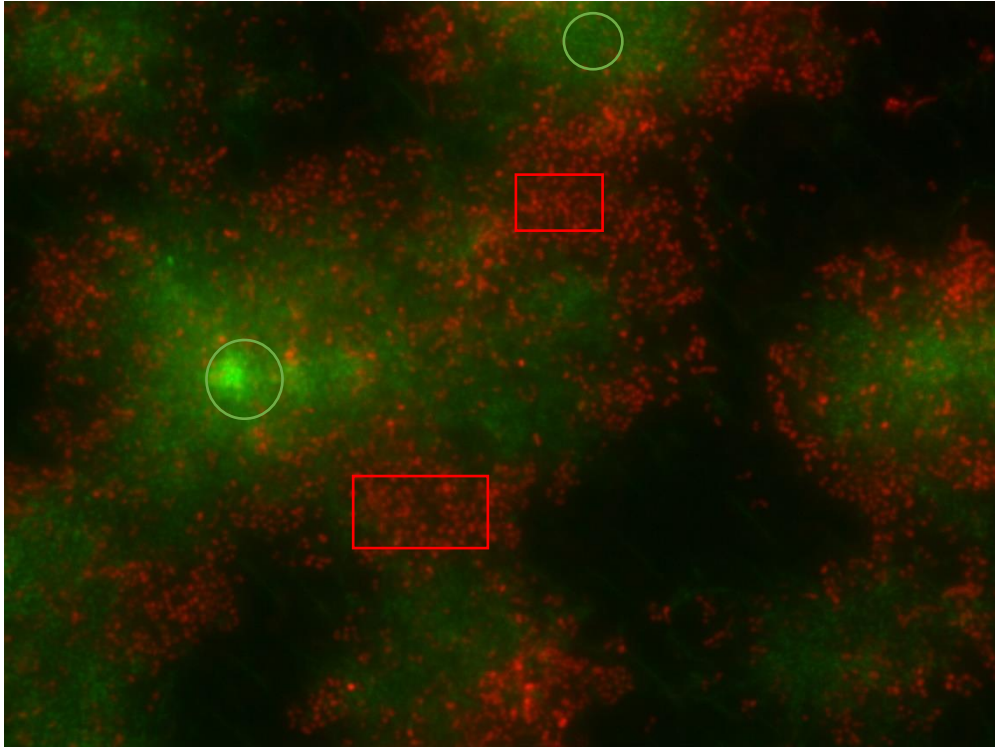
Figure 12 Fluorescence micrograph: green areas highlighted with a circle represent the living bacteria, whereas the red areas highlighted with a rectangle represent the dead bacteria. The black background represents the sample surface, in this case, the enamel surface, which is not stained by SYTO 9 or propidium iodide.

BacLight viability assay was carried out at room temperature in a 6-well-plate. One microliter of the SYTO 9 and 1 µl of propidium iodide was mixed in 1 ml saline solution (0.9% NaCl). This staining solution was vortexed before use. The specimens were covered with 10 µl staining solution and left 10 min in a dark chamber. Subsequently, samples were washed in saline solution two times, dried, fixed to a glass slide and mounted in BacLight oil for fluorescence microscopy analysis (KENSCHE et al., 2017).

3.6 Fluorescence microscopy (FM)

The detection of bacteria and their viability was conducted with FM at 1,000-fold magnification (Axioskop II, ZEISS MicroImaging GmbH, Göttingen, Germany), using AxioVision 4.8 (Carl Zeiss Microimaging GmbH, Göttingen, Germany) for image processing. Nine pictures per sample were taken (9 FM-micrographs per sample). These nine pictures are representative for each specimen (Figure 13).
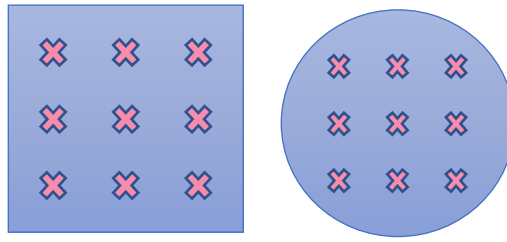
Figure 13 Illustration representing the approximately chosen positions where the pictures were taken on each square or round-shaped sample under the fluorescence microscope.

Semi-quantitative evaluation of the bacteria coverage was performed with the Sefexa Image Segmentation Tool, which is an open-source software for image segmentation available on www.fexovi.com/sefexa.html. To calculate the percentage of bacterial coverage, the program measures the total area of the selected picture (converted into grayscale) and, after setting a threshold, it is possible to separate the live and dead bacteria from the background, which gives the coverage area (Figure 14). Afterwards, the coverage percentage was determined with a simple proportion calculation. This procedure was repeated for all FM micrographs from one sample, and a medium coverage per sample was calculated in the end.
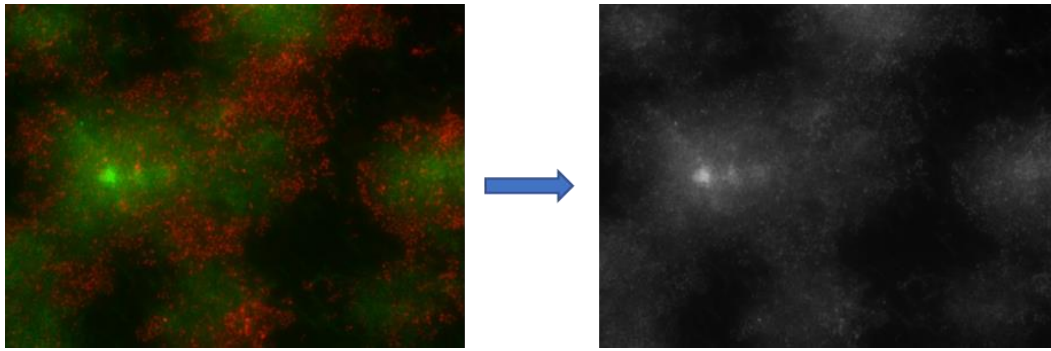
(a)
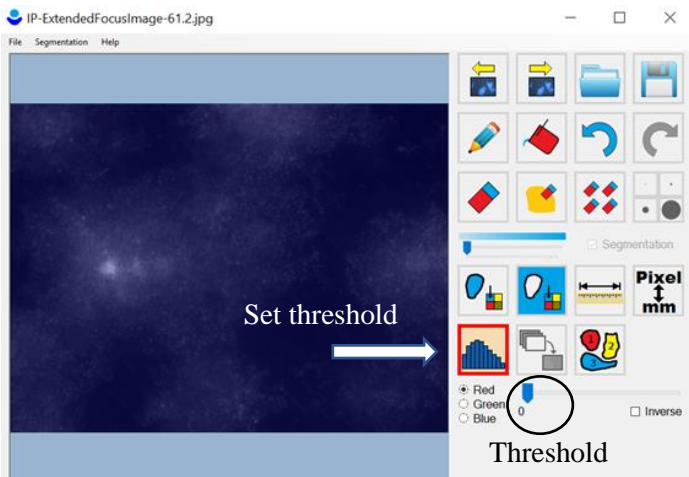
(b)
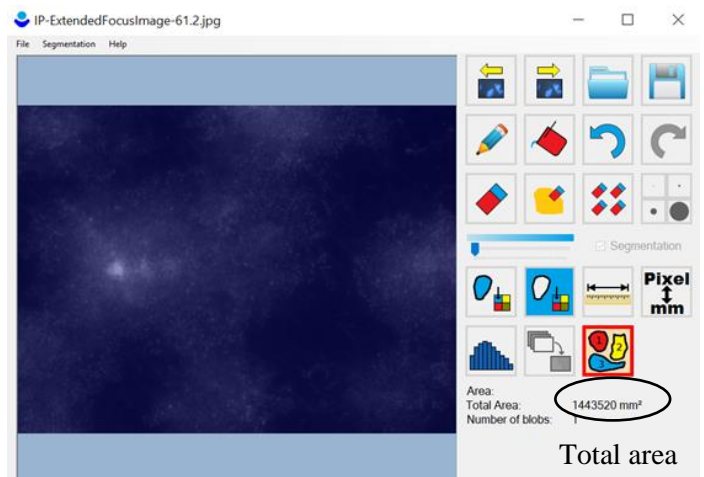
(c)
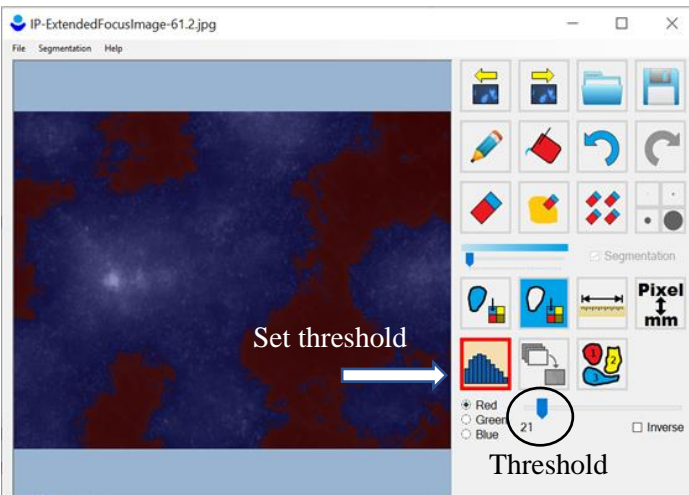
(d)
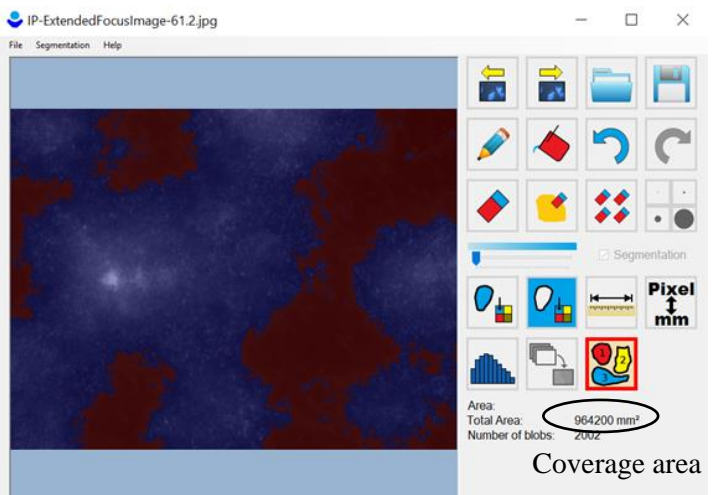
(e)

Figure 14 Bacterial coverage evaluation with Sefexa Image Segmentation Tool. (a) The micrograph generated by the AxioVision software was first converted into grayscale with GIMP free software. (b) A threshold of "0" is set for the total Figure's area. (c) The program gives the total area. (d) A new threshold is used to separate the bacteria area (blue) from the background (red) based on the tone of gray. (e) A new area is calculated based on this threshold.

Additionally, the live and dead cell correlation was performed with two different methods: scoring system and integrated density evaluation with ImageJ. It was decided to use the results from the ImageJ software in this thesis. Differences between them were further discussed in the "discussion of materials and methods" section (5.1.4).

3.6.1 Scoring system

The viability correlation between live (stained in green) and dead (stained in red) cells observed in the biofilm on the samples' surface was assessed and scored by two examiners, and it was based on the following scoring system table created by Rupf et al. (Table 3) (RUPF et al., 2012). This analysis was performed with five representative pictures per sample chosen from the pictures that were taken at 1,000-fold magnification under FM. When a disagreement was present, it was resolved through discussion (RUPF et al., 2012).

Table 3 Scoring system for the assessment of biofilm viability detected with BacLightTM viability assay

Score	Description
1	Mainly red fluorescence; ratio between red and green fluorescence 90:10 and higher.
2	More red fluorescence; ratio between red and green fluorescence 75:25 and higher.
3	Ratio between red and green fluorescence 50:50.
4	More green fluorescence; ratio between red and green fluorescence 25:75 and lower.
5	Mainly green fluorescence; ratio between red and green fluorescence 10:90 and lower.

3.6.2 ImageJ

ImageJ is a Java-based open-source software for image processing available for download at www.imagej.net. Five representative pictures per sample were chosen from the pictures that were taken at 1,000-fold magnification under FM to access the bacteria viability. Each figure contains a green (representing living cells) and a red (representing dead/damaged cells) channel in grayscale (Figure 15). With ImageJ, it was possible to measure the integrated density of both channels. Then the percentage of live cells could be calculated (Figure 15c).

Green channel   Red channel

(a)

Integrated density 1   Integrated density 2

(b)
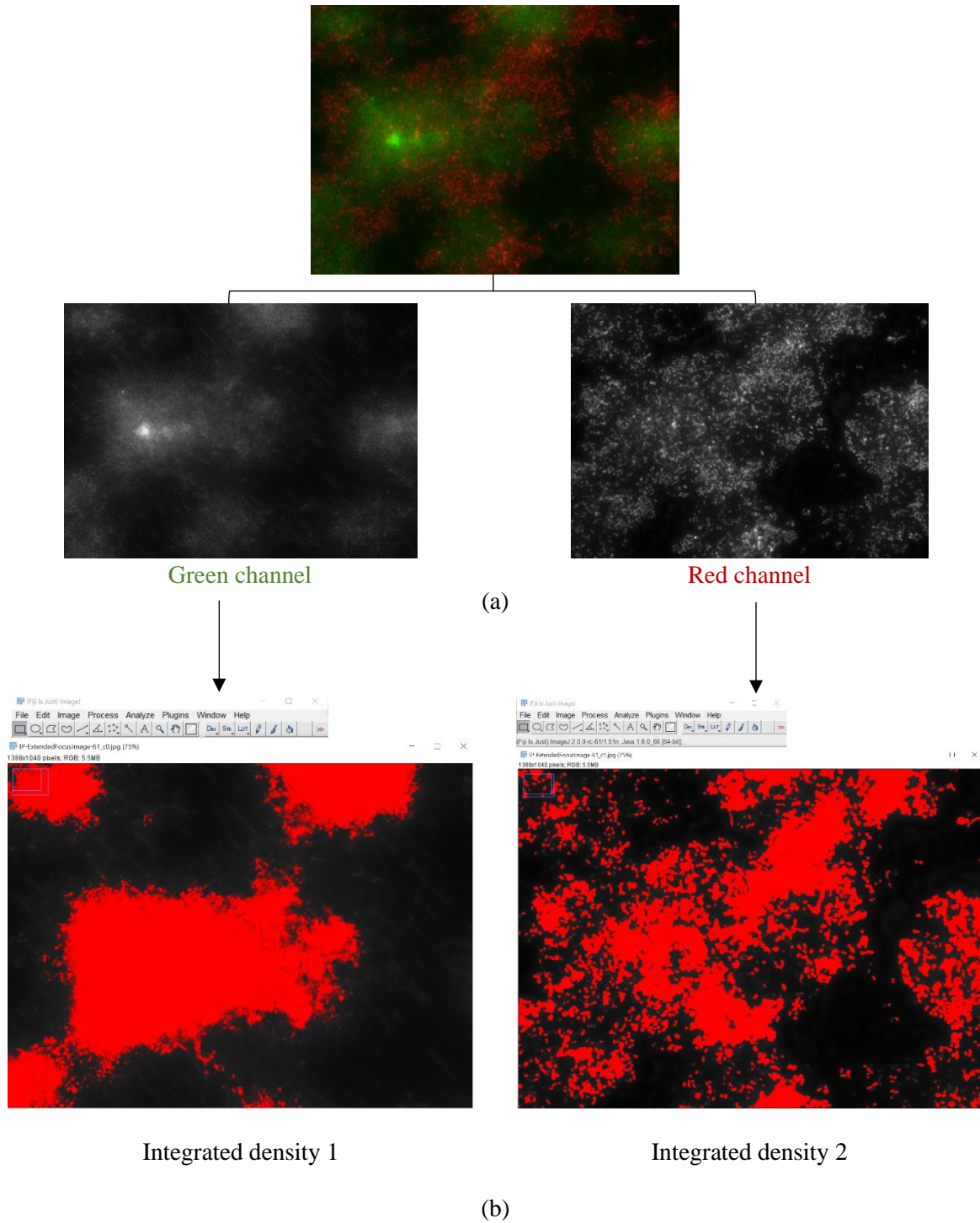
(integrated density 1) * 100 / (integrated density 1 + integrated density 2) = (bacteria viability) %

(c)

Figure 15 Bacterial viability evaluation with ImageJ software. (a) The green and red micrographs of the same section of the sample were evaluated separately. (b) After setting the same threshold for both channels, ImageJ provides the integrated density of each channel. The integrated density is calculated for all five pictures from the same sample. (c) With this data it is possible to calculate the bacteria viability percentage for each picture. Finally, a mean percentage is calculated for the sample.

3.7   Scanning electron microscopy (SEM)

All specimens also followed a fixation process for SEM analysis to visualize the bacterial coverage and the potential adherence of HAP particles to the pellicle and/or to the biofilm. After the total time of intraoral exposure for each protocol (Table 2), the samples were gently washed with sterile water to remove detached material, and the present biofilm was fixed following two different methods.

For the experiments from protocol 1, the samples were fixed with 1 ml of 2% Glutaraldehyde in 0.1 M cacodylate buffer during 2 h at 4 °C. Aiming to reduce the loss of hydroxyapatite particles, no further rinse with cacodylate buffer or alcohol was performed. Then, the samples were left to dry in the air chamber at room temperature overnight.

For the experiments from protocol 2 and 3, the samples were fixed with 1 ml 2% Glutaraldehyde in 0.1 M cacodylate buffer during 2 h at 4 °C. Next, samples were washed 5 times, 10 min each, with 1 ml of cacodylate buffer. A series of ethanol dehydration followed this procedure. Samples were immersed in various ethanol solutions accordingly: ethanol 50% (2x 10 min), ethanol 70% (1x 5 min), ethanol 80% (1x 5 min), ethanol 90% (1x 5 min) and ethanol 100% (2x 10 min). The samples were left to dry in the air chamber at room temperature overnight.

After dried, the samples from all protocols were sputter-coated with carbon and analyzed by SEM and energy dispersive X-Ray spectroscopy (EDX) evaluations in an XL30 ESEM FEG (FEI, Eindhoven, The Netherlands) at 5 kV and 10 kV, consecutively, at up to 20,000-fold magnification.

Additionally, the three hydroxyapatite nanoparticles solutions (HAP I, HAP II, HAP III) were directly applied to three different aluminum sample holders from the SEM to visualize the size and shape of the particles.

3.8   Transmission electron microscopy (TEM)

Five percent nano-hydroxyapatite solutions were prepared from each one of the analyzed powders (HAP I, HAP II, HAP III) to evaluate the particle's sizes. Each solution was directly applied on Pioloform-coated copper grids and analyzed in a TEM Tecnai 12 Biotwin (FEI, Eindhoven, The Netherlands) under magnifications of up to 100,000-fold.

Later in this study, to better understand the effects of the test solution on biofilm adhesion, it was also decided to investigate the ultrastructural characteristics of the obtained

biofilm. For this purpose, two volunteers that already participated in the experiments used again their upper jaw splint with mounted samples for protocols 2 and 3. Samples were prepared for TEM analysis using the following protocol.

The samples were washed with sterile water to remove not adhered bacteria after volunteers took off their splints. After washing, the samples were stored at 4 °C during 1 h in 1,5 ml tubes containing 1 ml of 1% Glutaraldehyde fixing solution. The next step following this primary fixation was washing the samples with 0.1 M cacodylate buffer 4 times with duration of 10 min each time, and store at 4 °C in cacodylate buffer. Next, fixation in osmium tetroxide during 1 h in a dark chamber at room temperature was performed, this procedure was followed by 5 times wash in distilled water (10 min each time) and, finally, immersion in 30% ethanol overnight. The next day, the TEM fixing procedures took place, and the dehydration process was performed at room temperature. This was carried out by immersing the samples in a series of ethanol solution, as follows: 50% (2x 10 min), 70% (2x 20 min), 90% (2x 30 min) and 100% (2x 30 min). Next, the samples were immersed in 100% acetone solution two times of 30 min duration, and finally stored at room temperature overnight in an acetone/Araldite mixture (Agarscientific, Stansted, United Kingdom) with an additional 3% accelerator (mixture A). The day next, the mixture A was poured out and the samples were stored at room temperature in the air chamber overnight in mixture B (Araldite mixture with 2% accelerator). On the following day, a new mixture B was used to fill half of the embedding forms. Identification tags were placed at the bottom side, and the embedding forms were filled until the top with mixture B. Then, samples were incubated for polymerization for 48 h at 65 °C. The following additional procedure was performed only for titanium and ceramics samples: after polymerization, titanium and ceramic were removed by treatment with hydrofluoric acid (5%) during 48 h, and the specimens were re-embedded in Araldite. The enamel was decalcified due to exposure in 0.1M HCl for 4 hours, and the specimens were re-embedded in Araldite.

As the final step, the specimens were cut in ultra-thin sections in an ultramicrotome with a diamond knife (Leica EM UC7, Germany) and mounted on Pioloform-coated copper grids and contrasted with aqueous solutions of uranyl acetate and lead citrate at room temperature. After an intensive wash with distilled water, biofilms could be analyzed with a TEM Tecnai 12 Biotwin (FEI, Eindhoven, The Netherlands) under a magnification of up to 100,000-fold.

3.9 Statistic

For protocol 1, it was performed a qualitative assessment of the SEM pictures. While for protocols 2 and 3, both qualitative (SEM and TEM images) and quantitative (FM results) methods were applied. Regarding the quantitative evaluation, the mean values were analyzed using GraphPad Prism 6. The following approach was used for protocol 2 and 3:

- Protocol 2
    - Two-way RM ANOVA with Tukey's multiple comparisons evaluated the difference of the same material in the different rinsing solutions for coverage and viability tests;
    - Two-way RM ANOVA with Tukey's multiple comparisons also assessed the difference between each material when the same solution was used to compare the HAP anti-adhesive properties against biofilm for each dental material.
- Protocol 3:
    - Mann-Whitney test was performed to evaluate the differences between polished and non-polished titanium samples for each solution used;
    - Kruskal-Wallis test with Dunn's correction for multiple comparisons test assessed differences between all polished samples in all solutions.

For all quantitative evaluations, statistical significance was established for $p \leq 0.05$.

4 Results

4.1 Subjects

During the experiments from Protocol 2, one subject was excluded due to the acquisition of infectious disease and the necessary use of antibiotics. The disease was not related to the experiments. Therefore, the evaluations for Protocol 2 was made with a total of 4 subjects.

4.2 Morphological and ultrastructural characterization of the hydroxyapatite particles

The particles' size and shape of each hydroxyapatite powder used in this study were analyzed by SEM (Figure 16, Figure 18, Figure 20) and TEM (Figure 17, Figure 19, Figure 21). The results for HAP I are shown in Figure 16 and Figure 17; Figure 18 and Figure 19 show the results for HAP II, and Figure 20 and Figure 21 reveal the characteristics of HAP III. The results of size measurements show that there is a variation of sizes for all products involved. HAP I and HAP II had a small size range, presenting a certain uniformity in the size of their particles. HAP I had particles ranging from 30 to 70 nm (Figure 16, Figure 17), while the size of HAP II particles ranged from 60 to 120 nm (Figure 18, Figure 19). HAP III had the biggest size variation, ranging from approximately 50 nm to particles even bigger than 1 µm (Figure 20, Figure 21).

Concerning the shape characteristics of the HAP powder, SEM and TEM confirmed the crystallite-like structures of the HAP I and HAP II particles (Figure 16 - 19). Figure 20 shows a majority of round-shaped particles for HAP III, but on the TEM figure (Figure 21), non-globular structures are also present. Thus, HAP III is composed of globular and a few non-globular particles with a significant size variation. Additionally, besides their different sizes and configuration, all of the three different hydroxyapatites tended to aggregate in aqueous solution, forming aggregates in different sizes and irregular shapes (Figure 16, 18, 20). Individual particles were more frequently seen in the HAP III solution, presenting a clear round-shaped conformation (Figure 20). HAP I and II rarely allowed observing individual crystallites when in watery solution (Figure 16, Figure 18).

HAP I – SEM analysis
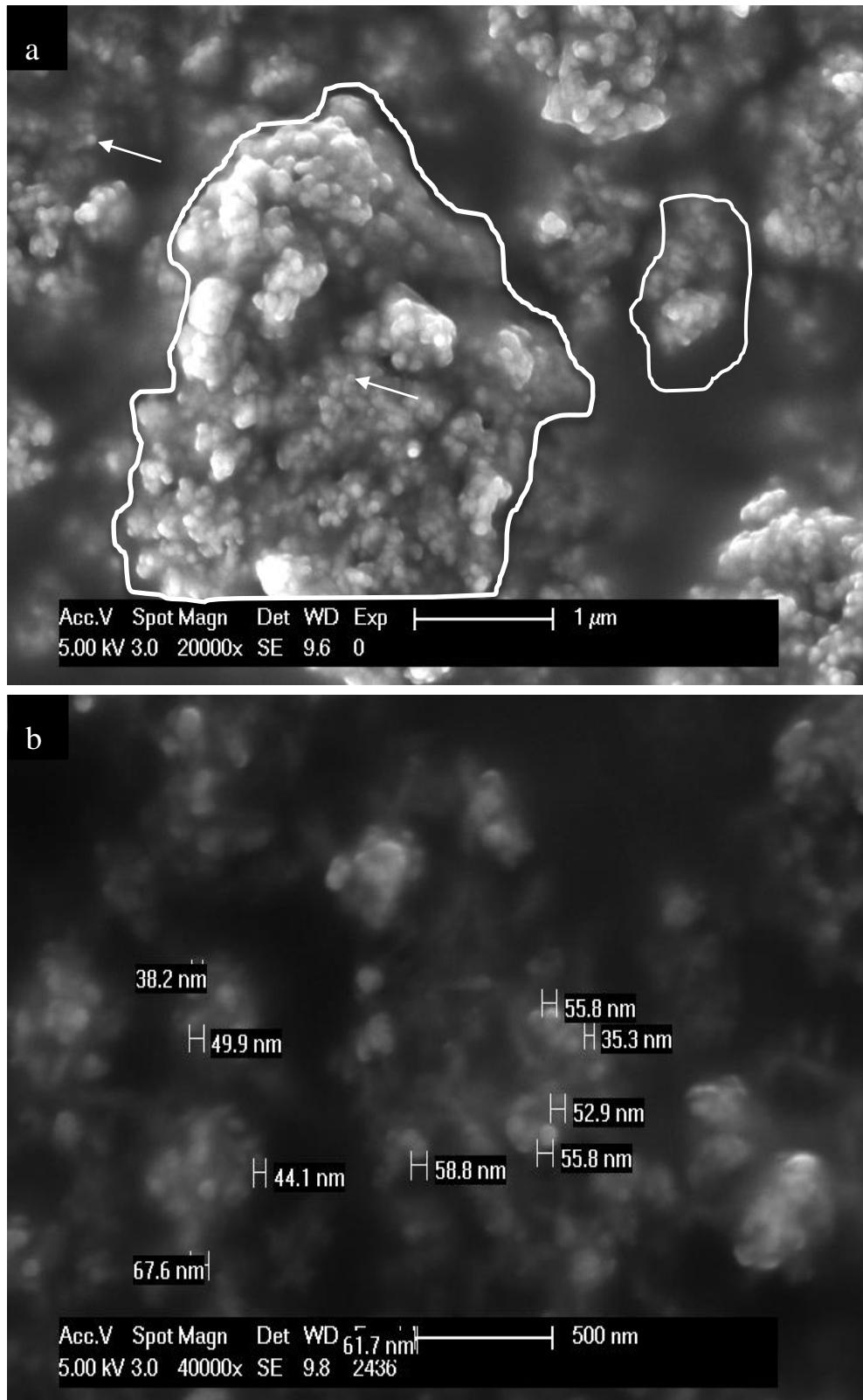
Figure 16 SEM micrographs at 20,000 (a) and 40,000-fold (b) magnifications from HAP I powder immersed in water solution. (a) The HAP particles formed agglomerates, delimited in white, which consist of single nanosized particles (white arrow). (b) Using the SEM measurement tool, it was possible to measure the size of single particles. It was visualized that the particles from HAP I ranged from 30 to 70 nm, approximately. Figure 16a published in NOBRE et al., 2020.

HAP I – TEM analysis
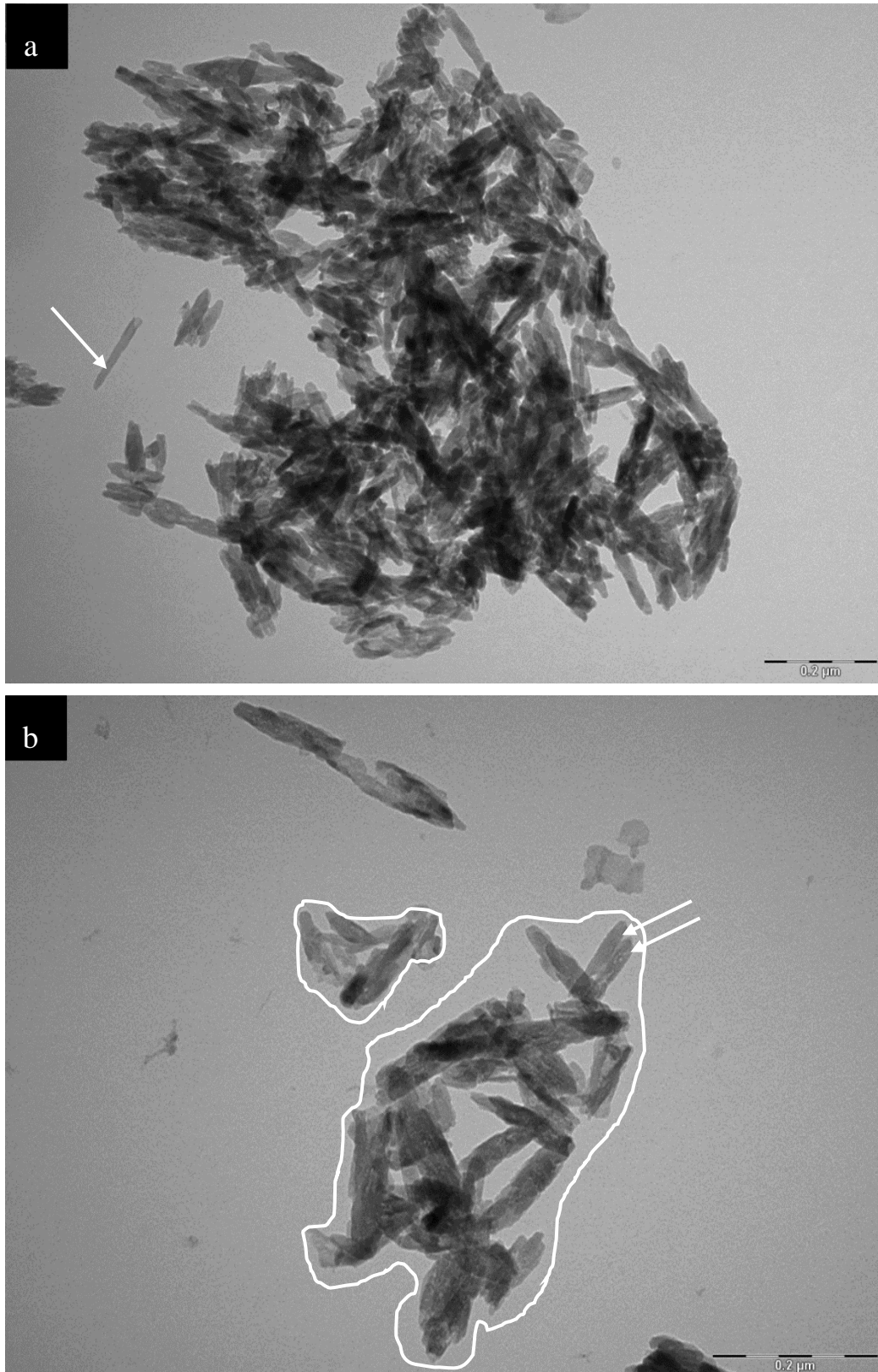
Figure 17 TEM micrographs at 68,000 (a) and 98,000-fold (b) magnifications from HAP I powder immersed in water solution. TEM provided the visualization of the particle´ shape. The particles tend to form aggregates in different sizes and conformations (delimited in white), which are composed by single particles presenting an elongated needle-like structure (white arrows). Figure 17a published in NOBRE et al., 2020.

HAP II – SEM analysis
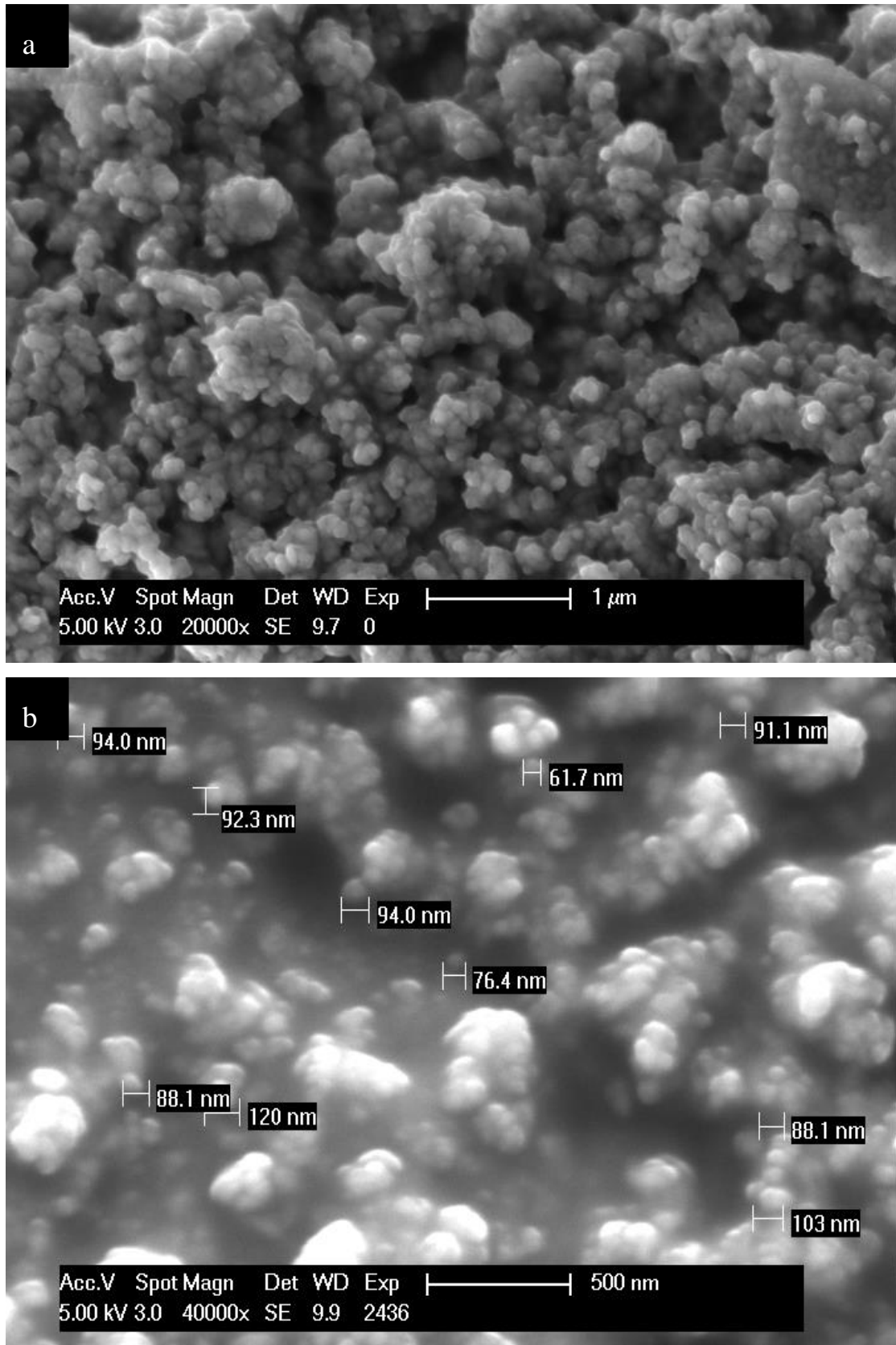
Figure 18 SEM micrographs at 20,000 (a) and 40,000-fold (b) magnifications from HAP II powder immersed in water solution. (a) HAP II particles formed dense and homogeneous agglomerates. (b) The size of the single particles ranged from 60 to 120 nm, approximately. Figure 18a published in NOBRE et al., 2020.

HAP II – TEM analysis
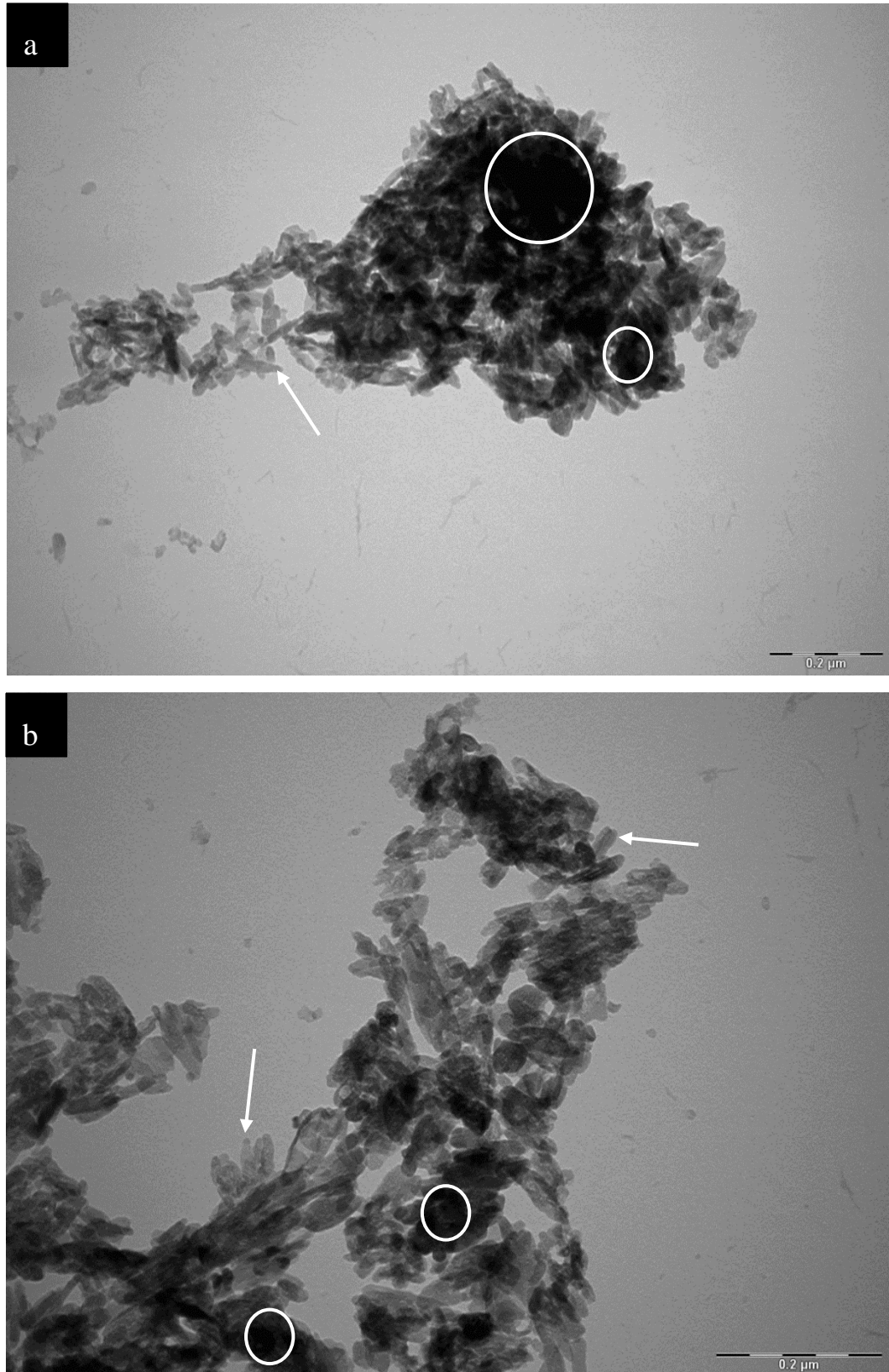
Figure 19 TEM micrographs at 68,000 (a) and 98,000-fold (b) magnifications from HAP II powder immersed in water solution. HAP II particles have a similar arrangement as HAP I. However, the agglomerates present a denser conformation, which can be confirmed by the black areas highlighted by the white circles. These areas represent single particles that are overlapped. The white arrows are pointing to the needle-shaped single particles. Figure 19a published in NOBRE et al., 2020.

41

HAP III – SEM analysis
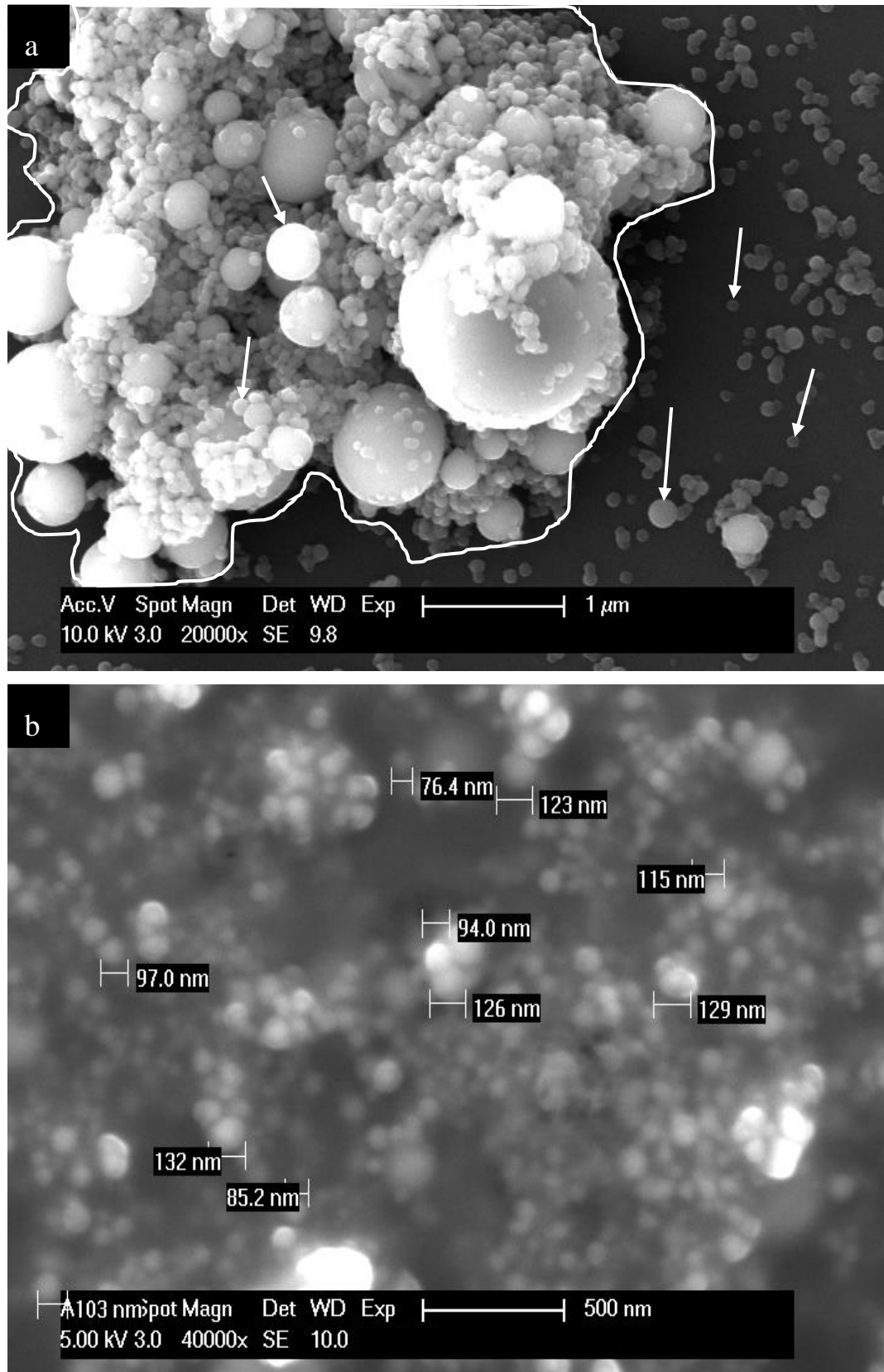
Figure 20 SEM micrographs at 20,000 (a) and 40,000-fold (b) magnifications from HAP III powder immersed in water solution. (a) The single particles can be easily identified (white arrows) and they are present scattered across the surface, as well as united in clusters (highlighted by white circle line). (b) The single particles from HAP III present a highly variable size, with a range from 50 nm to 1 µm, approximately. Figure 20a published in NOBRE et al., 2020.

HAP III – TEM analysis
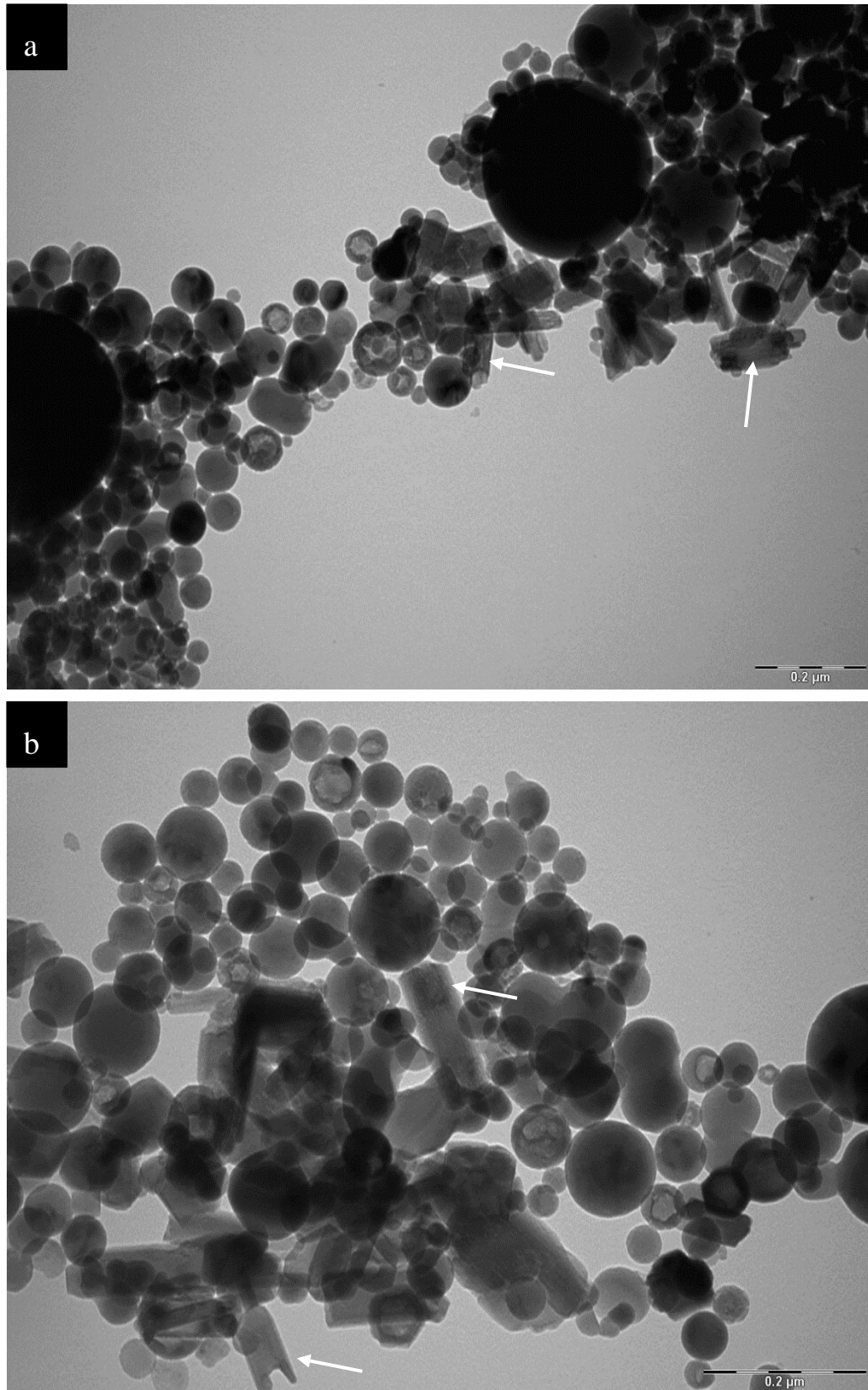
Figure 21 TEM micrographs at 68,000 (a) and 98,000-fold (b) magnifications from HAP III powder immersed in water solution. TEM micrographs provided the visualization of HAP III particles. There are not only globular, but also non-globular shaped particles (white arrows) with different electron density. Figure 21a published in NOBRE et al., 2020.

As mentioned before, hydroxyapatite is a calcium-phosphate compound, therefore mostly composed of calcium (Ca) and phosphate (P) elements. EDX images of particles clusters (Figure 22) show that the red selected area in the three pictures presents high peaks of Ca and P, which are compounds present in the hydroxyapatite molecule ($Ca_{10}(PO_4)_6(OH)_2$). Oxygen (O) is present in high levels due to the water medium in addition to being compound of the hydroxyapatite particle. The presence of carbon (C) is justified by the carbon sputter-coating procedure, which is essential for the SEM analysis.

HAP I

Element	Wt%	At%
C	27.06	40.54
O	37.19	41.83
P	11.90	6.91
Ca	23.86	10.71

HAP II

Element	Wt%	At%
C	32.83	46.95
O	35.63	38.25
P	10.22	5.67
Ca	21.32	9.13

HAP III

Element	Wt%	At%
C	12.20	22.13
O	33.52	45.66
P	16.86	11.86
Ca	37.43	20.35
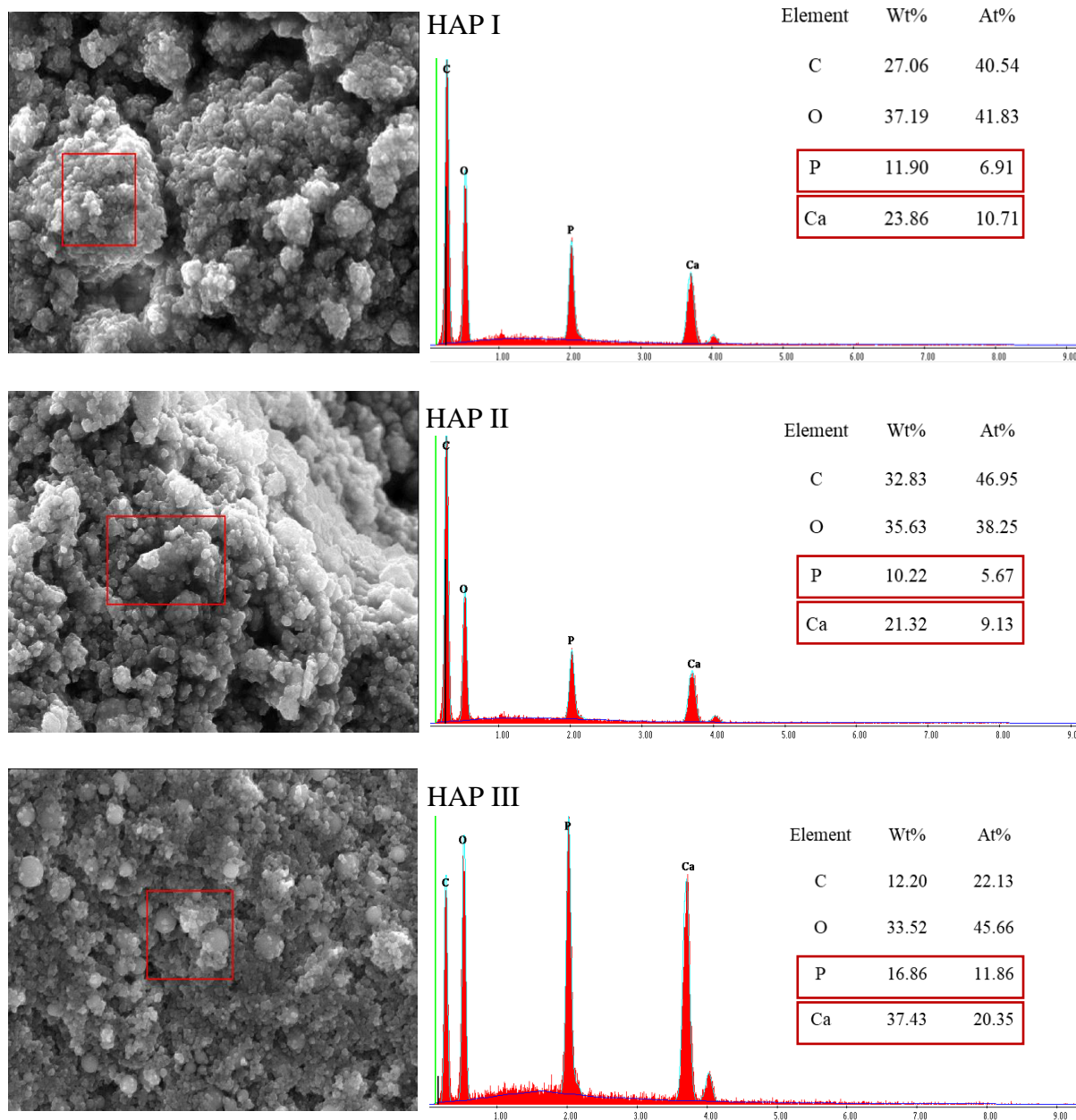
Figure 22 EDX analysis of the tested hydroxyapatite powders immersed in water solution: HAP I, HAP II and HAP III. The element analysis took place within the red window, and it was made at 5,000-fold magnification. The presence of Ca and P peaks indicate the presence of the hydroxyapatite particle. (Wt% = weight percentage; At% = atomic percentage). Figure 22 published in NOBRE et al., 2020.

44

4.3 Hydroxyapatite adherence to the pellicle

Protocol 1 was performed to evaluate the capability of adhesion of the applied HAP particles to the oral pellicle formed on the different dental materials (enamel, titanium, ceramic and PMMA).

Beforehand, it is important to understand the characteristics of each surface after the polishing process and before performing the intraoral exposure.

- The enamel surface (Figure 23a) is characterized by scratches, from the polishing procedures, arranged in parallel to each other, according to the enamel crystals organization. The small grains present in this figure may represent debris from the polishing process, which were not properly removed.
- The titanium surface (Figure 23b) also present scratches, however they are not well defined and not well organized; being present in several directions.
- Differently, the ceramic sample (Figure 23c) present a smooth surface with discreet scratches.
- The PMMA surface (Figure 23d), on the other hand, has a surface with a different arrangement. To prepare the PMMA resin, two compounds are mixed: the monomer and the powder polymer, which is composed by pre-polymerized PMMA round-shaped particles. After the autopolymerising process, some pre-polymerized particles are not well dissolved. They are, therefore, embedded in the cured resin structure (Figure 24). These particles are embedded in the resin in a disorganized manner, being present at different depths. Thus, during the polishing, these grain structures will be polished as well, creating the craters-like configurations over the entire surface visible in Figure 23d and in the following figures where PMMA was applied.
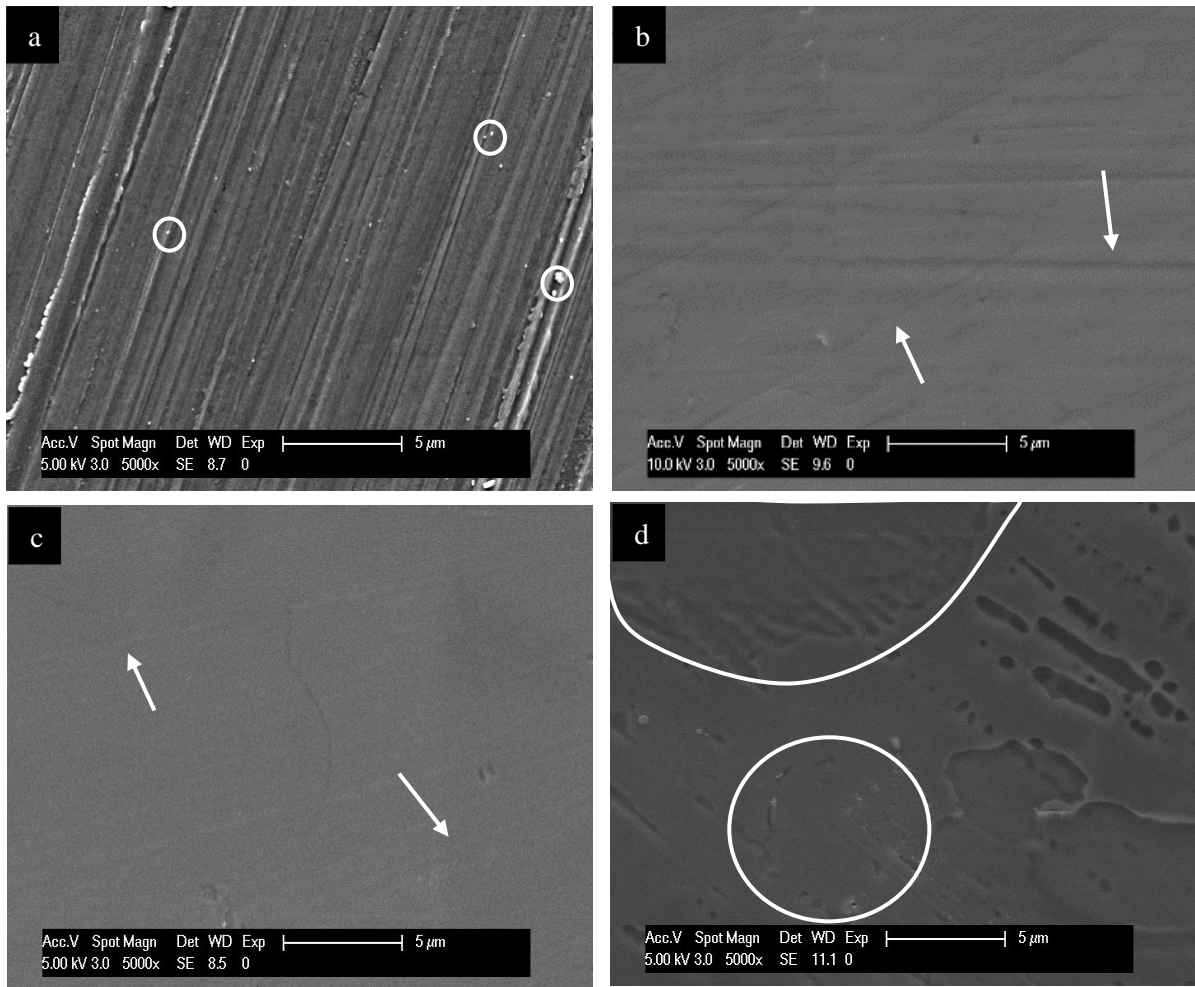
Figure 23 SEM micrographs at 5,000-fold magnifications of the dental materials used in this experiment (without oral exposure): enamel (a), titanium (b), ceramic (c) and PMMA (d). (a) The circles highlight the grains present on the enamel surface, possible representing debris from the polishing process. (b) and (c): The arrows point to scratches over the titanium and ceramic surfaces, respectively, resulting from the polishing procedures. (d) The circle delimitates the "crater-like" structure commonly visible on the PMMA surfaces, which could be a prepolymerized globular particle.
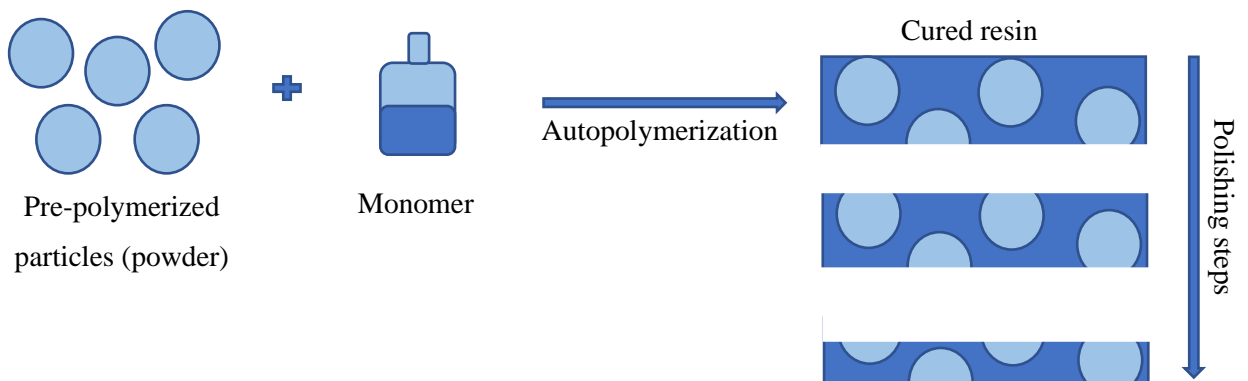
Figure 24 Illustration of PMMA resin preparation and further configuration after polishing. The blue circles inside the rectangle represent the remaining pre-polymerized PMMA particles embedded into the cured resin structure.

46

4.3.1 HAP particles adherence on pellicle-covered enamel

Pellicle formation over 2 h on the control samples, enamel specimens rinsed with water, is shown in Figure 25. The Figure 26, 27 and 28 demonstrate the adherence of HAP particles after rinsing with the watery solutions of HAP I, II and III, respectively.

After exposure to the oral cavity, the SEM micrographs from the enamel sample showed that it was already possible to detect a thin pellicle with globular structures on the surface even after three minutes of intraoral exposure followed by a water rinse (Figure 25a). The scratches from the enamel surface were masked by these globular-shaped particles, which represent the salivary proteins from the acquired pellicle. Over time, the thickness and coverage area of this globular film increased, masking even more the enamel surface (Figure 25b). A homogeneous and globular pellicle was visible on the enamel after 2 h (Figure 25c).

Immediately after rinsing with any hydroxyapatite solution (HAP I, HAP II, HAP III) there was a distinct change of the surface's morphology. Besides the presence of the proteins from the acquired pellicle, the enamel surfaces were heterogeneously covered with hydroxyapatite particles and clusters with large variations of size and shapes (Figure 26, Figure 27a, Figure 28a). HAP I and HAP II presented bigger cluster structures with sizes up to 4 µm, whereas HAP III revealed a more homogeneous coverage distribution immediately after rinsing with the HAP solutions.

On the specimens removed from the splints thirty minutes after rinsing, the same pattern was observed for the three tested HAP solutions: the number of adhered hydroxyapatite particles decreased compared to the pattern immediately after rinsing. Small clusters and single particles could be seen dispersed over the enamel surfaces (Figure 26b, Figure 27b, Figure 28b).

Finally, 2 h after rinsing with the HAP solutions, the enamel surfaces are characterized by a globular network-like pellicle coverage. The HAP particles are integrated within the pellicle, hampering the differentiation between the HAP particles and the proteins from the pellicle. Smaller hydroxyapatite particles were visible on the enamel surfaces, and small clusters were still visible, most of them with a size below 1 µm (Figure 26c, Figure 27c, Figure 28c).

Enamel – Water rinsing
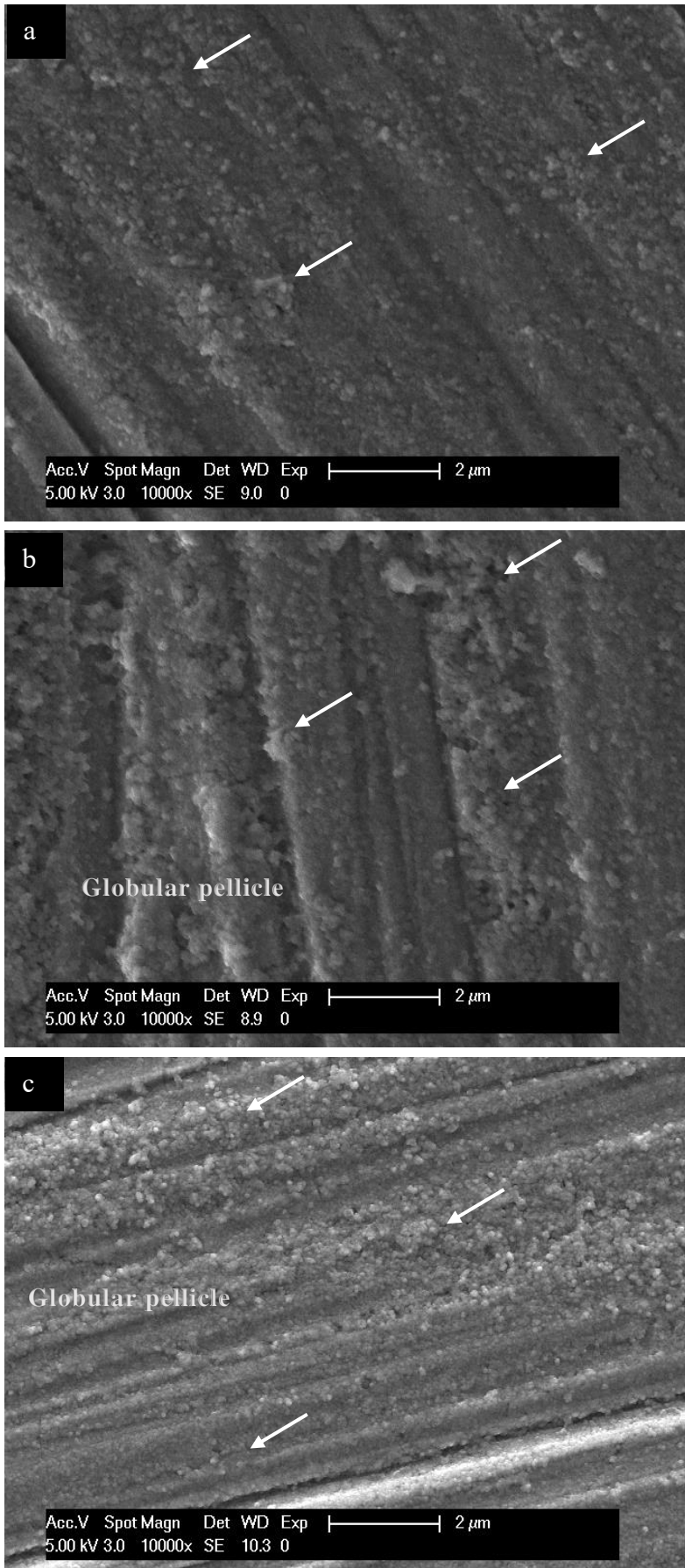
Figure 25 SEM micrographs at 10,000-fold magnifications of enamel samples after rinsing with water according to protocol 1. The pellicle formation and progression are visible at three different time-points: immediately (a), 30 min (b) and 2 h (c) after rinsing. The white arrows are pointing to the globular structures from the acquired pellicle.

48

Enamel – HAP I
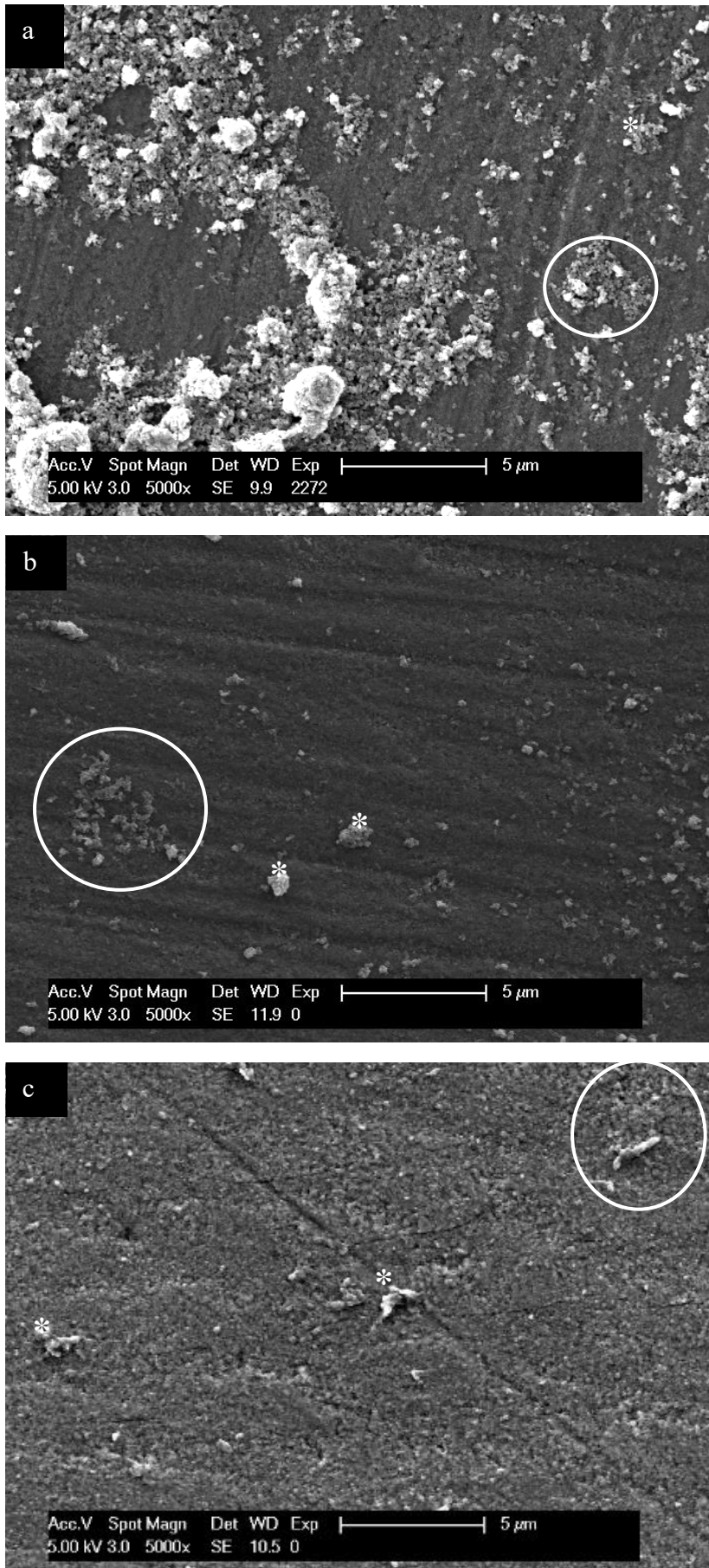
Figure 26 SEM micrographs at 5,000-fold magnifications of enamel samples after rinsing with HAP I according to protocol 1. Clusters (white asterisks) and hydroxyapatite agglomerates (white circles) are visible at three different time-points: immediately (a), 30 min (b) and 2 h (c) after rinsing. The particles are over the globular 2 h-pellicle layer. Adherent HAP particles decrease with increasing intraoral exposure time. Figure 26 published in NOBRE et al., 2020.

Enamel – HAP II
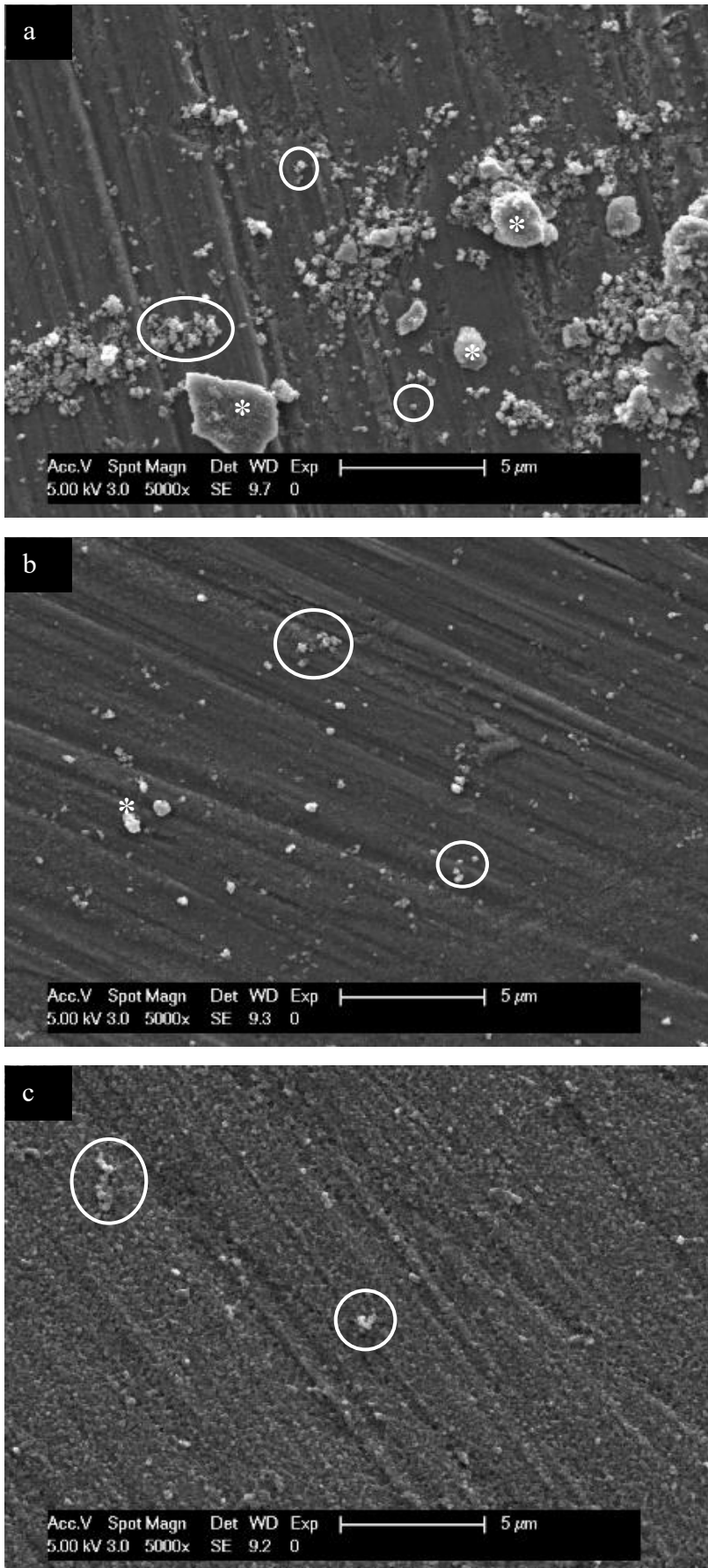
Figure 27 SEM micrographs at 5,000-fold magnification of enamel samples after rinsing with HAP II according to protocol 1. (Hydroxyapatite clusters white asterisks) and agglomerates (white circles) are visible at three different time-points: immediately (a), 30 min (b) and 2 h (c) after rinsing. The particles are over the globular 2 h-pellicle layer. Adherent HAP particles decrease with increasing intraoral exposure time. Figure 27 published in NOBRE et al., 2020.

HAP III - Enamel
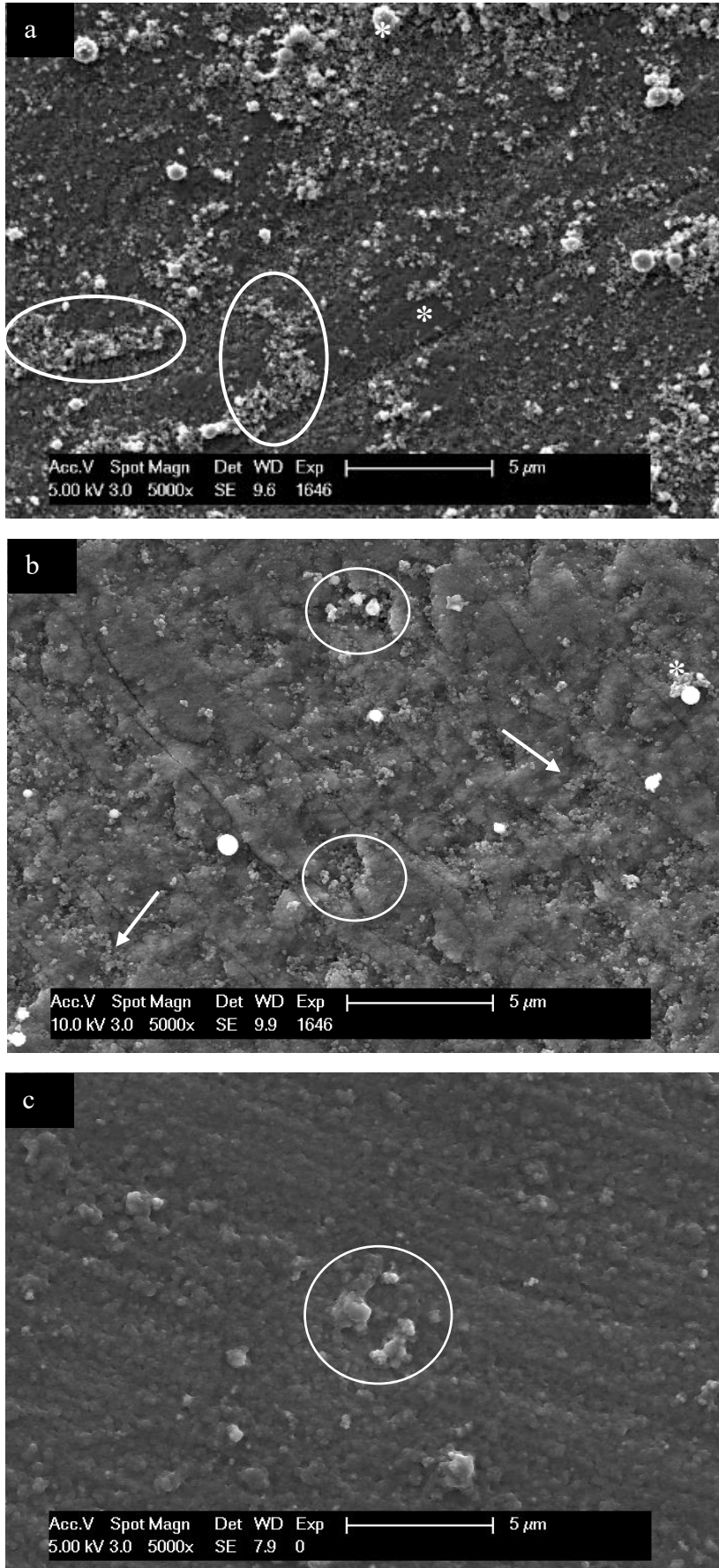
Figure 28 SEM micrographs at 5,000-fold magnifications of enamel samples after rinsing with HAP III according to protocol 1. Hydroxyapatite particles (white arrows), clusters (white asterisk) and agglomerates (white circles) are visible at three different time-points: immediately (a), 30 min (b) and 2 h (c) after rinsing. The particles are over the globular 2 h-pellicle layer. Adherent HAP particles decrease with increasing intraoral exposure time. Figure 28 published in NOBRE et al., 2020.

4.3.2 HAP particles adherence on pellicle-covered titanium

Pellicle formation over 2h on the control samples, titanium specimens rinsed with water, is shown in Figure 29. The Figure 30, 31 and 32 demonstrate the adherence of HAP particles after rinsing with the watery solutions of HAP I, II and III, respectively.

The globular structures representing the proteins from the three minutes pellicle are visible in small quantity over the titanium surface, which was removed from the splint immediately after the rinsing with the water solution (Figure 29a). As with enamel, the number of proteins present on the titanium surface increased after 30 minutes (Figure 29b) and after 2 h (Figure 29c) of intraoral exposure after rinsing with water solution, leaving a homogeneous pellicle coverage on the titanium surface.

When the volunteers used the HAP rinsing solutions, some differences between the HAP formulations were present. The titanium samples that were removed immediately after the 30 seconds rinse followed a similar pattern for all three HAP solutions: the nanoparticles were randomly distributed over the samples' surface, as single particles, and forming clusters and aggregates (Figure 30a, Figure 31a, Figure 32a). HAP III had a higher amount of particles covering the titanium surface immediately after rinsing in comparison with HAP I and HAP II (Figure 32a).

Thirty minutes after rinsing, the number of adhered particles decreased, and more dispersed particles and small aggregates could be seen (Figure 30b, Figure 31b, Figure 32b). Several particles from HAP II and HAP III were accumulated in retention areas from the titanium surface (Figure 31b and Figure 32b). Surprisingly, almost all nanoparticles were washed out on titanium samples rinsed with HAP I (Figure 30b).

After two hours of exposure to the HAP solutions, HAP II and III solutions were more effective in adhering to the titanium samples, while the hydroxyapatite particles from HAP I were almost absent. On Figure 31c, it is possible to visualize elongated and bridge-like structures in-between the HAP II particles and between the HAP II particles and the pellicle.

Titanium - Control
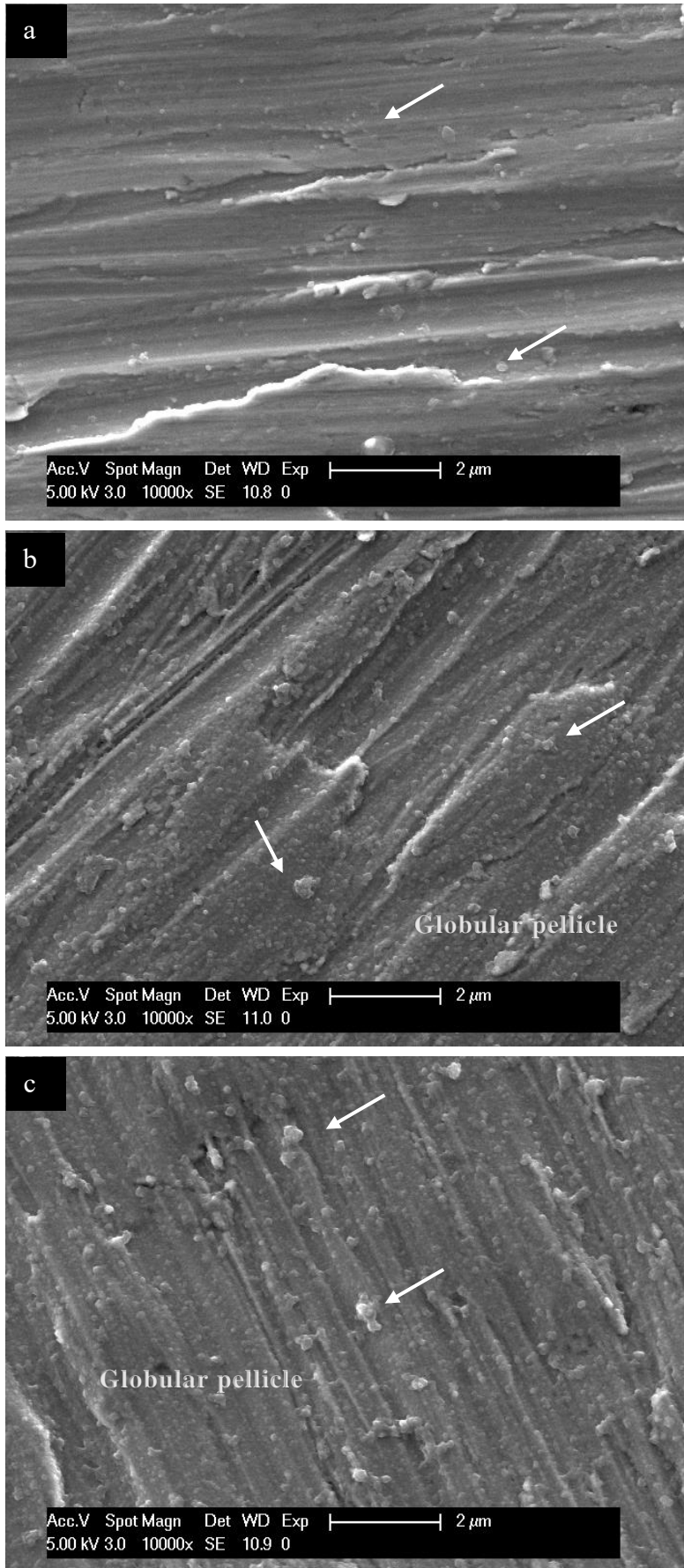
Figure 29 SEM micrographs at 10,000-fold magnifications of titanium samples after rinsing with water. Pellicle formation is visible at three different time-points: immediately (a), 30 min (b) and 2 h (c) after rinsing. The white arrows are pointing to the globular structures from the acquired pellicle.

Titanium – HAP I
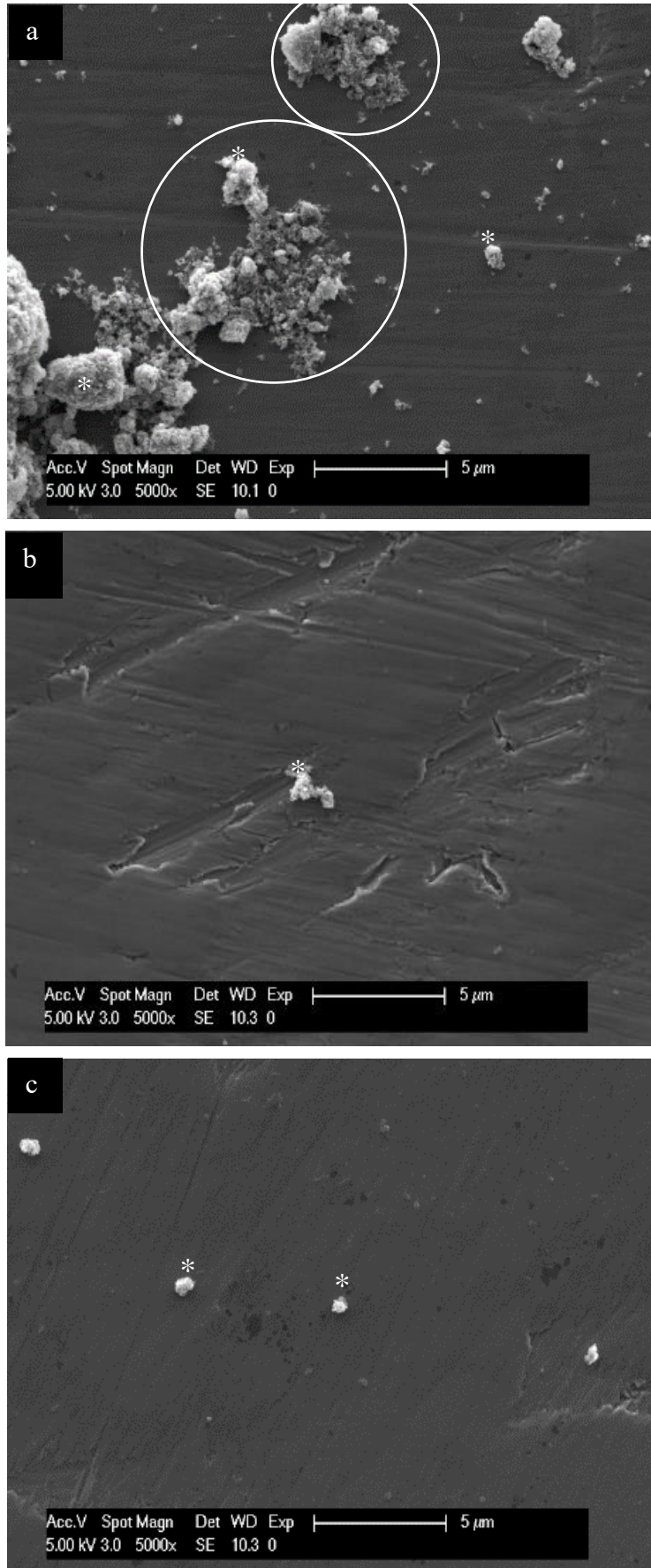
Figure 30 SEM micrographs at 5,000-fold magnifications of polished titanium samples after rinsing with HAP I according to protocol 1. Hydroxyapatite clusters (white asterisks) and agglomerates (white circles) are visible at three different time-points: immediately (a), 30 min (b) and 2 h (c) after rinsing. HAP I particles were present in low amount on titanium surfaces 2 h after rinsing. Figure 30 published in NOBRE et al., 2020.
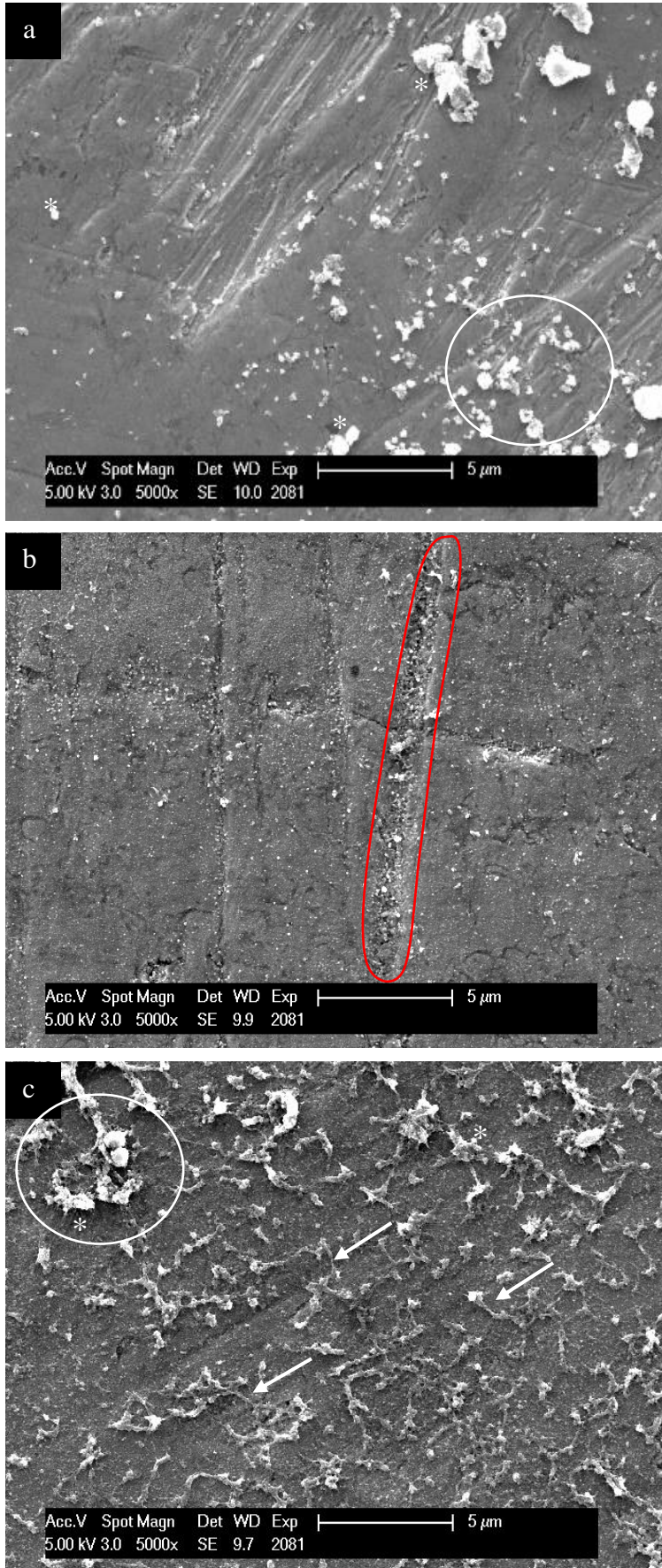
Titanium – HAP II

Figure 31 SEM micrographs at 5,000-fold magnifications of polished titanium samples after rinsing with HAP II. Hydroxyapatite clusters (white asterisks) and agglomerates (white circles) are visible at three different time-points: immediately (a), 30 min (b) and 2 h (c) after rinsing. (b) The retention area delimited by the red ellipse is an area where HAP particles tend to accumulate. (c) Bridge-like structures (white arrow) are visible connecting not only the HAP particles to each other, but also connecting the HAP particles to the proteins from the pellicle. Figure 31 published in NOBRE et al., 2020.

Titanium – HAP III
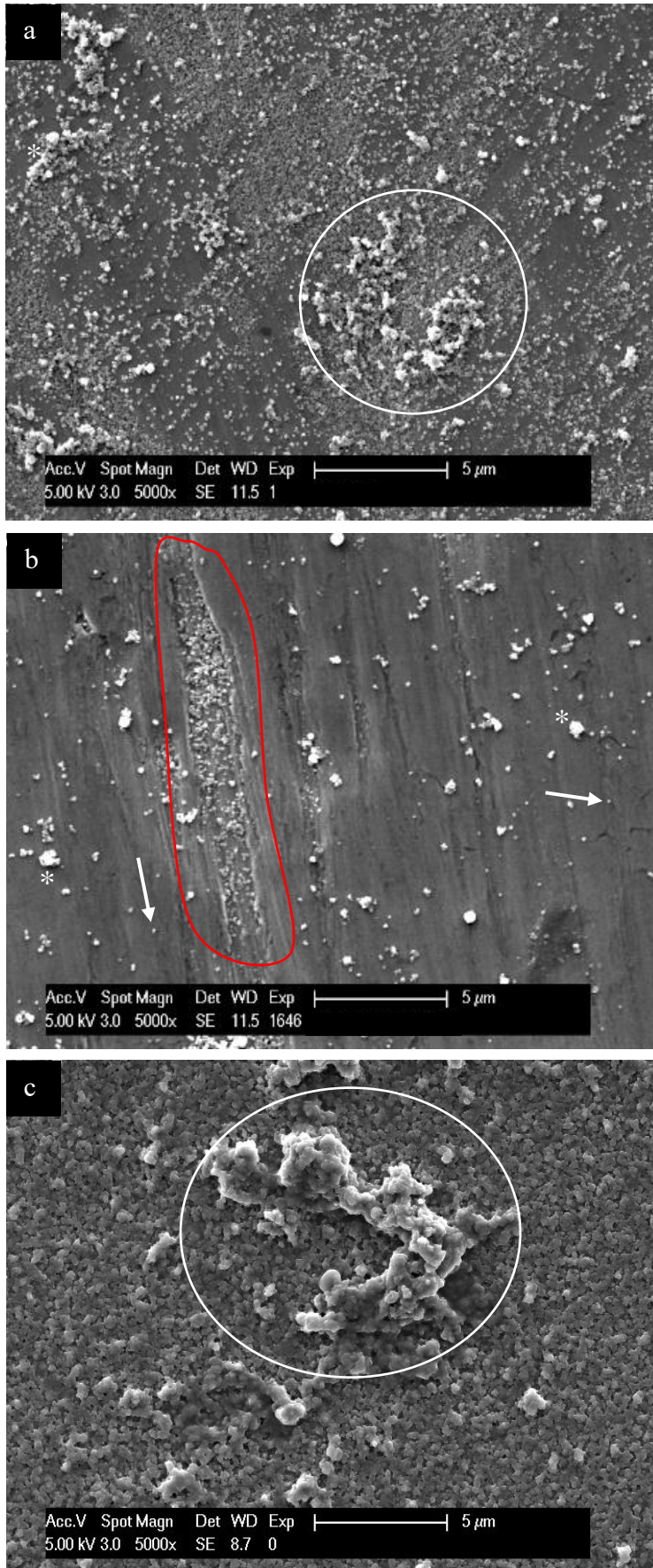
Figure 32 SEM micrographs at 5,000-fold magnifications of polished titanium samples after rinsing with HAP III. Hydroxyapatite single particles (white arrow), clusters (white asterisks) and agglomerates (white circles) are visible at three different time-points: immediately (a), 30 min (b) and 2 h (c) after rinsing. Micrograph "b" shows HAP III particles accumulated on retention areas (highlighted in red) from the titanium surface. The particles are over the globular 2 h-pellicle layer. Figure 32 published in NOBRE et al., 2020.

56

4.3.3 HAP particles adherence on pellicle-covered ceramic

Pellicle formation over 2h on the control samples, ceramic specimens rinsed with water, is shown in Figure 33. The Figure 34, 35 and 36 demonstrate the adherence of HAP particles after rinsing with the watery solutions of HAP I, II and III, respectively.

The progression of the pellicle formation on ceramic samples rinsed with water was similar to the findings on enamel and titanium surfaces. During this two-hour experiment, there was an increasing number of globular particles covering the smooth ceramic surface over time, until the formation of a homogeneous and multilayer proteinaceous coverage after 2 h (Figure 33).

The characteristics of the HAP particles distribution immediately after rinsing was not different for the ceramic samples as compared to enamel and titanium samples. The Figure 34a, 35a and 36a reinforces the propensity of the particles present in the HAP I, HAP II and HAP III solutions to aggregate and form clusters in different sizes and shapes.

Thirty minutes after rinsing, the number of adhered particles decreased. Clusters with more than 5 µm size were still present at this stage when HAP II or HAP III were applied. While the hydroxyapatite particles from HAP II were more disperse, the particles from HAP I and HAP III formed a more homogeneous coverage on their respective ceramic surfaces (Figure 34b, Figure 35b, Figure 36b).

Finally, 2 h after rinsing, in most of the cases, even smaller particles were visible on those surfaces, and clusters were still visible (Figure 34c, Figure 35c, Figure 36c). The amount and the size of the hydroxyapatite clusters on each material surface decreased over time, except for HAP II (Figure 35c). The SEM results showed that ceramic samples had a lower HAP deposition after 2 h when compared to the other materials. Figure 36c shows that, after 2 h, particles from HAP III were mostly accumulated on surface irregularities caused by the polishing process.

Ceramic – Control
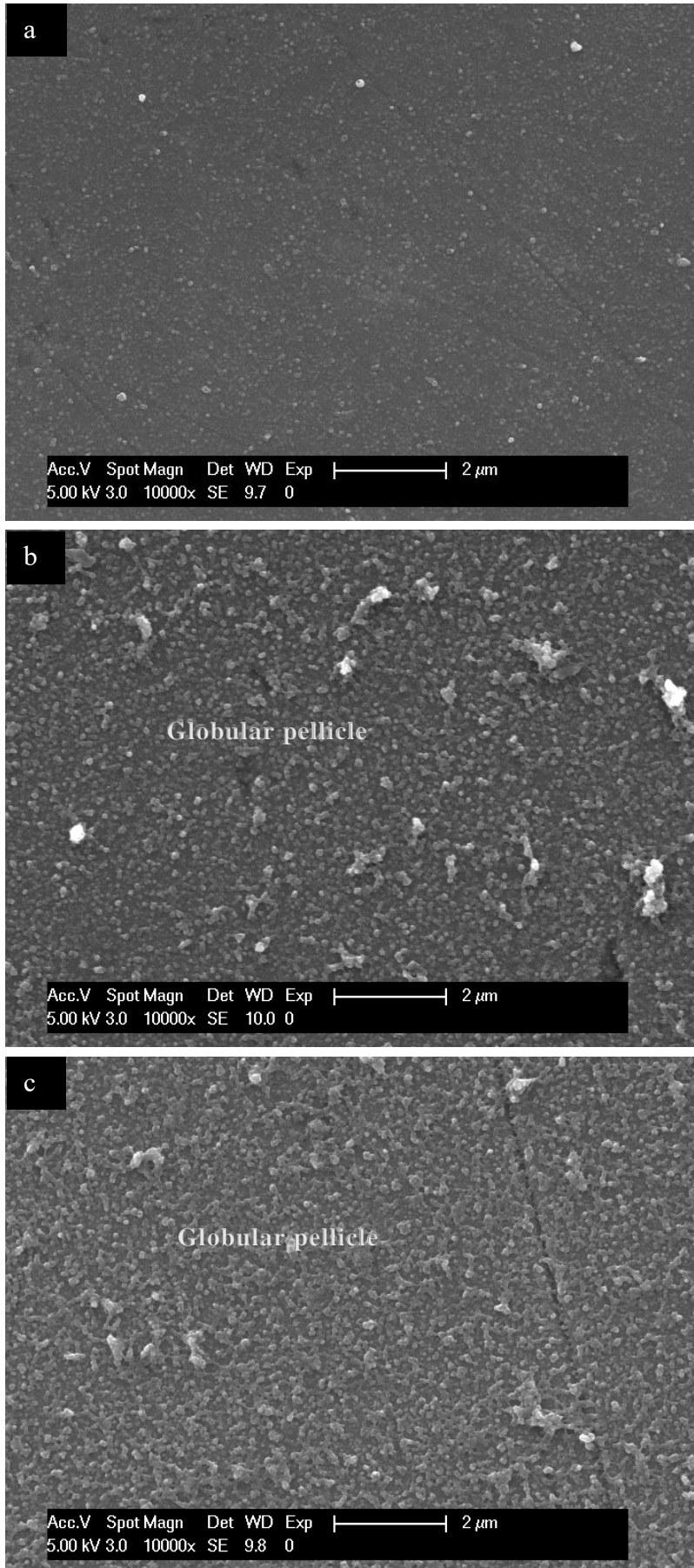
Figure 33 SEM micrographs at 10,000-fold magnifications of ceramic samples after rinsing with water. Pellicle structures are visible at three different time-points: immediately (a), 30 min (b) and 2 h (c) after rinsing. The progression of the pellicle formation is visible, and it is characterized by an increasing number of globular structures over time.

Ceramic - HAP I
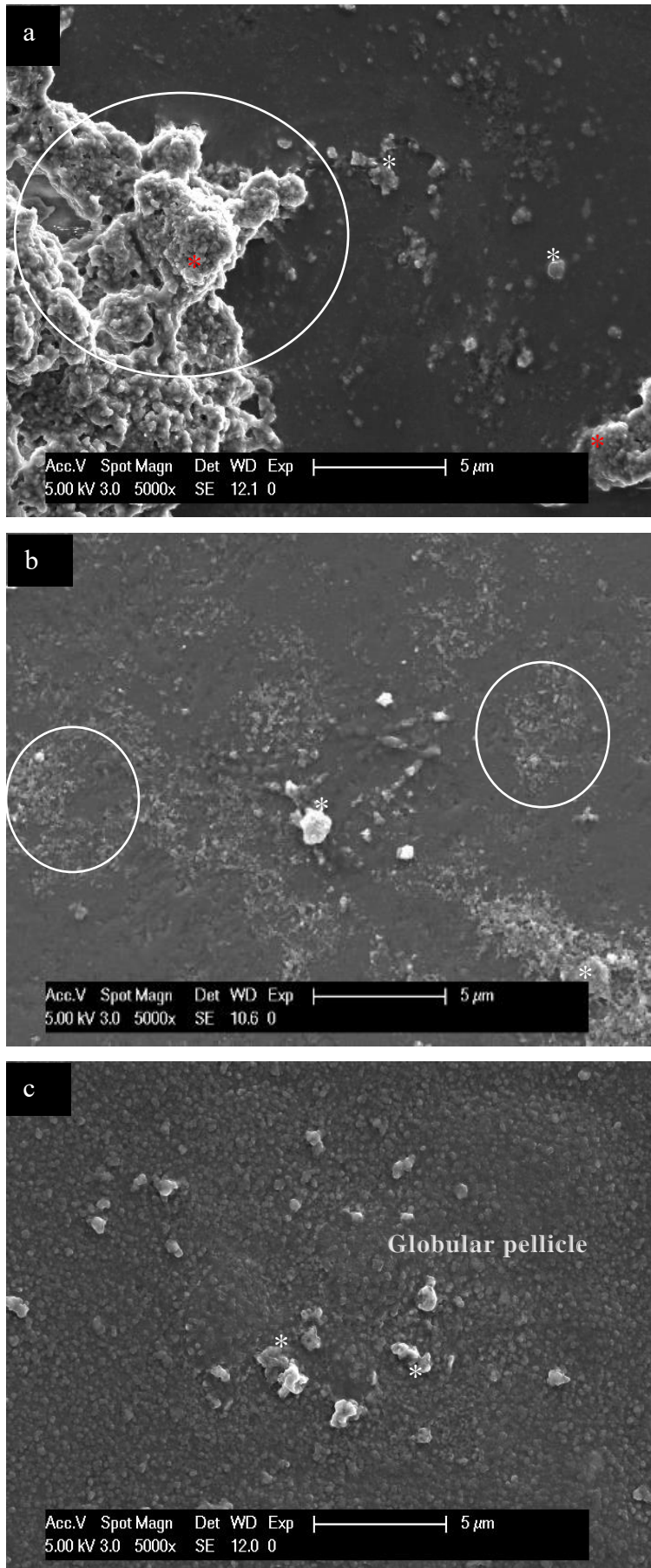
Figure 34 SEM micrographs at 5,000-fold magnifications of ceramic samples after rinsing with HAP I. Hydroxyapatite clusters (red and white asterisks) and agglomerates (white circles) are visible at three different time-points: immediately (a), 30 min (b) and 2 h (c) after rinsing. (a) Clusters bigger than 5 μm (red asterisk) are visible immediately after rinsing with HAP I on the ceramic surface. (b) After 30 min of rinsing, there were HAP particles aggregates (white circles) covering the ceramic surface. The particles are over the globular 2 h-pellicle layer. Figure 34 published in NOBRE et al., 2020.
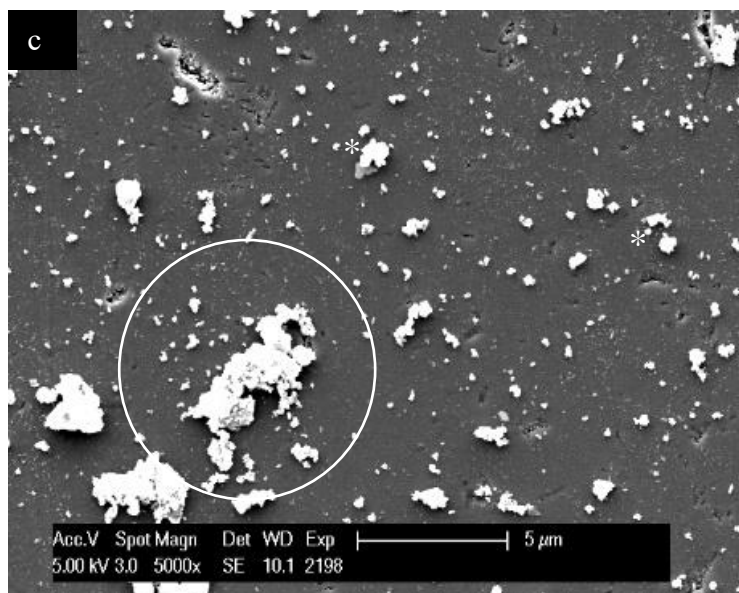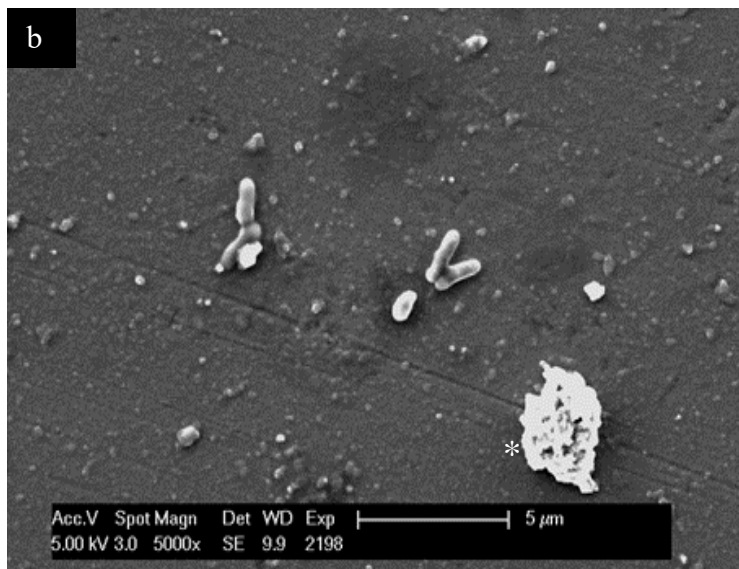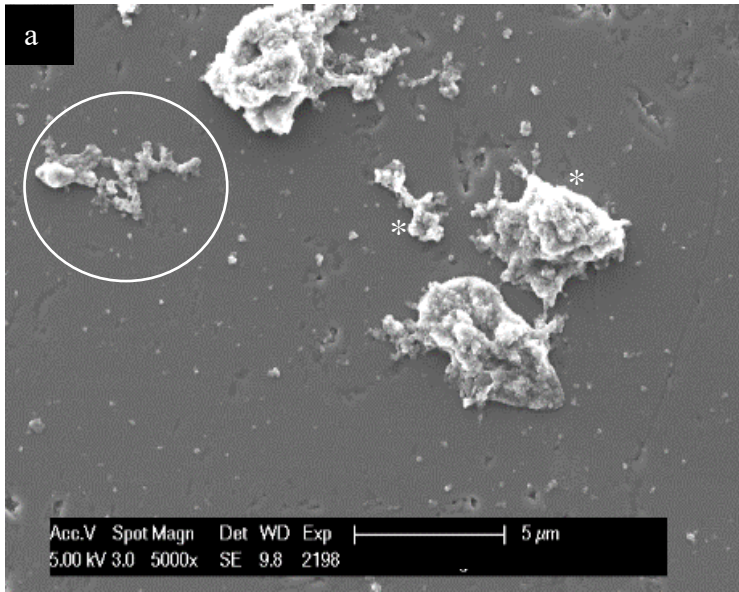
Ceramic - HAP II

Figure 35 SEM micrographs at 5,000-fold magnifications of ceramic samples after rinsing with HAP II. Hydroxyapatite, clusters (white asterisks) and agglomerates (white circles) are visible at three different time-points: immediately (a), 30 min (b) and 2 h (c) after rinsing. The presence of clusters was a common finding on ceramic surfaces after rinsing with HAP II. Figure 35 published in NOBRE et al., 2020.

Ceramic - HAP III
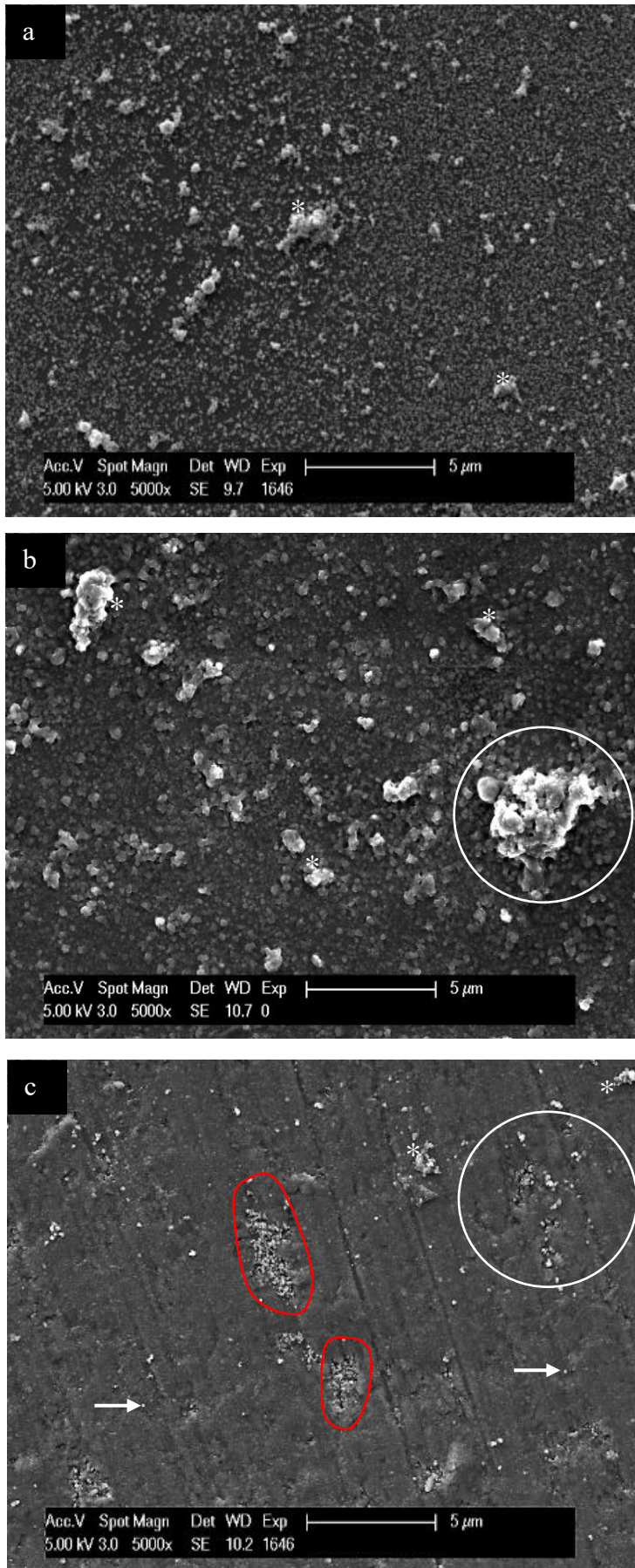
Figure 36 SEM micrographs at 5,000-fold magnifications of ceramic samples after rinsing with HAP III. Hydroxyapatite single particles (white arrow), clusters (white asterisks) and agglomerates (white circles) are visible at three different time-points: immediately (a), 30 min (b) and 2 h (c) after rinsing. Highlighted in red on micrograph "c", the hydroxyapatite particles were also accumulated on the irregularities of the ceramic surface. Adherent HAP particles decrease with increasing intraoral exposure time. Figure 36 published in NOBRE et al., 2020.

4.3.4 HAP particles adherence on pellicle-covered PMMA

Pellicle formation over 2h on the control samples, PMMA specimens rinsed with water, is shown in Figure 37. The Figure 38, 39 and 40 demonstrate the adherence of HAP particles after rinsing with the watery solutions of HAP I, II and III, respectively.

Despite the characteristic surface texture of PMMA with integrated round-shaped prepolymerized particles, it is clear that the pattern of the acquired pellicle formation was also repeated for this material and similar to the three previous materials: enamel, titanium and ceramics. The amount of globular structures on PMMA surface gradually increased after three minutes of intraoral exposure followed by a water rinse over 2 hours (Figure 37).

Immediately after the mouthwash with the 5% HAP solutions, the nanoparticles were randomly distributed covering more than 40% of the PMMA surfaces (Figure 38a, Figure 39a, Figure 40a). In PMMA samples rinsed with HAP I the presence of clusters was higher than in samples rinsed with HAP II or HAP III (Figure 38-40).

Thirty minutes after rinsing, the number of adhered particles decreased, but was still higher than on the other tested materials (Figure 38b, Figure 39b, Figure 40b). Two hours after rinsing, single as wells as clustered hydroxyapatite particles could be detected on the PMMA surfaces (Figure 38c, Figure 39c, Figure 40c). The surface rinsed with HAP III solution had the less homogeneous coverage (Figure 40c).

Compared to the other materials, higher amounts of hydroxyapatite particles were found on PMMA samples after the same time of intraoral exposure.

PMMA - Control

a

Acc.V Spot Magn   Det WD Exp ├─────────┤   2 μm
5.00 kV 3.0 10000x SE   11.0 0

b

Acc.V Spot Magn   Det WD Exp ├─────────┤   2 μm
5.00 kV 3.0 10000x SE   10.6 0

c

Globular pellicle

Acc.V Spot Magn   Det WD Exp ├─────────┤   2 μm
5.00 kV 3.0 10000x SE   10.7 0
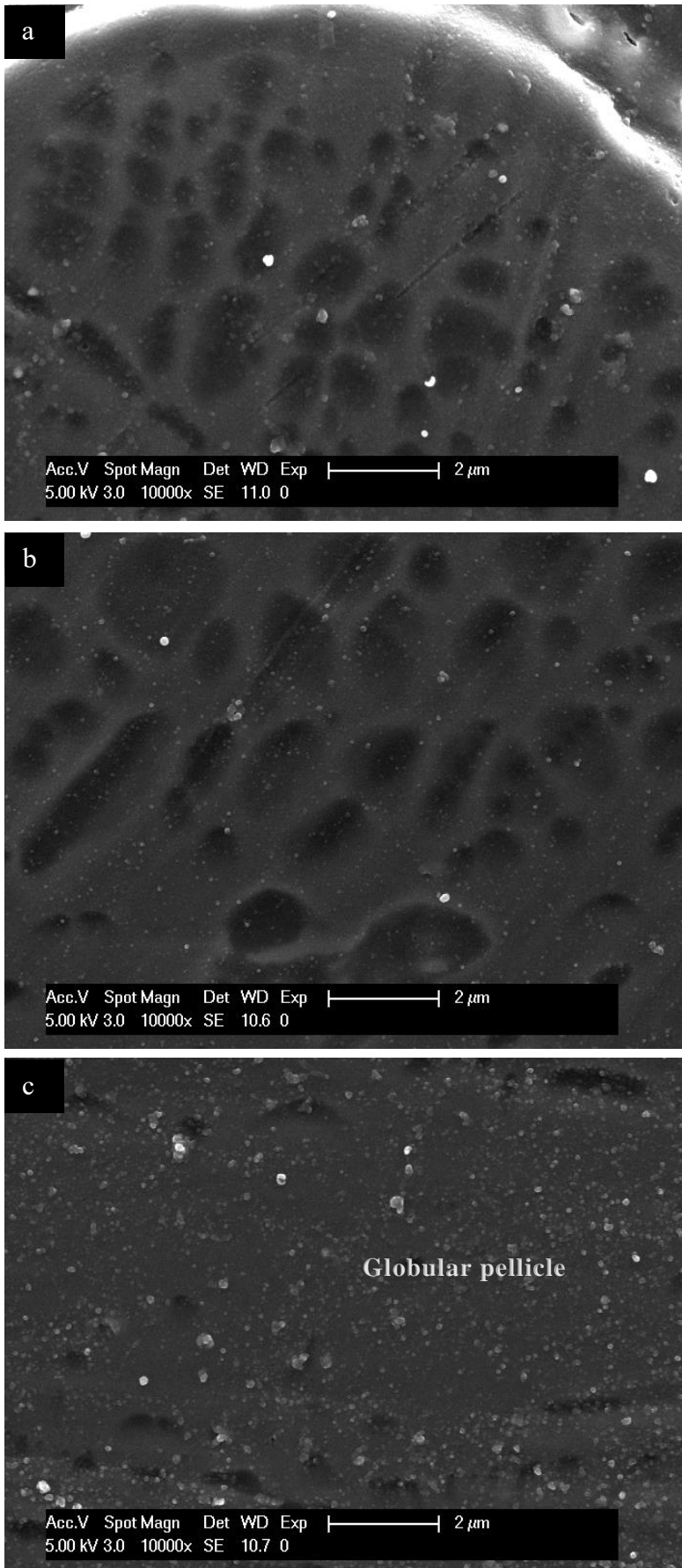
Figure 37 SEM micrographs at 10,000-fold magnifications of PMMA samples after rinsing with water. Pellicle formation is visible at the three different time-points: immediately (a), 30 min (b) and 2 h (c) after rinsing. The progression of the pellicle formation is visible, and it is followed by the increasing number of globular structures over time.

PMMA - HAP I
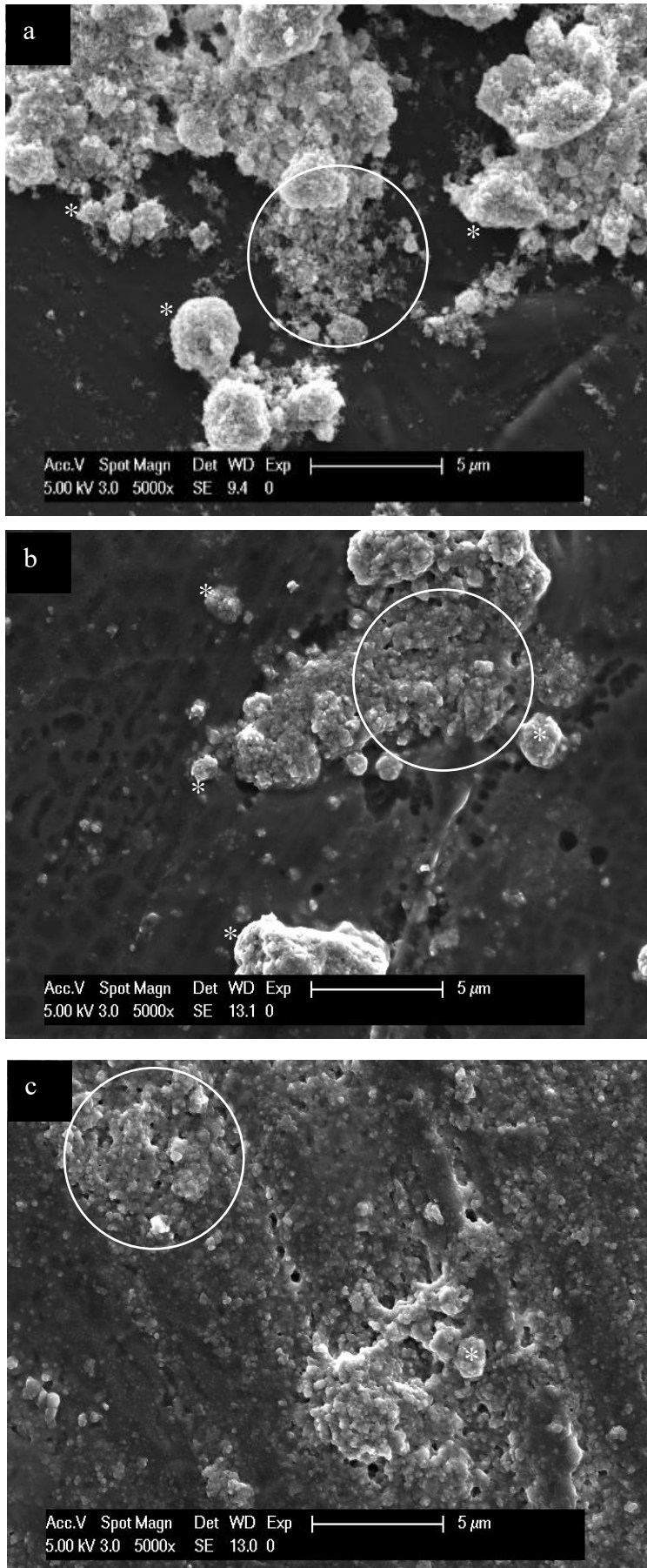
Figure 38 SEM micrographs at 5,000-fold magnifications of PMMA samples after rinsing with HAP I. Hydroxyapatite clusters (white asterisks) and agglomerates (white circles) are visible at three different time-points: immediately (a), 30 min (b) and 2 h (c) after rinsing. Clusters with various sizes and shapes were present at all time points on PMMA surfaces rinsed with HAP I solution. Figure 38 published in NOBRE et al., 2020.

PMMA - HAP II
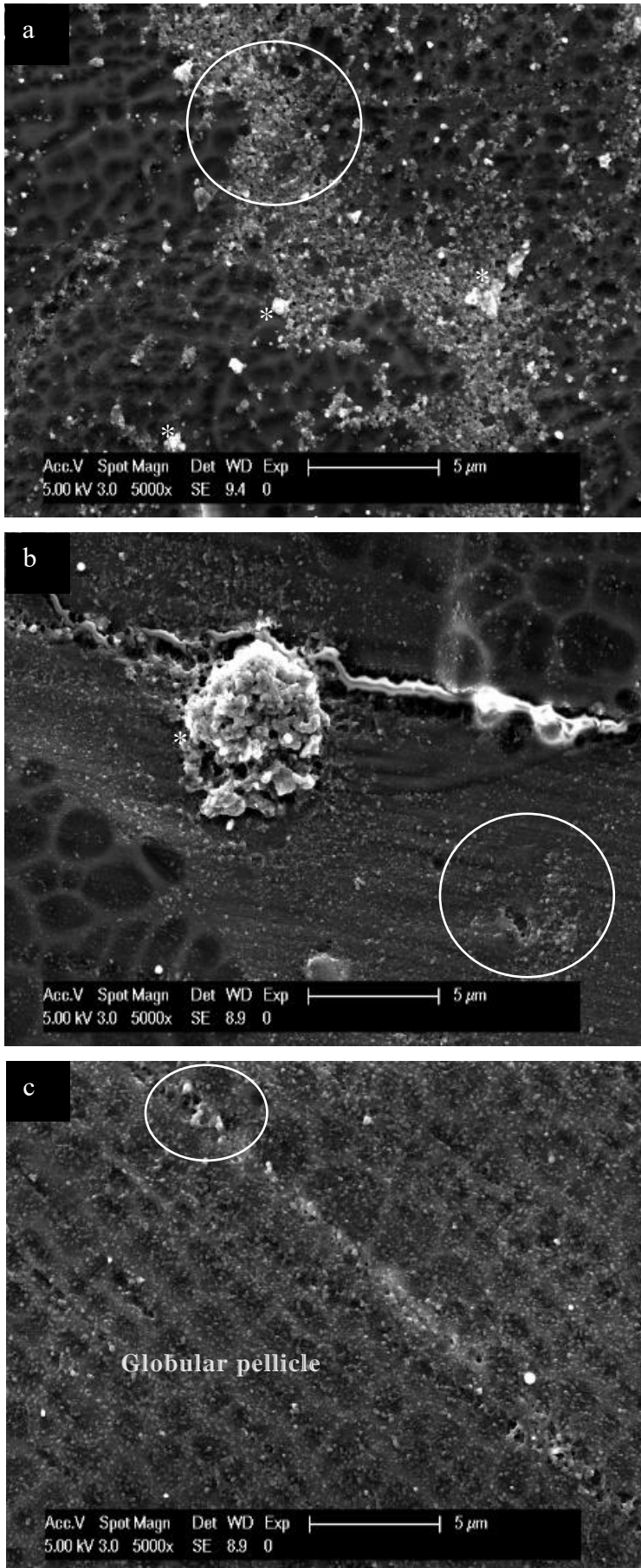
Figure 39 SEM micrographs at 5,000-fold magnifications of PMMA samples after rinsing with HAP II. Hydroxyapatite clusters (white asterisks) and agglomerates (white circles) are visible at three different time-points: immediately (a), 30 min (b) and 2 h (c) after rinsing. Figure 39 published in NOBRE et al., 2020.

PMMA - HAP III

Acc.V Spot Magn Det WD Exp ⊢————————⊣ 5 μm
5.00 kV 3.0 5000x SE 11.6 0

Globular pellicle

Acc.V Spot Magn Det WD Exp ⊢————————⊣ 5 μm
5.00 kV 3.0 5000x SE 11.4 0

Acc.V Spot Magn Det WD Exp ⊢————————⊣ 5 μm
5.00 kV 3.0 5000x SE 9.1 0
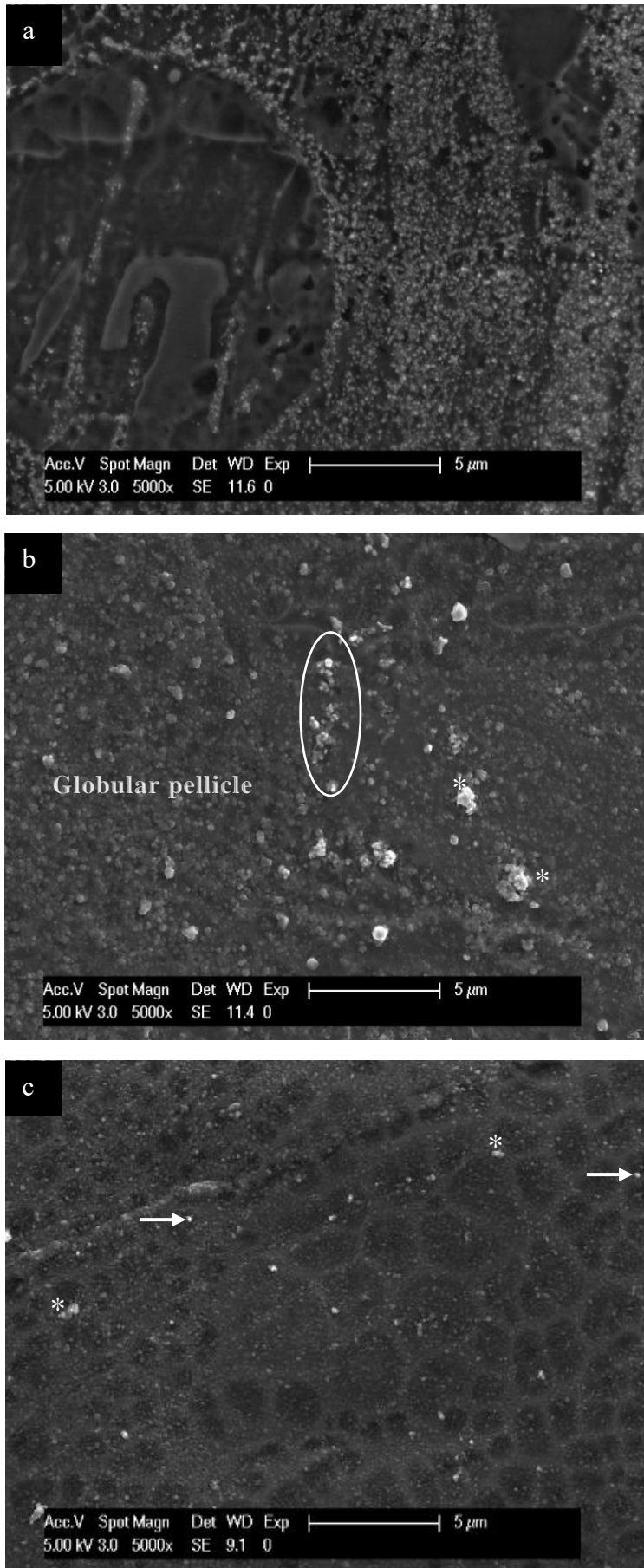
Figure 40 SEM micrographs at 5,000-fold magnifications of PMMA samples after rinsing with HAP III. Hydroxyapatite single particles (white arrows), clusters (white asterisks) and agglomerates (white circles) are visible at three different time-points: immediately (a), 30 min (b) and 2 h (c) after rinsing. Figure 40 published in NOBRE et al., 2020.

4.3.5 Additional observations considering the adherence of HAP particles to the pellicle-covered surfaces

Results obtained after performing the experiments according to protocol 1 indicate that scattered single hydroxyapatite particles from the three HAP solutions were visible on all materials surface two hours after rinsing with to the respective solutions. Higher SEM magnification was used to visualize the possible interactions between the accumulated nano-HAP and the pellicle that covered each substrate surface. Interestingly, when the hydroxyapatite containing solutions were applied, it was possible to observe connective structures between these particles and the pellicle formed on enamel, titanium and PMMA surfaces after 2 h of rinsing with the respective solutions (Figure 41). On ceramics, these connective structures could not be detected.

Furthermore, in the experiments according to protocol 2, it was found that particles from all hydroxyapatite solutions tested were present on all samples even 12 h after the last 30s rinsing (Figure 42 and Figure 43). It was possible to detect HAP particles on the pellicle-covered surface of each material after the two-times rinsing with the HAP solution during the 24 h oral exposure. Furthermore, these figures show that hydroxyapatite nanoparticles may adhere not only to the pellicle surface, but also to the bacterial surface.

Finally, Figure 44, from protocol 3, shows that hydroxyapatite particles and aggregates (HAP II) could be detected randomly on the Ti surface after 48 h of intraoral exposure, when rinsing each 12 h with the HAP II test solution. EDX analysis endorsed the SEM results, confirming the presence of HAP through elements quantification (Figure 44).
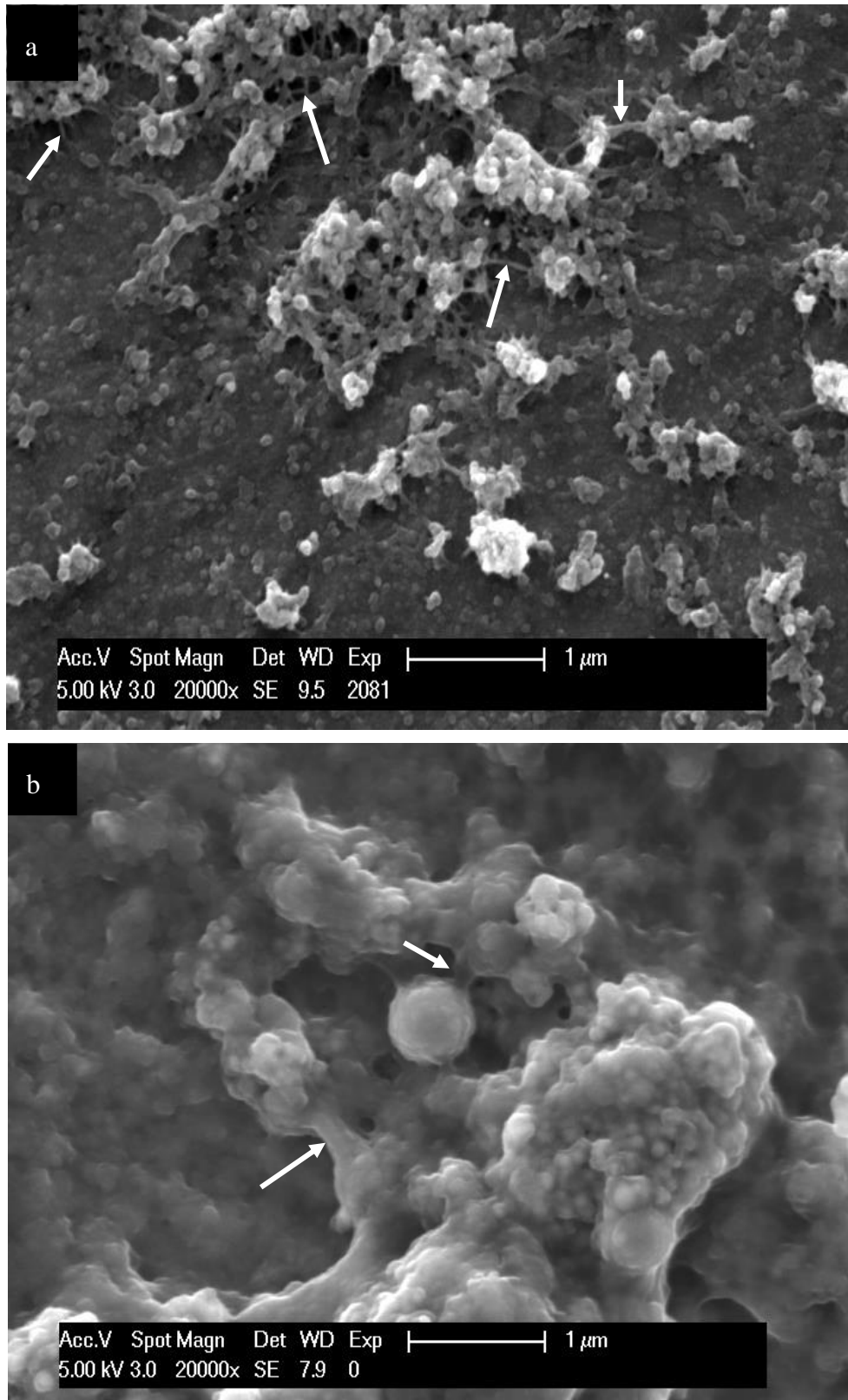
Figure 41 SEM micrograph at 20,000-fold magnification showing connective structures between HAP II particles and the pellicle-covered titanium surface (a) and HAP III and the pellicle-covered enamel surface (b) 2 h after oral exposure to these HAP solutions. The HAP particles are in direct contact with globular structures from the acquired pellicle, showing a high affinity to the salivary proteins. Arrows point to connective bridges between the HAP particles and between the HAP particles and the pellicle. Figure 41 published in NOBRE et al., 2020.
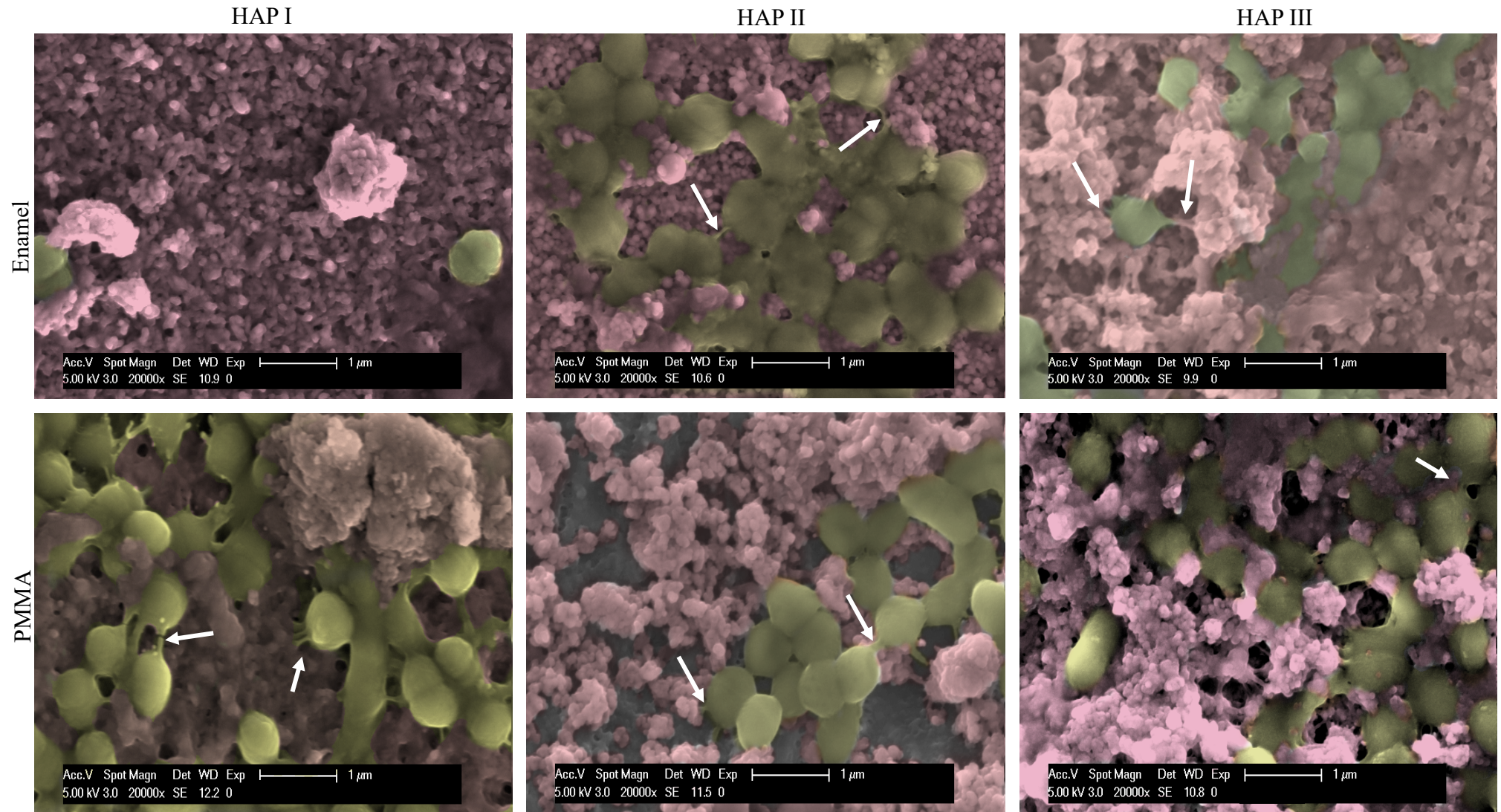
Figure 42 SEM images at 20,000-fold magnifications from enamel and PMMA samples after 24 h of intraoral exposure and two times rinsing with HAP I, HAP II and HAP III. The pink color on those micrographs show the hydroxyapatite particles, which were accumulated not only on enamel and PMMA surfaces but were also detected on top of the bacteria. The yellow color represents the adhered bacteria community, composed mostly by coccoid specimens. Also, in yellow, there are bridge-like structures (white arrows) connecting the bacteria to other bacteria or to the HAP particles. The greyish zone may represent a thicker 24-h pellicle on the PMMA surface.
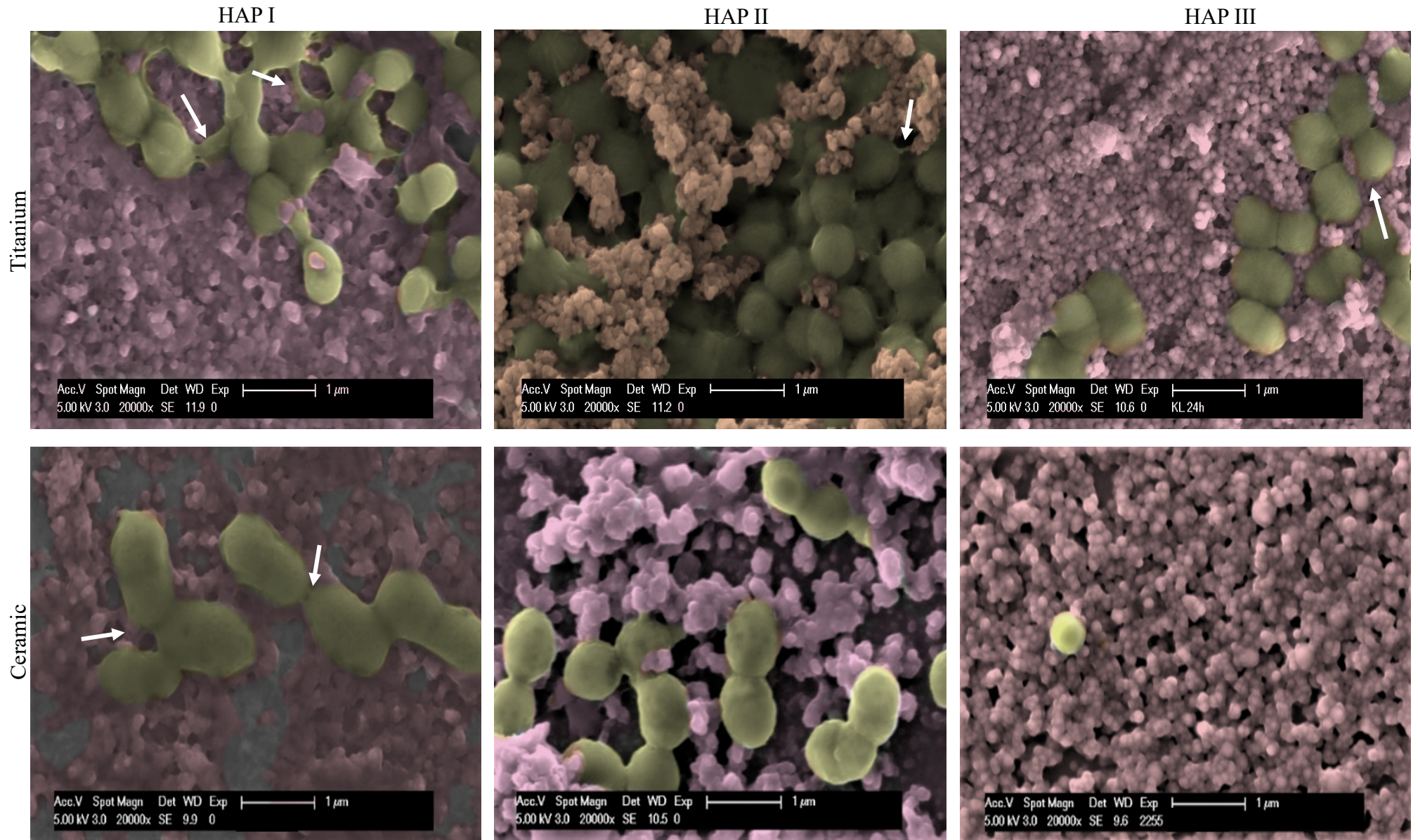
Figure 43 SEM micrographs at 20,000-fold magnifications from titanium and ceramic samples after 24 h of intraoral exposure and two times rinsing with HAP I, HAP II and HAP III. The pink color represents the hydroxyapatite particles, which were accumulated on titanium and ceramic surfaces. Single bacteria and bacterial colonies were detected (highlighted in yellow). As on enamel and PMMA samples, there are bridge-like structures (white arrows) connecting the bacteria to other bacteria or to the HAP particles
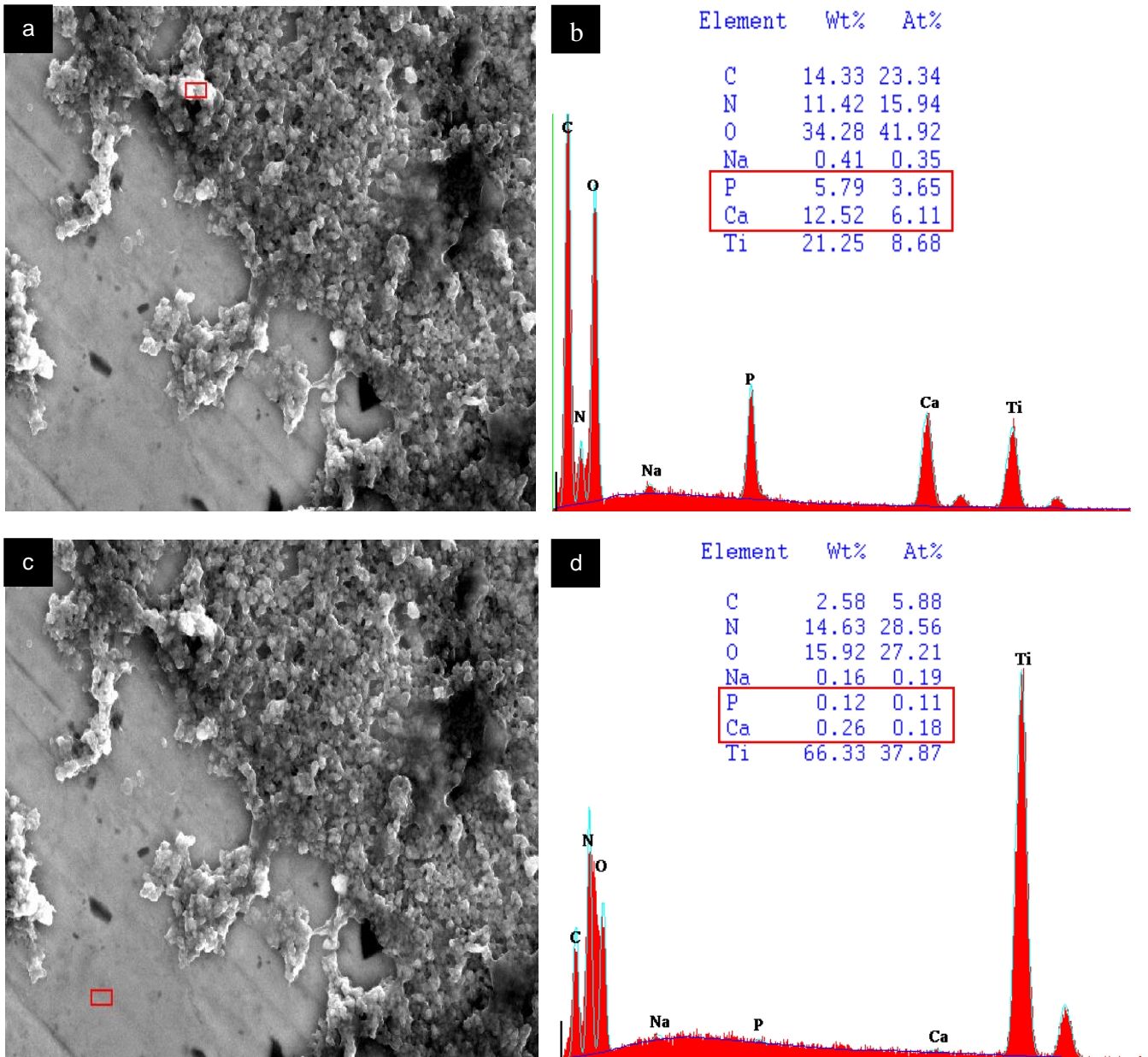
Figure 44 SEM images at 10,000-fold magnifications allowed the visualization of hydroxyapatite particles (HAP II) which accumulated the titanium surfaces. The element analysis took place within the red window on micrographs "a" and "c". Higher values of P and Ca detected by the EDX analysis (b) confirmed the presence of hydroxyapatite. Low percentages of P and Ca, as well as the high Ti percentage (d), corroborated to this result as a negative control, showing the presence of only titanium in the demarcated area (c).

71

4.4   HAP solutions effects on the 24-h biofilm

4.4.1 BacLight assay: biofilm coverage and viability

After 24 h of intraoral exposure, biofilms were present on all samples (Figure 45-48). Fluorescence microscopic investigations of the 24-h biofilm allowed bacterial coverage visualization and differentiation between live (green) and dead (red) bacteria cells. The black background area on the following FM micrographs represents the respective material surfaces, which are not stained.

Regarding the biofilm coverage analysis, samples rinsed with water presented a significant denser biofilm than samples rinsed with any other solutions tested ($p < 0.0001$) (Figure 49). A nearly homogeneous coverage with mostly green cells was present on enamel, ceramic and PMMA samples rinsed with water (Figure 45, Figure 47, Figure 48). On titanium, the bacterial cells covered more than 50% of the surface (Figure 46). On the contrary, a significantly lower number of bacteria was detected when CHX rinse was applied compared with the negative control ($p = 0.0099$) (Figure 49). Most samples treated with the HAP solutions showed lower biofilm coverage, without a significant difference from the CHX rinsed samples, except for titanium and ceramic samples rinsed with HAP III (Figure 49). The differences considering biofilm formation on the different the materials applied in this study after rinsing with the HAP solutions were subtle. Enamel, titanium and ceramics specimens presented a lower quantity of bacteria than PMMA for all HAP solutions (Figure 49).

Regarding the biofilm viability results, the samples rinsed with any of the HAP solutions had a higher number of live bacteria, represented by the green shapes on Figures 45 to 48. The living cells were mostly detected within small islands surrounded by dead single cells or small aggregates of dead cells (Figure 45-48). Such result revealed significant differences when compared with the samples rinsed with CHX ($p < 0.0001$), where most bacteria were dead (red) (Figure 50). However, no significant difference was found between the samples rinsed with the HAP solutions and the samples rinsed with water. Thus, both solutions presented a majority of living cells, stained in green (Figure 45-48, Figure 50).

Additionally, independent of the solution used as mouthrinse, there was no significant difference in bacteria viability between the applied materials, when the same rinsing solution was used (Figure 50).

Enamel
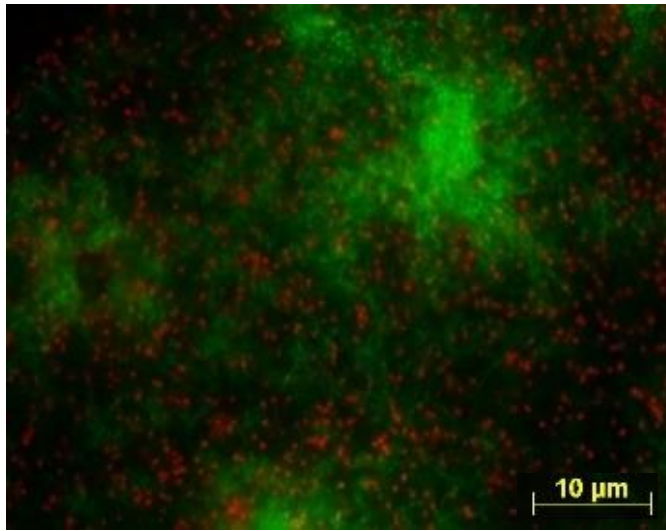
HAP I
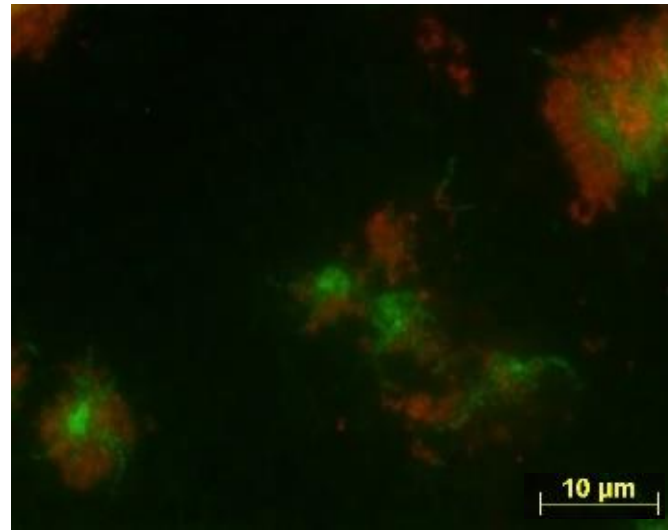
HAP II
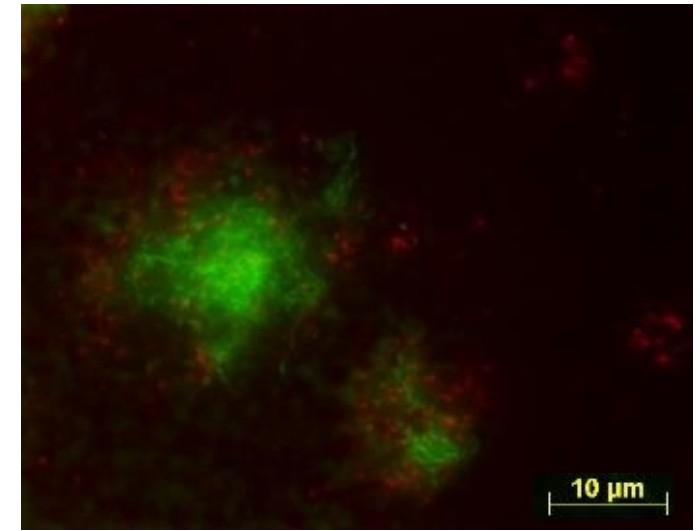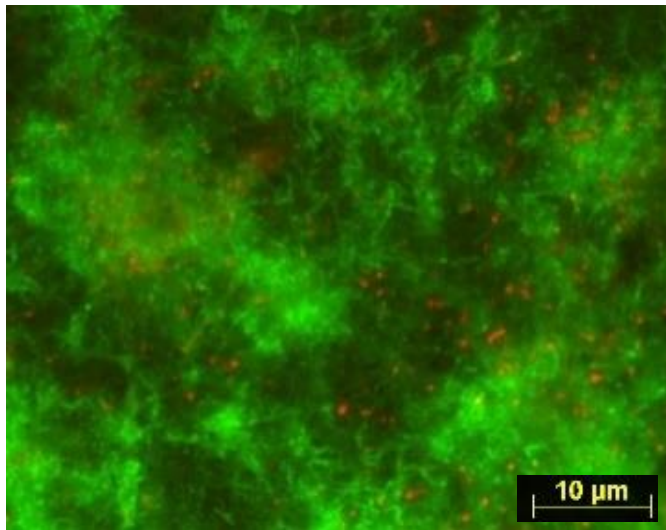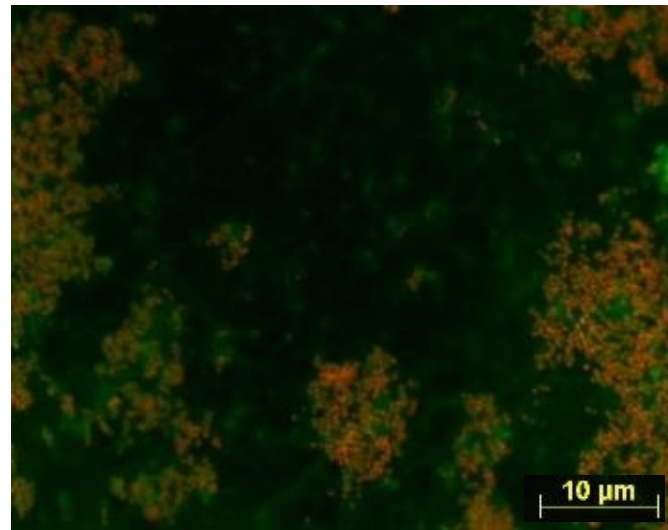
HAP III

Water

CHX

Figure 45 Fluorescence microscopic investigation of Live/Dead stained 24-h biofilm on enamel slabs after two times rinsing with HAP I, HAP II, HAP III, CHX and water. Water control was densely covered with live cells and a few single dead cells. The specimens rinsed with CHX presented mostly dead bacteria, but also some green colonies were visible. HAP samples presented a similar pattern, with mainly living bacteria, but surrounded by single dead cells or small colonies of dead cells. They had a lower biofilm coverage than the sample rinsed with water.
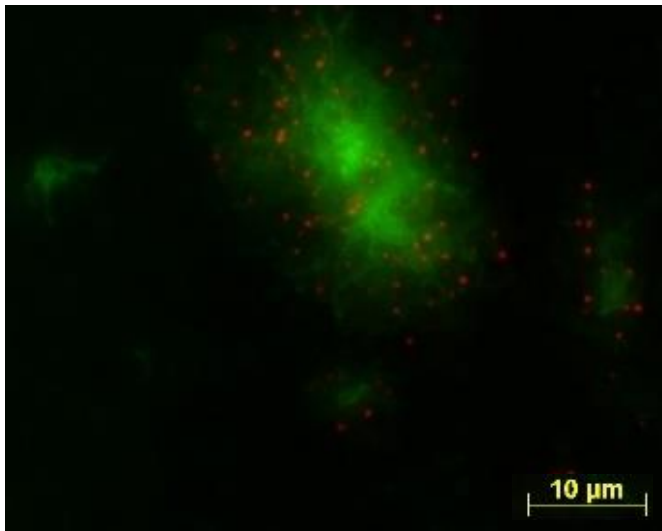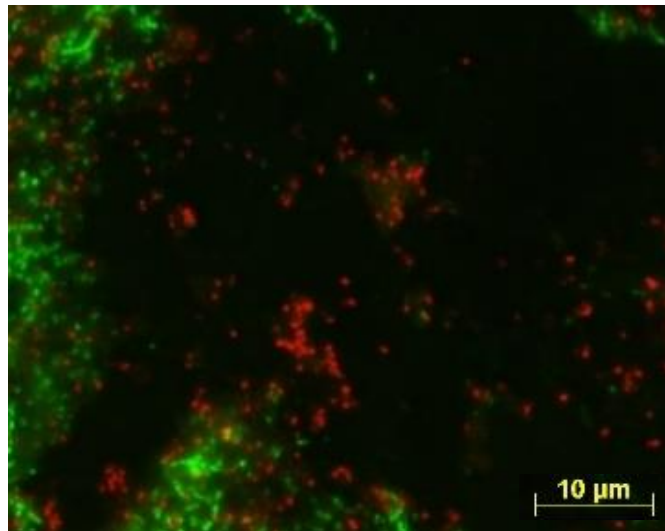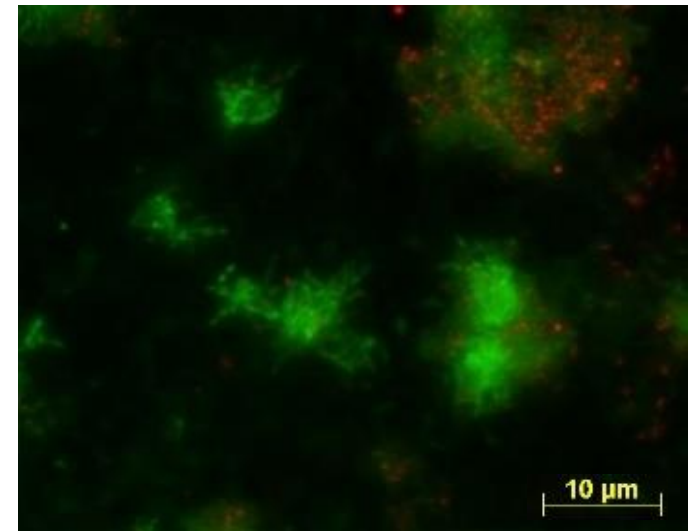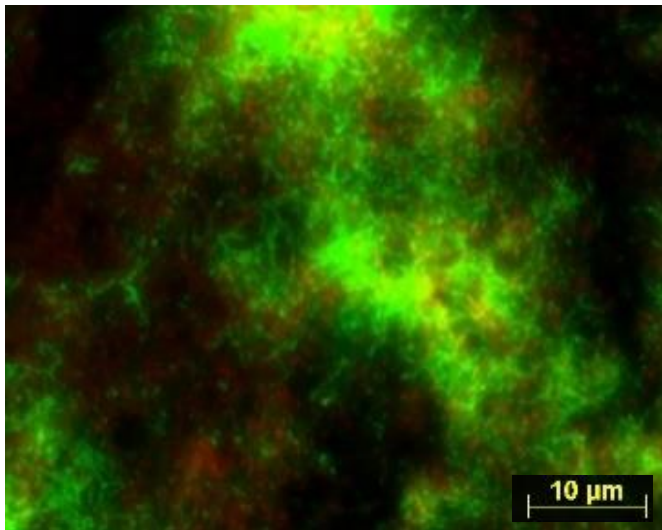
HAP I
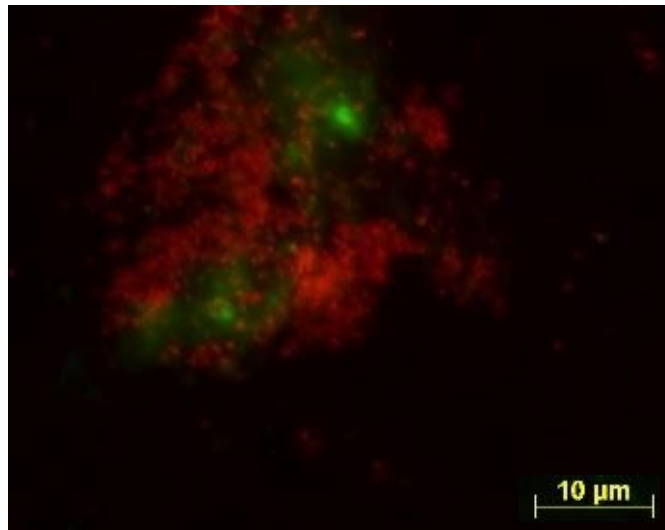
HAP II

HAP III

Water

CHX

Figure 46 Fluorescence microscopic investigation of Live/Dead stained 24-h biofilm on titanium after two times rinsing with HAP I, HAP II, HAP III, CHX and water. The quantity of bacteria on titanium samples was lower than on enamel and on PMMA samples.

Ceramic
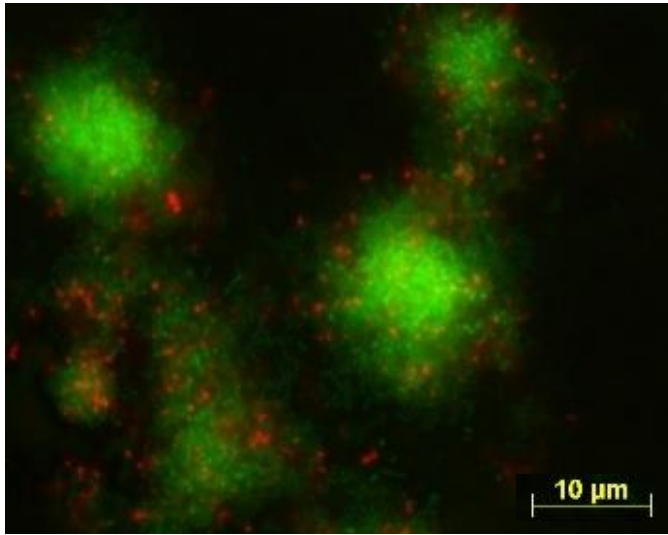
HAP I
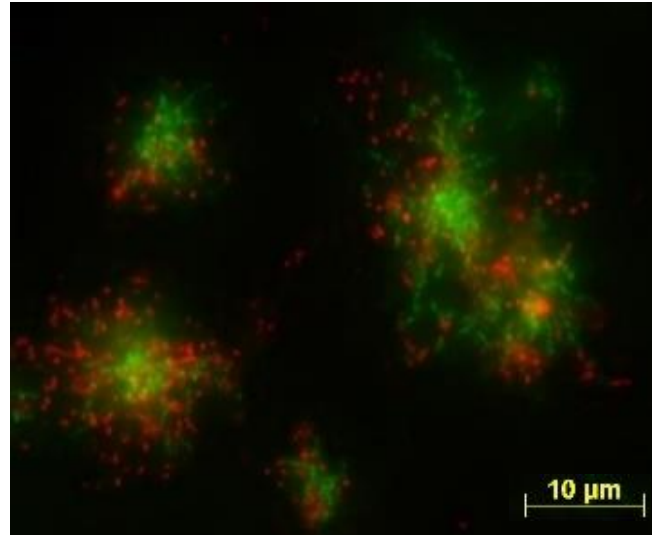
HAP II
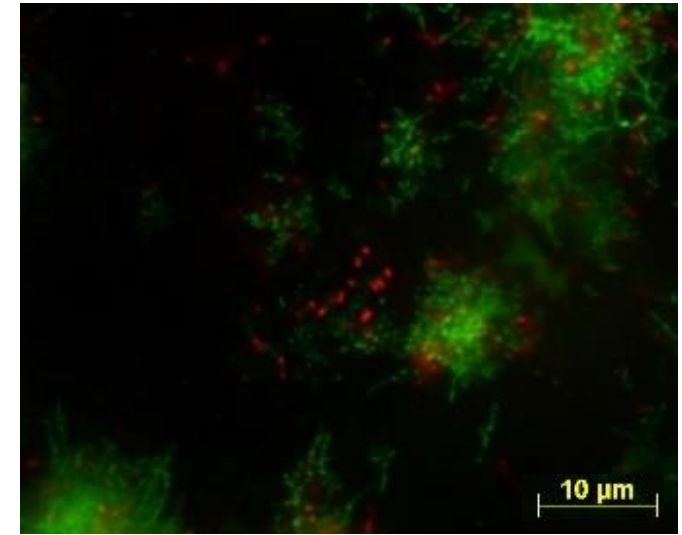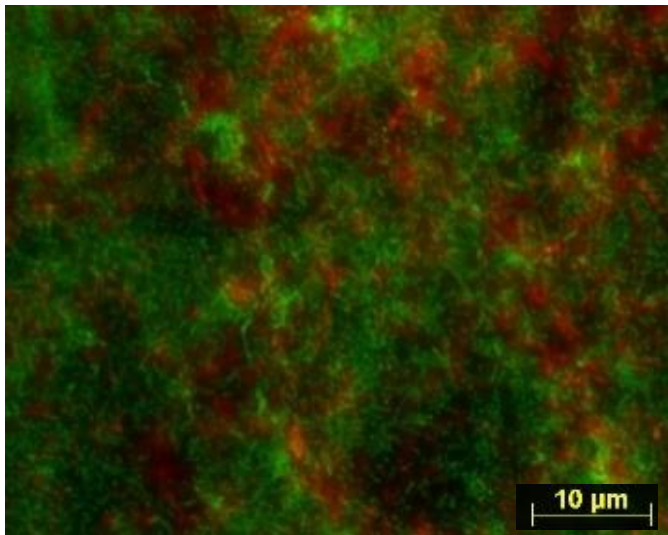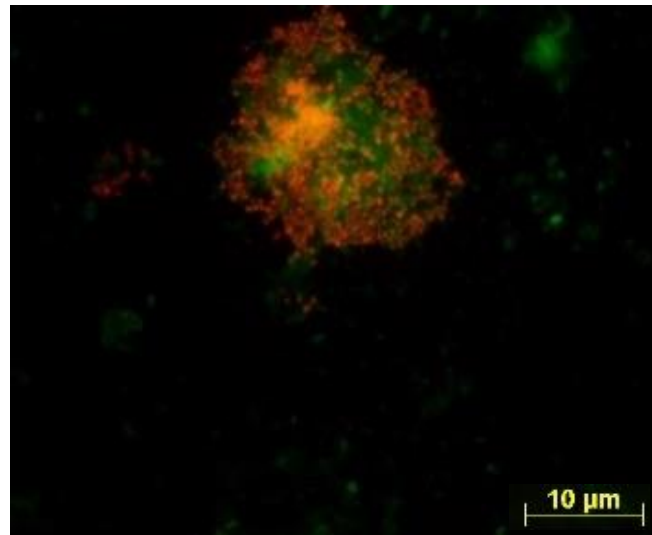
HAP III

Water

CHX

Figure 47 Fluorescence microscopic investigation of Live/Dead stained 24-h biofilm on ceramic after two times rinsing with HAP I, HAP II, HAP III, CHX and water. As on titanium samples, lower numbers of bacteria were found on ceramic slabs, when compared to enamel and PMMA. Green islands of bacteria surrounded by red single cells were detected on samples rinsed with the HAP solutions.
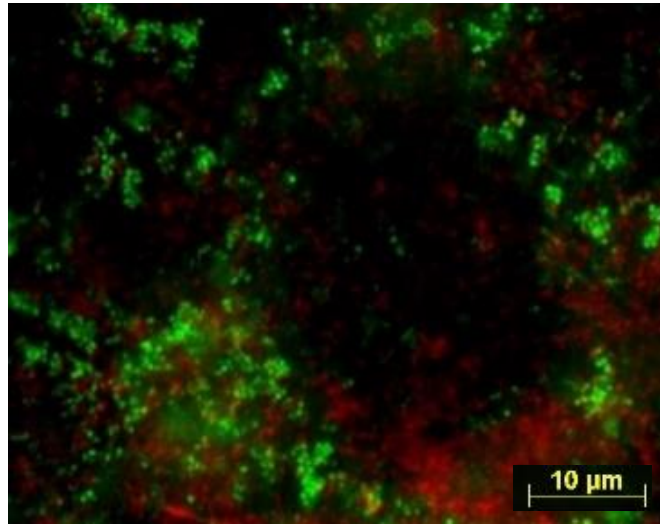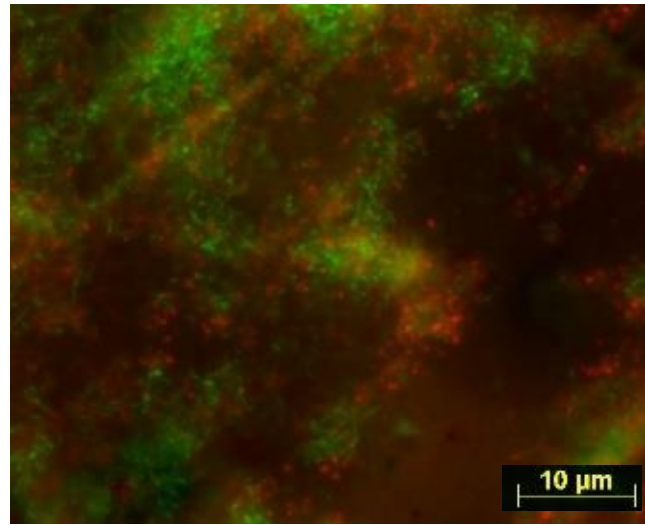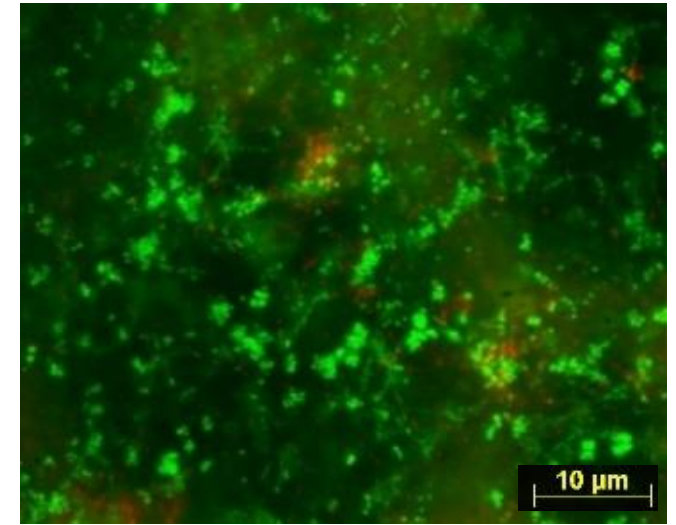
PMMA
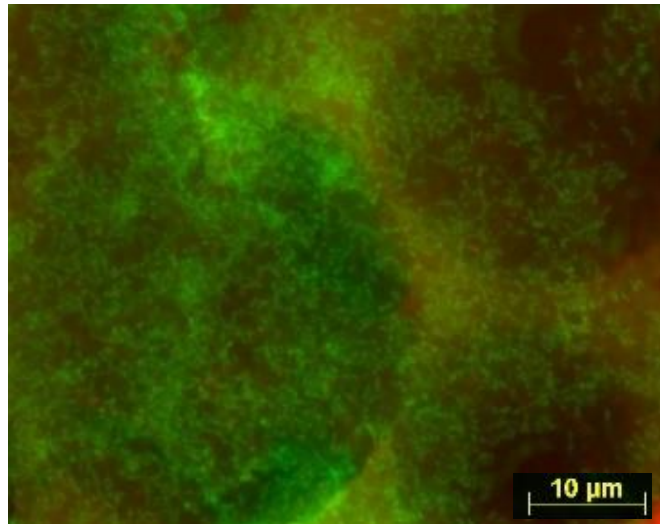
HAP I
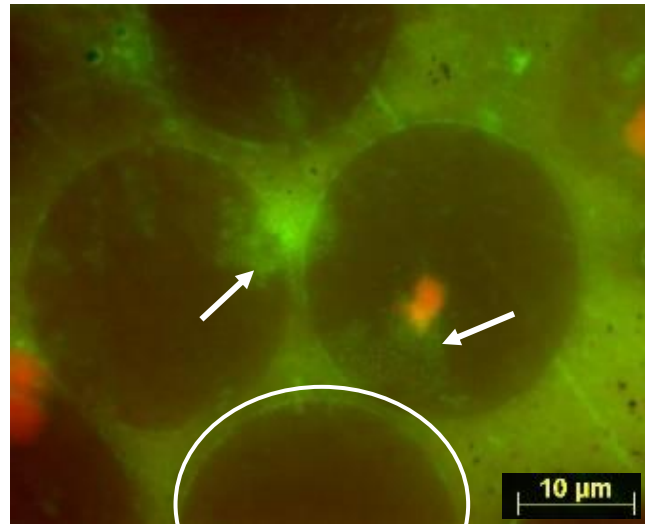
HAP II

HAP III

Water

CHX

Figure 48 Fluorescence microscopic investigation of the Live/Dead stained 24-h biofilm on PMMA after two times rinsing with HAP I, HAP II, HAP III, CHX and water. These samples presented slightly more bacteria than all the other materials. Colonies of living bacteria are also visible when chlorhexidine was applied (white arrows). The superficial layer of the PMMA surface was usually stained in red or in green, which is visible on micrographs from HAP II and CHX. The white circle delimitates the prepolymerized PMMA particles.
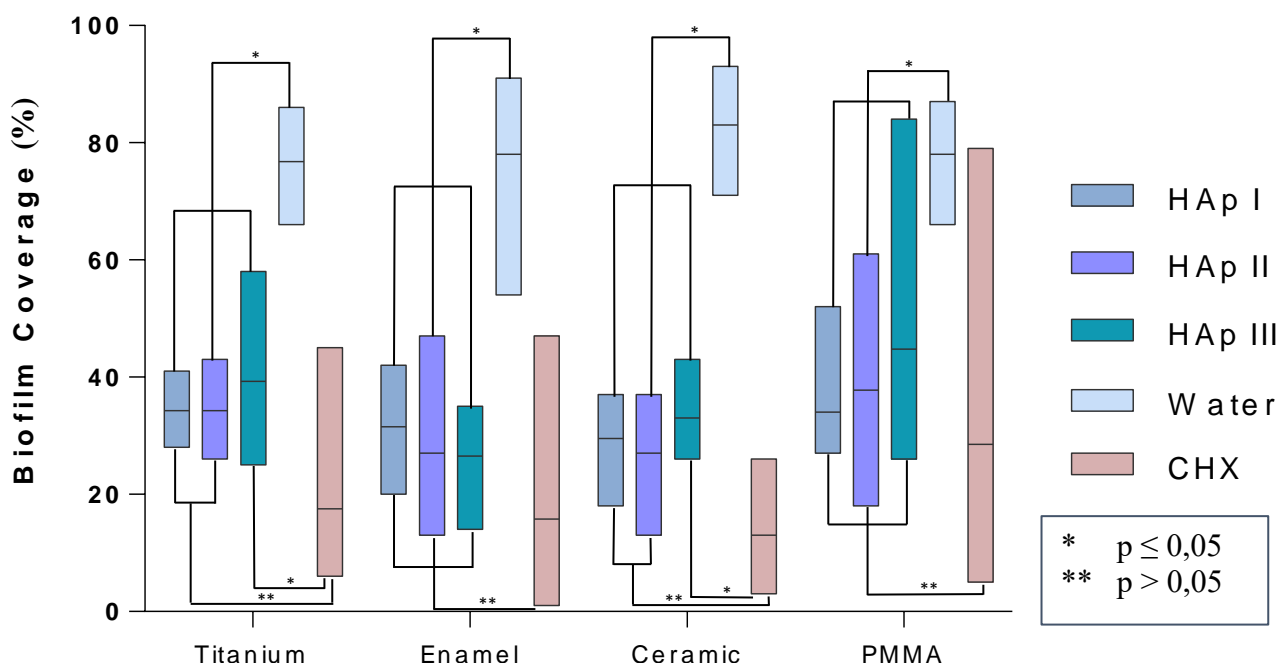
Figure 49 24-h biofilm coverage on different dental material samples. Samples rinsed with water presented a significant denser biofilm than samples rinsed with any other solutions tested ($p < 0.0001$). A significantly lower number of bacteria was detected when CHX rinse was applied compared with the negative control ($p = 0.0099$). Most samples treated with the HAP solutions showed lower biofilm coverage, without a significant difference from the CHX rinsed samples, except for titanium and ceramic samples rinsed with HAP III. Enamel, titanium and ceramics specimens presented a lower quantity of bacteria than PMMA for all HAP solutions.
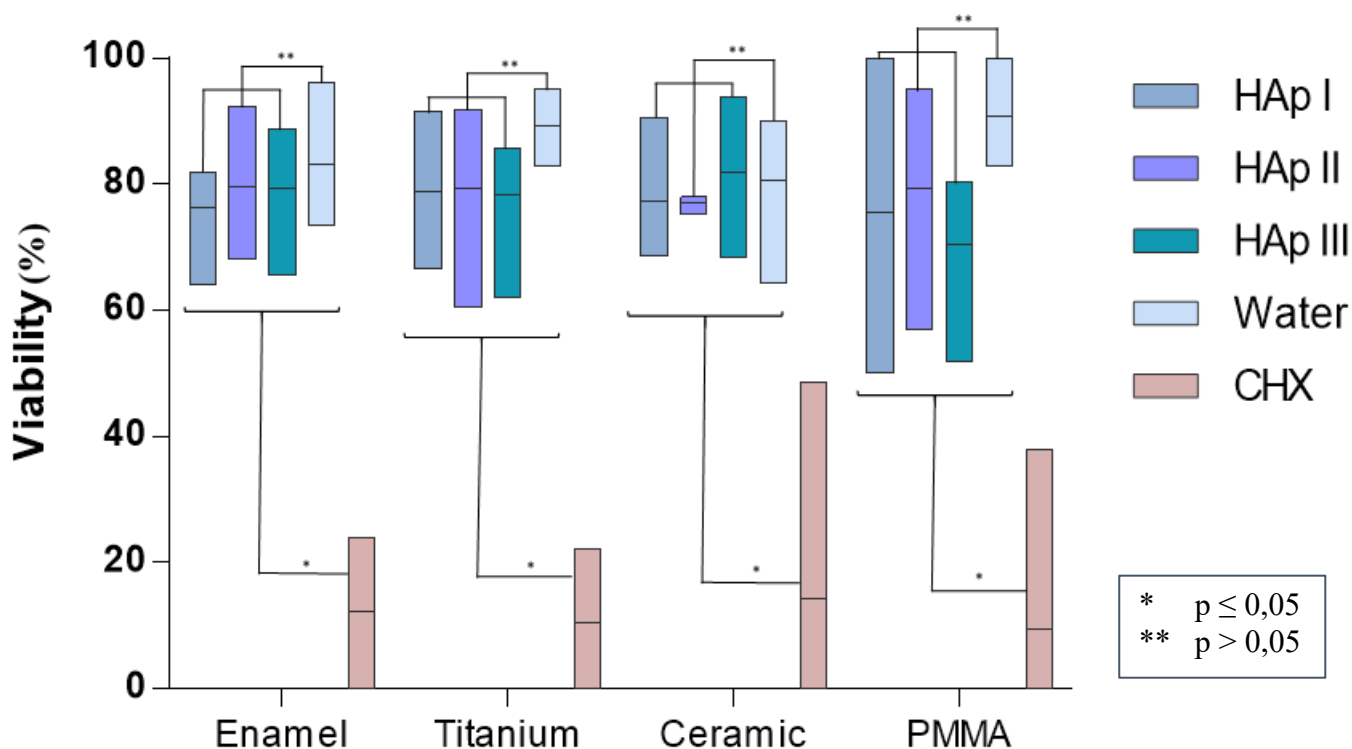
Figure 50 Bacteria viability results of the 24-h biofilm formed on different dental materials. There was a significant difference when comparing the samples rinsed with any of the HAP solutions with the samples rinsed with CHX ($p < 0.0001$), where most bacteria were dead. However, no significant difference was found between the samples rinsed with the HAP solutions and the samples rinsed with water. Additionally, independent of the solution used as mouthrinse, there was no significant difference in bacteria viability between the applied materials, when the same rinsing solution was used.

4.4.2 Scanning electron microscopy

In protocol 2, the SEM analyses were performed on four different polished surfaces: enamel, titanium, ceramic, and PMMA previously presented on Figure 23. After 24 h of intraoral exposure, the *in situ* formed biofilm consisted mainly of coccoid bacteria, independent of the dental material or solution used (Figures 51-54). A few rod-shaped bacteria were detected on titanium samples rinsed with water (Figure 52).

The micrographs presented in Figures 51-54 showed that the SEM investigations confirmed the results from the fluorescence microscopic analysis. SEM results also detected a dense and multilayered biofilm on samples rinsed with water. On the other hand, when CHX was applied, only a few isolated bacteria, small bacterial conglomerates or no bacterial cells were visualized (Figures 51-54). Specimens rinsed with any of the HAP solutions revealed considerably less biofilm than the water rinsed control samples. This biofilm was usually present in colonies over the surfaces (Figures 51-54). Hydroxyapatite particles were often detected on top of some bacterial cells (Figures 51-54). Furthermore, the PMMA samples presented more biofilm on their surface in comparison to the other materials (Figure 54).

Additionally, SEM evaluation at higher magnifications enabled a better visualization of a bridge-like structure, indicating a possible interaction between the hydroxyapatite particles and bacterial cells (Figure 55). The nanoparticles were visible attached to the bacterial cells and accumulate in their surroundings.

78
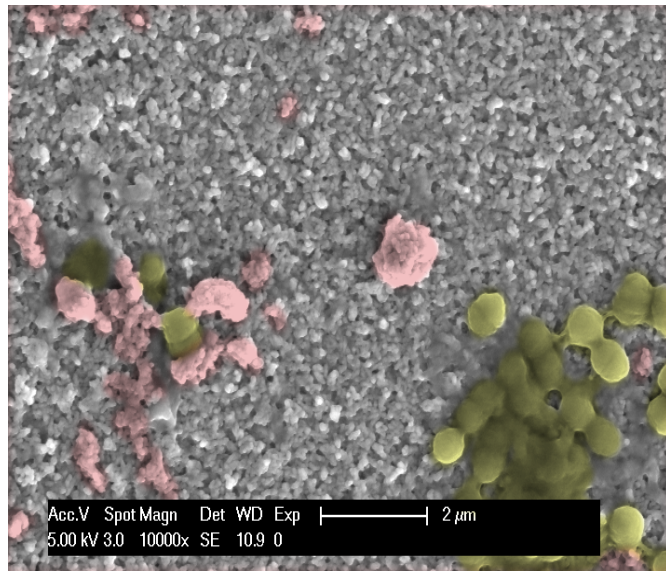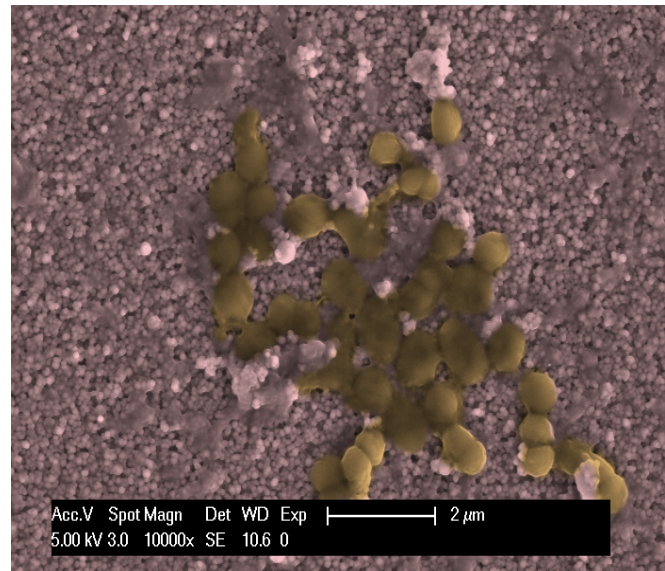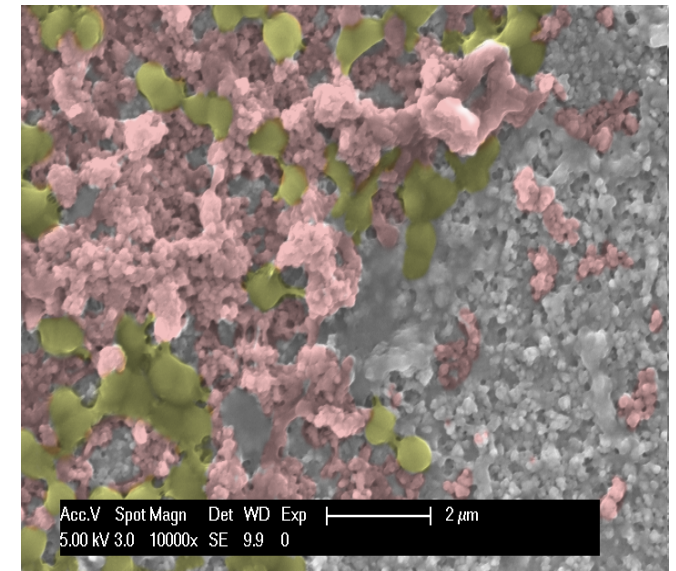
Enamel
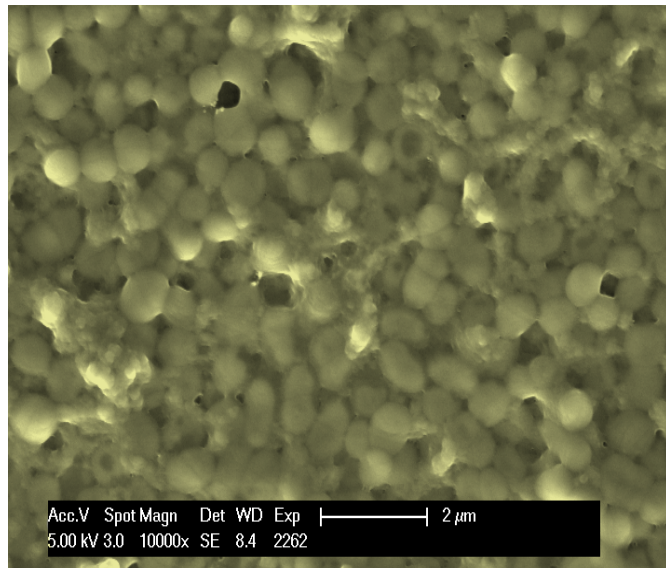
HAP I
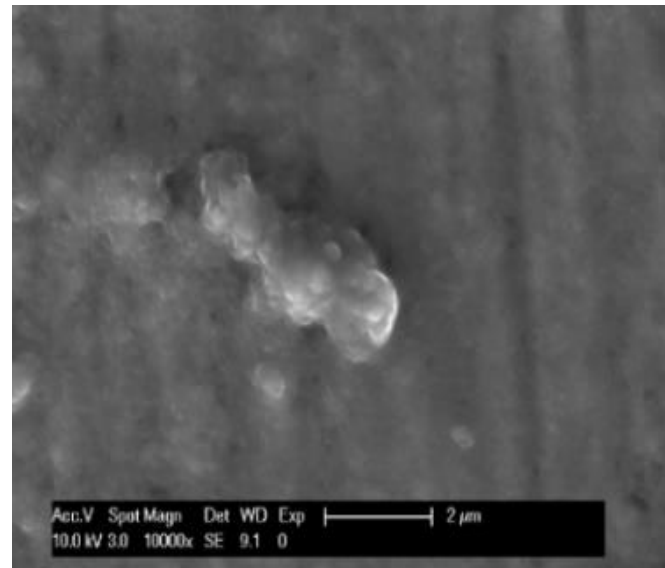
HAP II

HAP III

Water

CHX

Figure 51 SEM at 10,000-fold magnification shows the variation of biofilm amount on the enamel surface after 24 h of intraoral exposure and two times rinsing with HAP I, HAP II, HAP III, CHX and water. The yellow color represents coccoid shaped bacteria. The pink color represents the HAP particles. The grey color represents the material surface covered with a thick 24-h pellicle, and possibly with HAP particles on top on samples rinsed with the HAP solutions. It was not possible to distinguish the pellicle's globular particles from the small agglomerates of hydroxyapatite.

Titanium
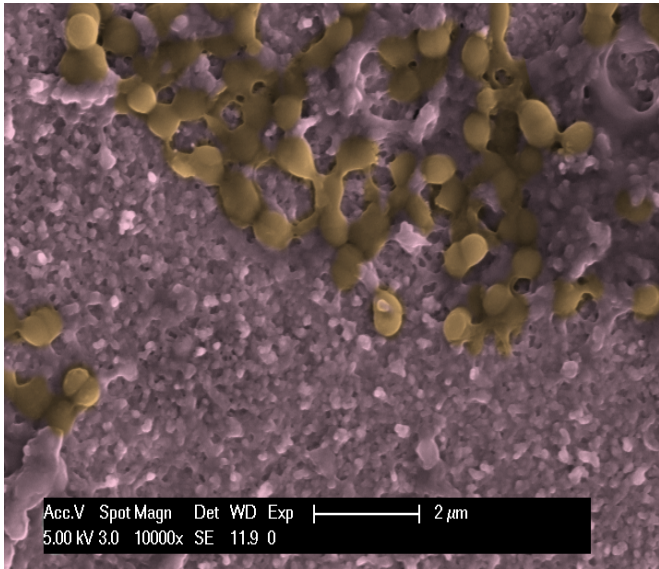
HAP I
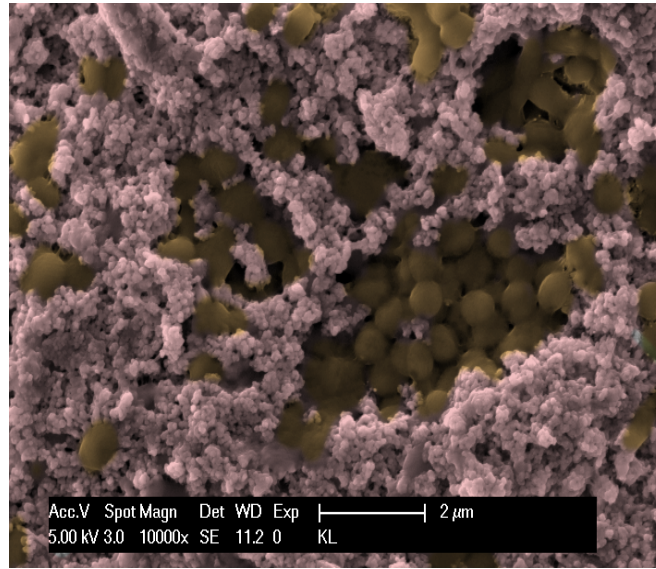
HAP II
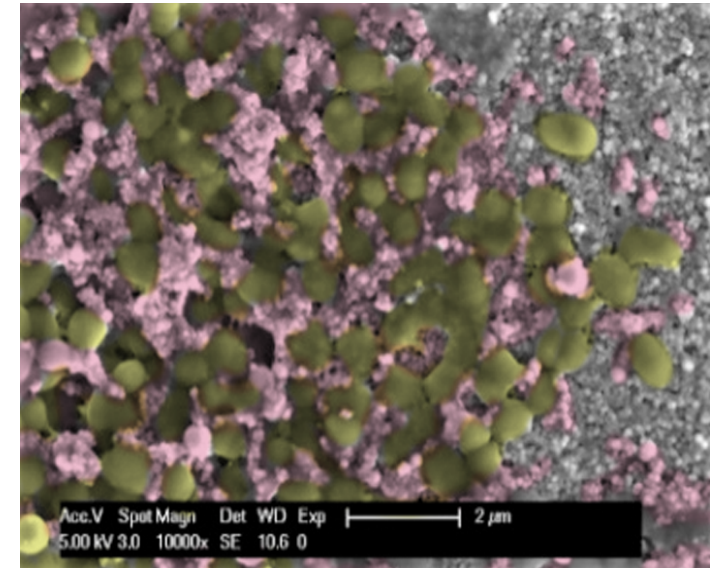
HAP III
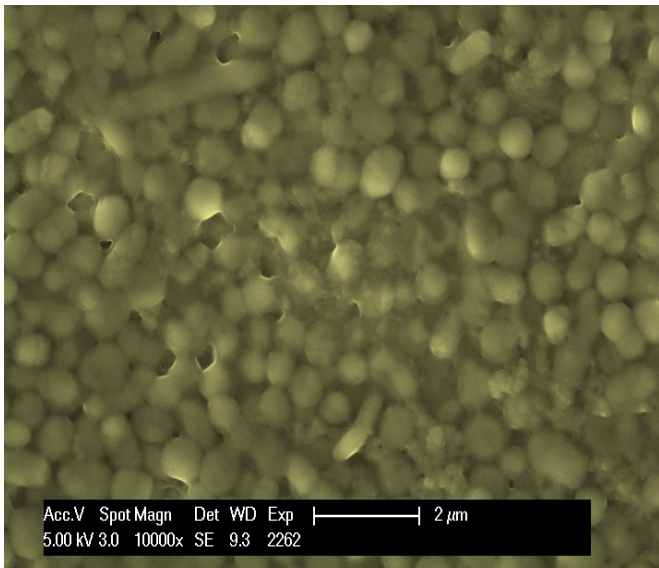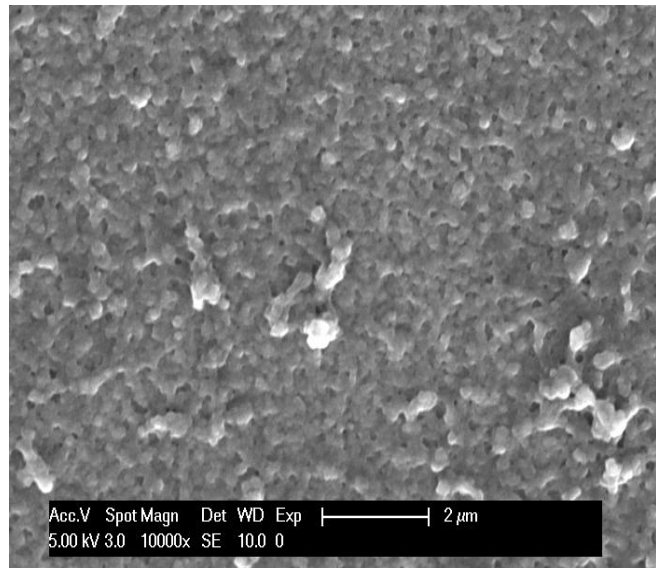
Water

CHX

Figure 52 SEM at 10,000-fold magnification shows the variation on biofilm amount on the titanium surface after 24 h of intraoral exposure and two times rinsing with HAP I, HAP II, HAP III, CHX and water. The yellow color represents the coccoid shaped bacteria. The pink color represents the HAP particles. The grey color represents the material surface covered with a thick 24-h pellicle, and possibly with HAP particles on top on samples rinsed with the HAP solutions.

Ceramic
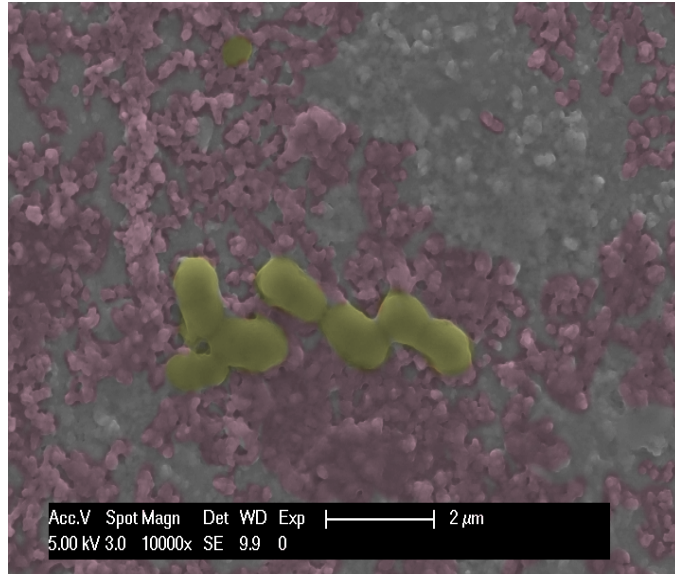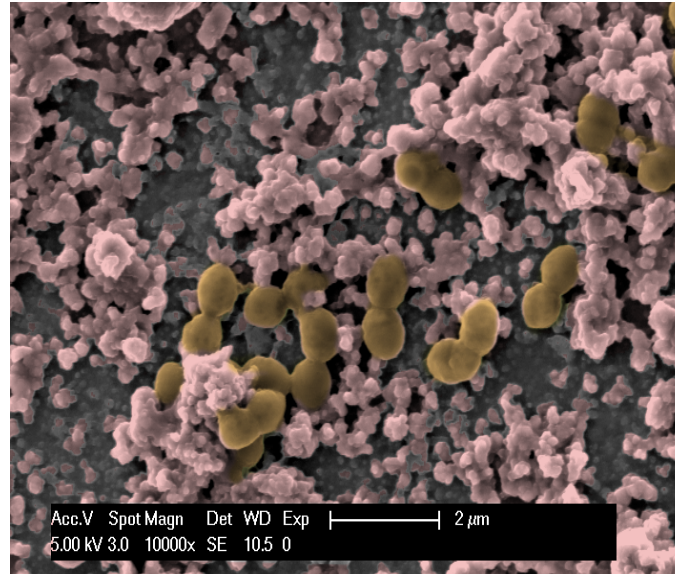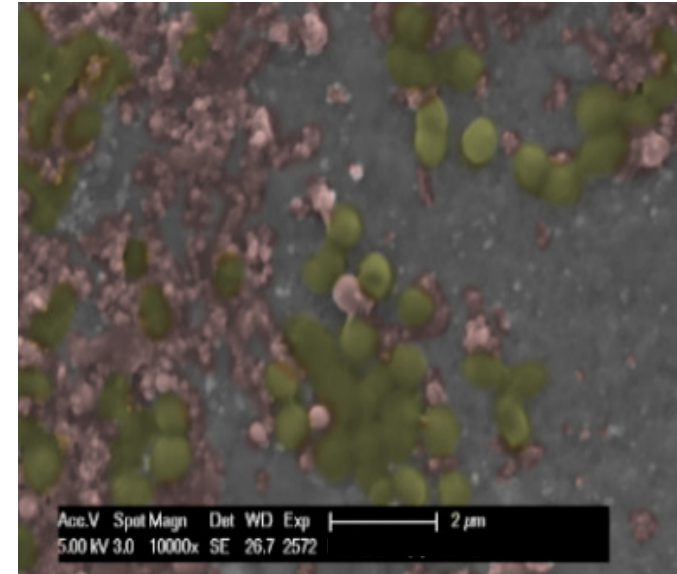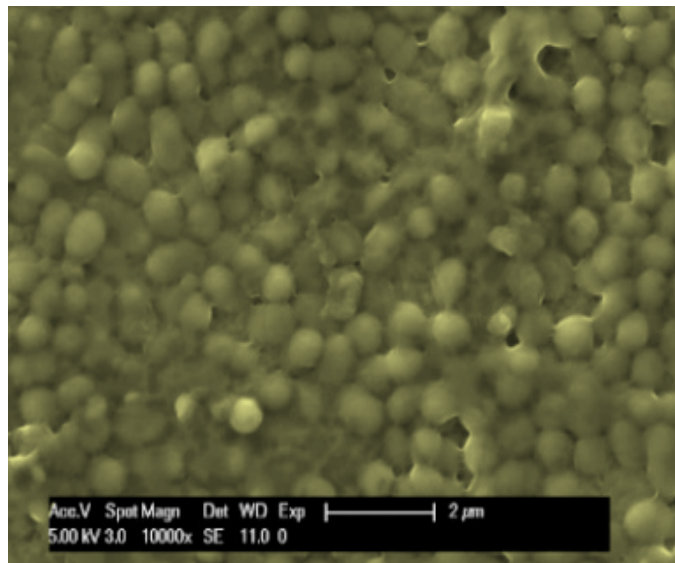
HAP I
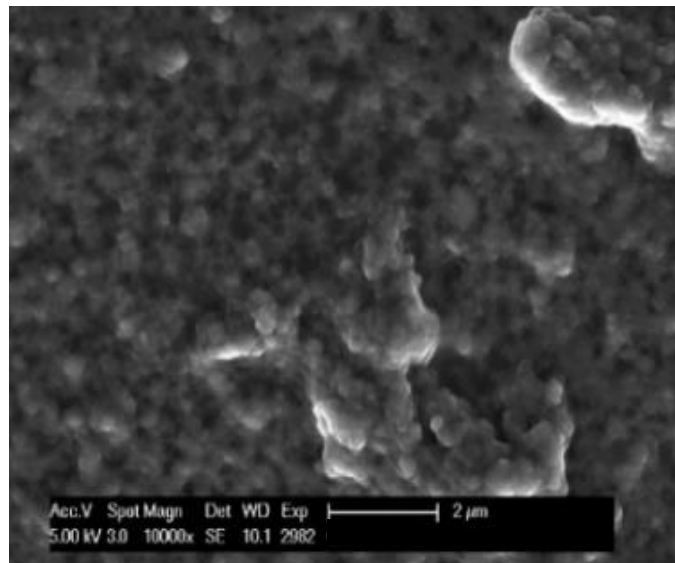
HAP II

HAP III

Water

CHX

Figure 53 SEM at 10,000-fold magnification shows the variation on biofilm amount on the ceramic surface after 24 h of intraoral exposure and two times rinsing with HAP I, HAP II, HAP III, CHX and water. The yellow color represents the coccoid shaped bacteria. The pink color represents the HAP particles. The grey color represents the material surface covered with a thick 24-h pellicle, and possibly with HAP particles on top on samples rinsed with the HAP solutions.
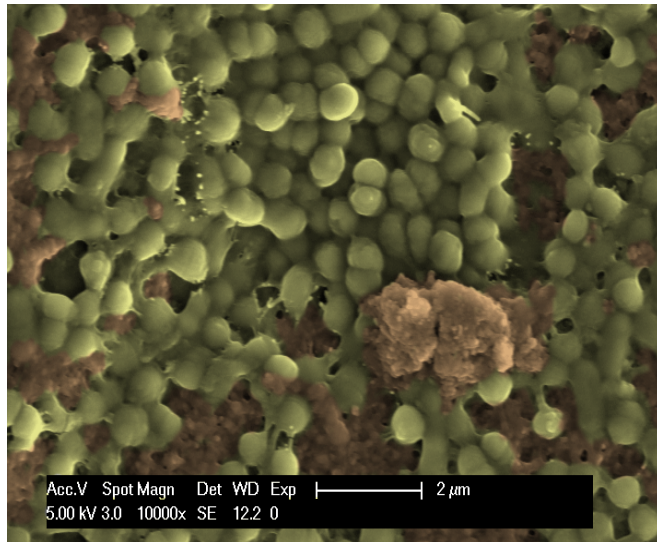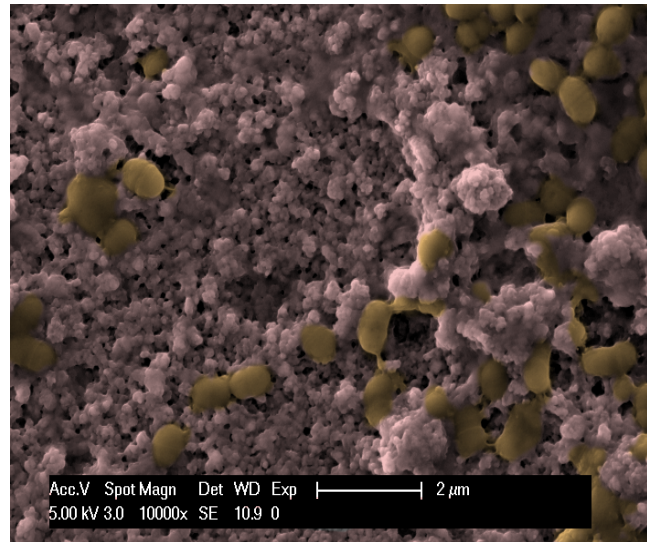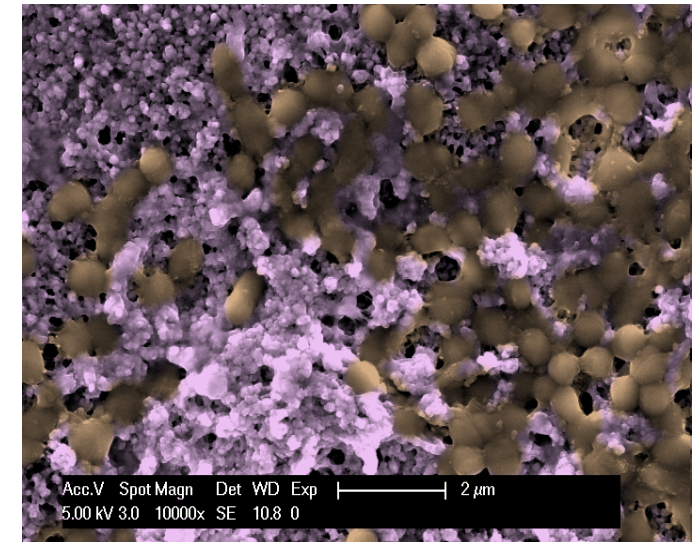
PMMA
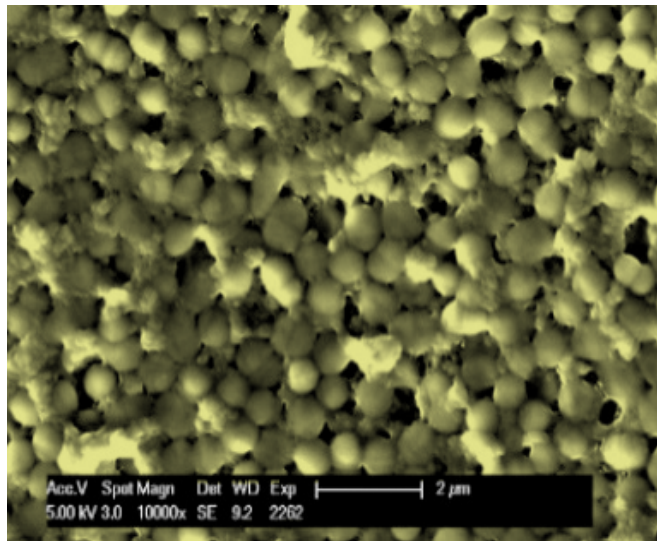
HAP I
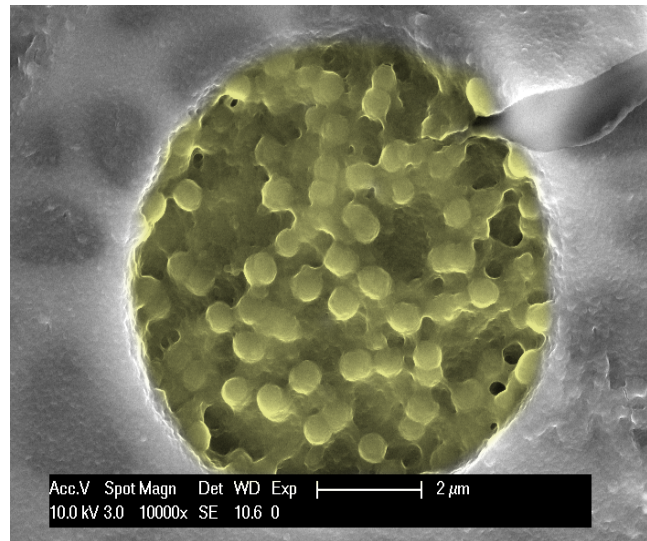
HAP II

HAP III

Water

CHX

Figure 54 SEM at 10,000-fold magnification shows the variation on biofilm amount on the PMMA surface after 24 h of intraoral exposure and two times rinsing with HAP I, HAP II, HAP III, CHX and water. Bacterial colonies were also visible on samples rinsed with CHX. They were located in retention areas of the PMMA surface. The yellow color represents the coccoid shaped bacteria. The pink color represents the HAP particles. The grey color represents the material surface covered with a thick 24-h pellicle, and possibly with HAP particles on top on samples rinsed with the HAP solutions.
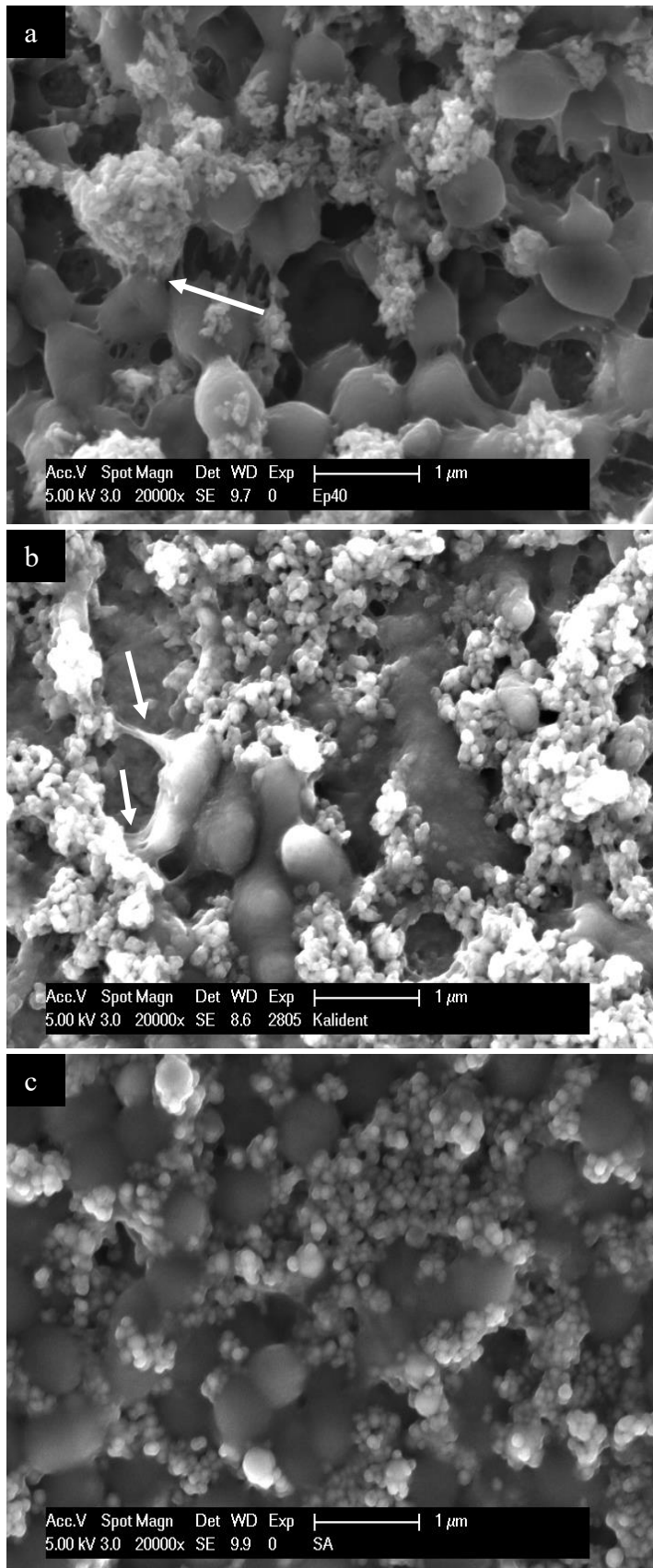
Figure 55 SEM at 20,000-fold magnification of HAP I (a), HAP II (b) HAP III (c) particles on the 24-h biofilm formed on enamel, under the effect of two times rinsing with the respective HAP solutions. The micrographs show the accumulation of HAP particles on the bacteria surface. It is also visible the bacteria-hydroxyapatite interaction through the presence of connective structures (white arrows) between them.

4.4.3 Transmission electron microscopy

First, it was unviable to analyze the PMMA samples by TEM. It was not possible to visualize any structure by TEM microscopy with the methodology applied. The biofilm structures might have been dissolved in the aceton-Araldite mixture during the embedding procedure. Therefore, TEM evaluation was performed only with enamel, titanium, and ceramics samples.

Samples rinsed with water showed the typical 24-h pellicle ultrastructure with an electron-dense basal layer and a granular second layer (Figure 56). Depending on the materials applied (enamel, titanium, ceramics), some differences in the characteristics of the pellicle's ultrastructure were visible (Figure 56). Pellicle layers formed on enamel samples presented a heterogeneous, diffuse and not well-defined basal layer, while this same layer on ceramics and titanium samples was thicker and appeared as a clear line in contact with the material surface (Figure 56). On enamel, the granular second outer layer was a thick and loose structure, while on ceramics, the outer layer was also thick, but very compact (Figure 56). On titanium, this second layer was thin and very dispersed (Figure 56). Another similar point on all samples rinsed with water was the presence of a mono or double layer of integrated bacteria on top of the pellicle's outer layer, representing the 24-h biofilm. It was possible to visualize filiform structures around the bacteria, representing their mechanism of adhesion.

When HAP I (Figure 57), HAP II (Figure 58) or HAP III (Figure 59) were used as rinsing solutions, the samples followed a similar pattern concerning the pellicle's basal and outer layer on each material. Additionally, there were peculiarities concerning each hydroxyapatite solution. Biofilm samples rinsed with HAP I or HAP II presented some black spots randomly scattered on their surfaces, which could represent residues from single particles and clusters of hydroxyapatite nanoparticles (Figure 57 and Figure 58). Differently, on all samples rinsed with HAP III brighter and round-shaped "empty" structures were detected (Figure 59). These structures might be the hydroxyapatite particles that were dissolved during the TEM processing (Figure 59). Furthermore, most of the bacteria presented changes on their inner morphology, containing these same brighter and round-shaped structures of low electron density (Figure 59).

In contrast, when CHX was applied (Figure 60), a similar pellicle ultrastructure was present on enamel, titanium, and ceramics. The basal and the second layers were thicker (*c.* 300 – 2000 nm) and more electron-dense without the presence of adherent bacteria (Figure 60).

Water
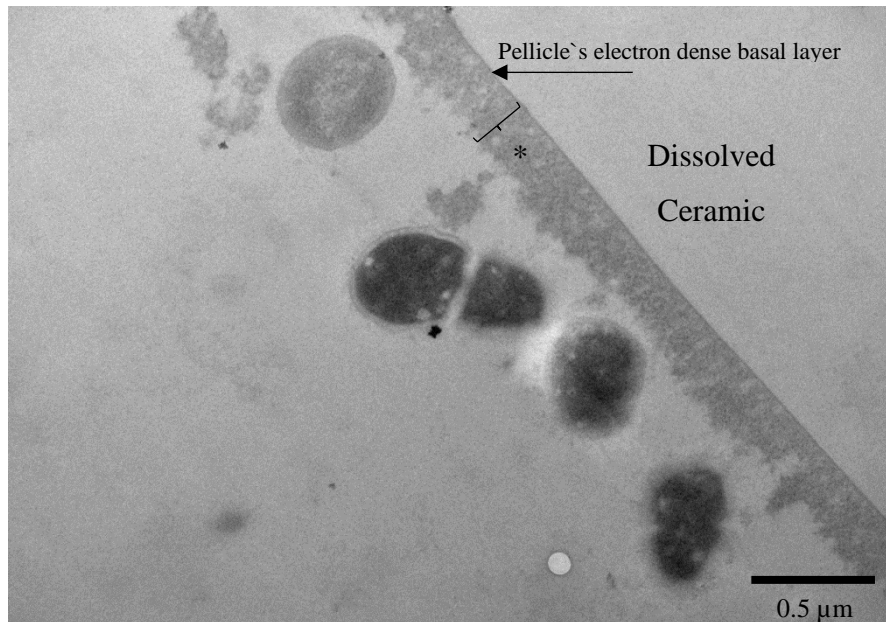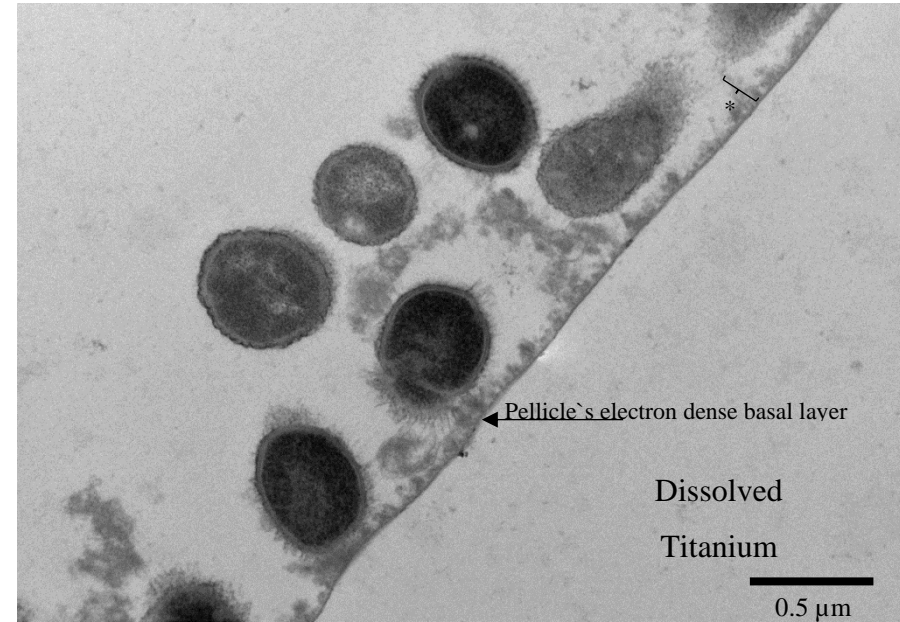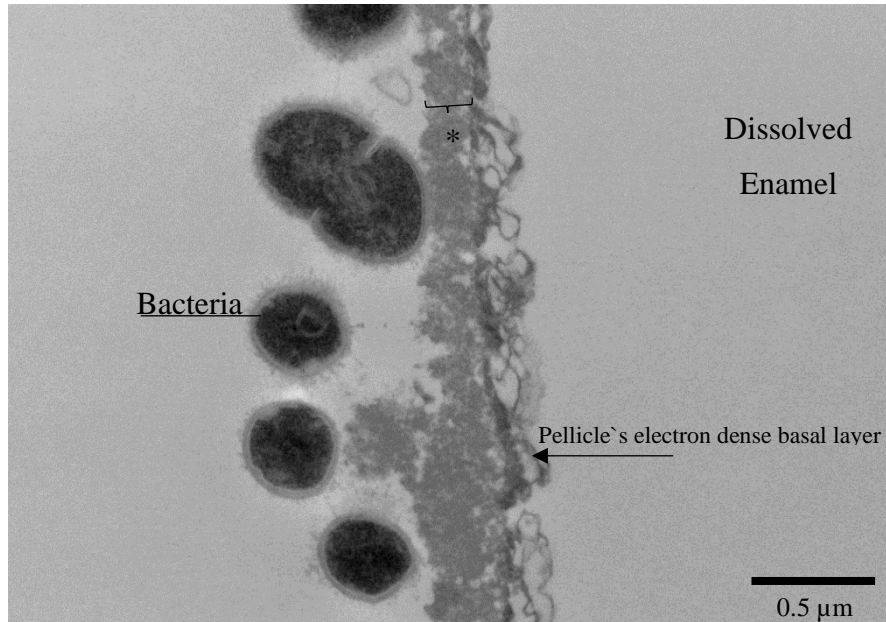
Figure 56 TEM micrographs at 30,000-fold magnifications of a 24-h biofilm on enamel, titanium and ceramic surfaces after water rinsing according to protocol 2. Bacterial cells are adhered onto the pellicle formed on all surfaces. On the bacteria surface fimbriae could be observed. The asterisks represent the pellicle`s outer layer.
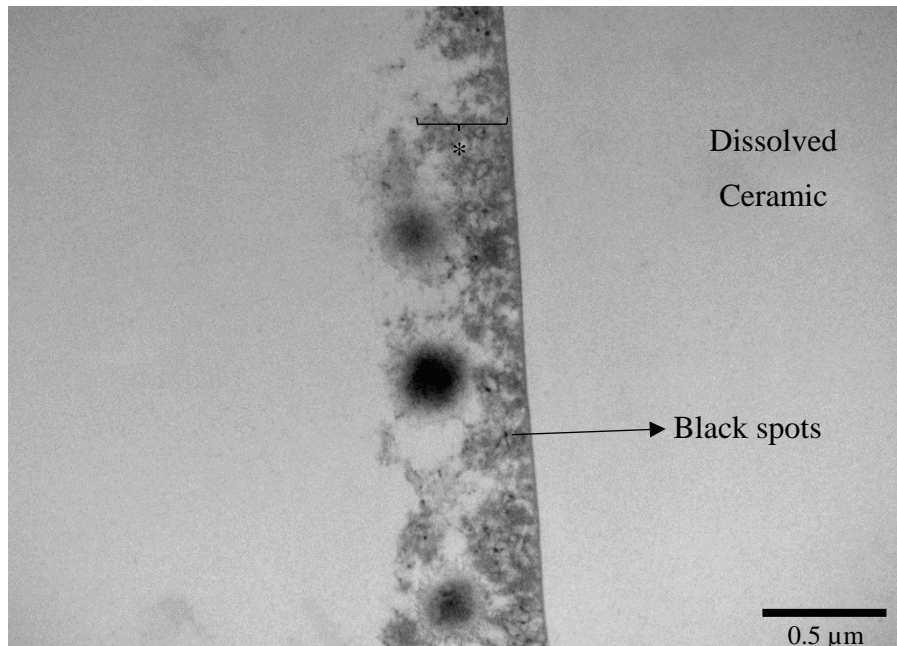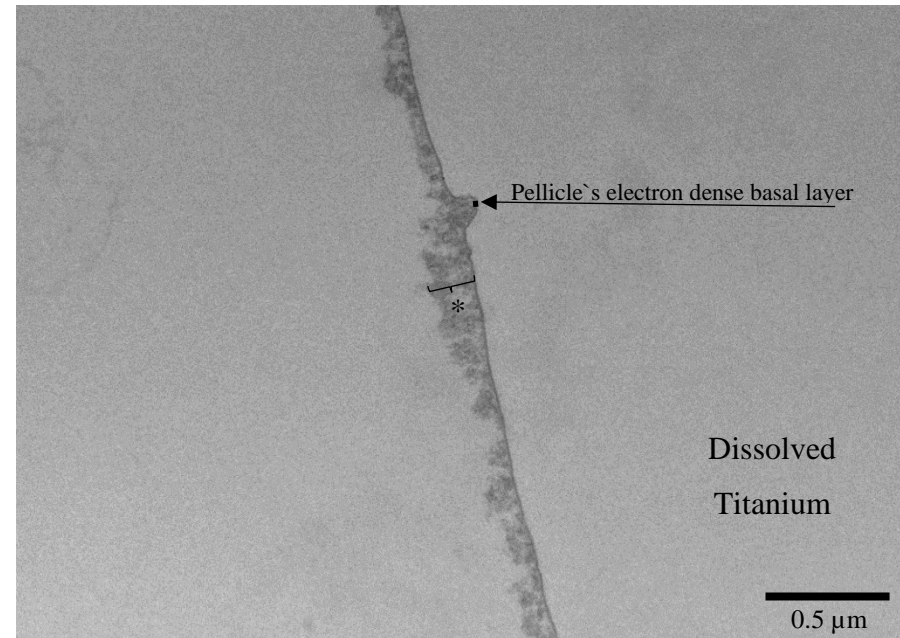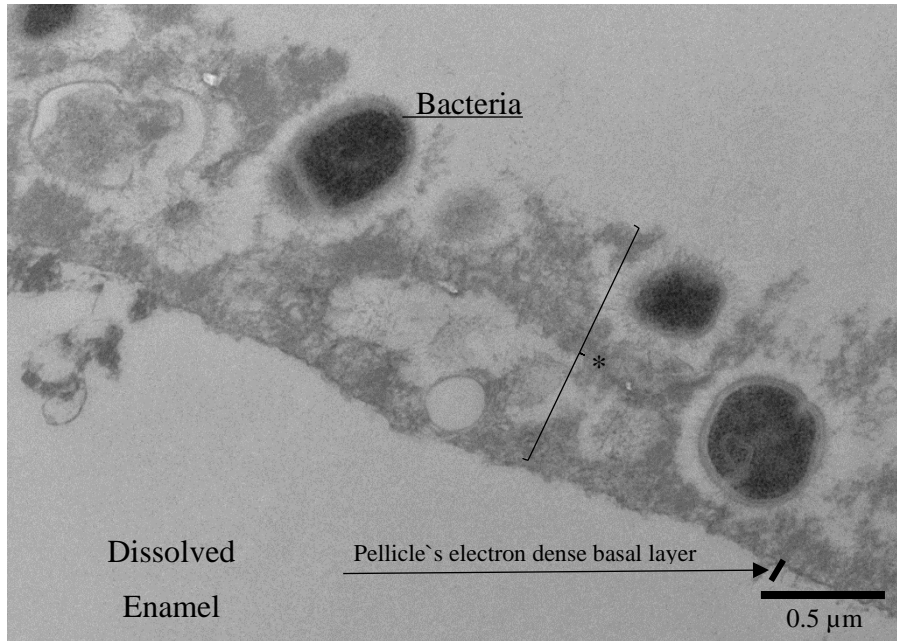
Figure 57 TEM micrographs at 30,000-fold magnifications of a 24-h biofilm formed on enamel, titanium and ceramic surfaces after rinsing with HAP I, according to protocol 2. Attached bacteria are visible in lower amount on titanium and ceramic surfaces. The asterisks represent the pellicle`s outer layer. Some small black spots scattered randomly on the sample were detected. They may represent single particles and clusters of hydroxyapatite nanoparticles that were not dissolved during the TEM processing steps.
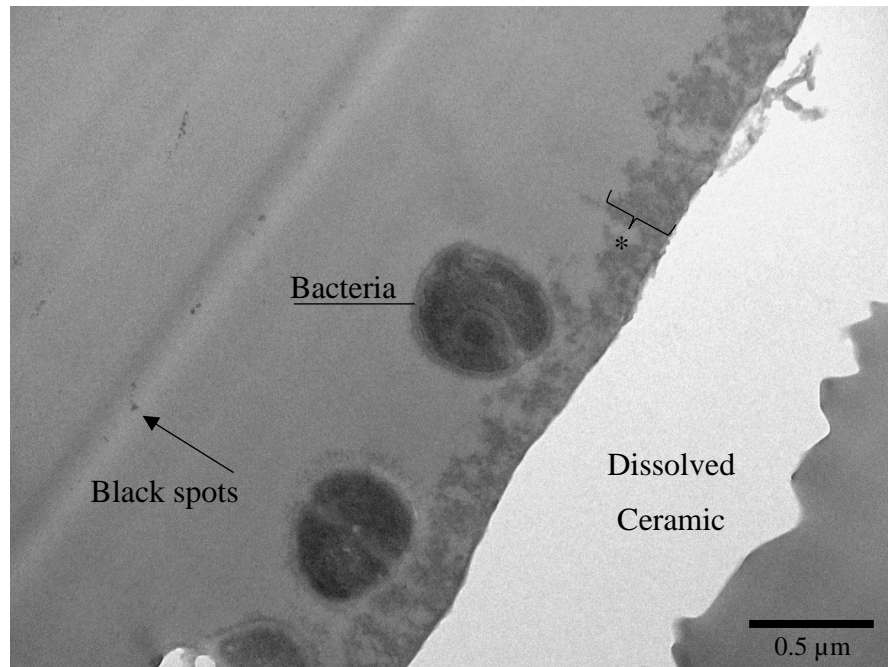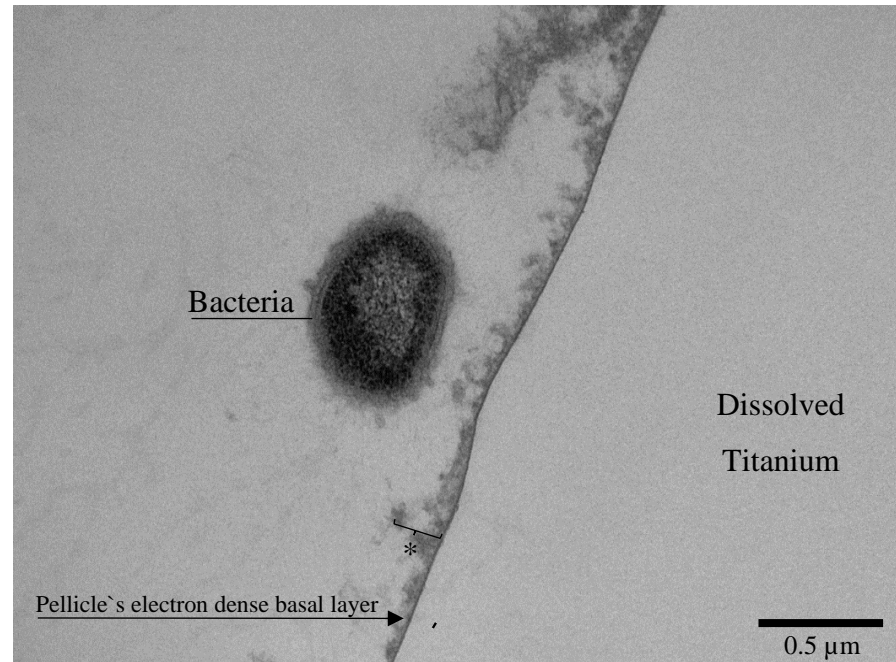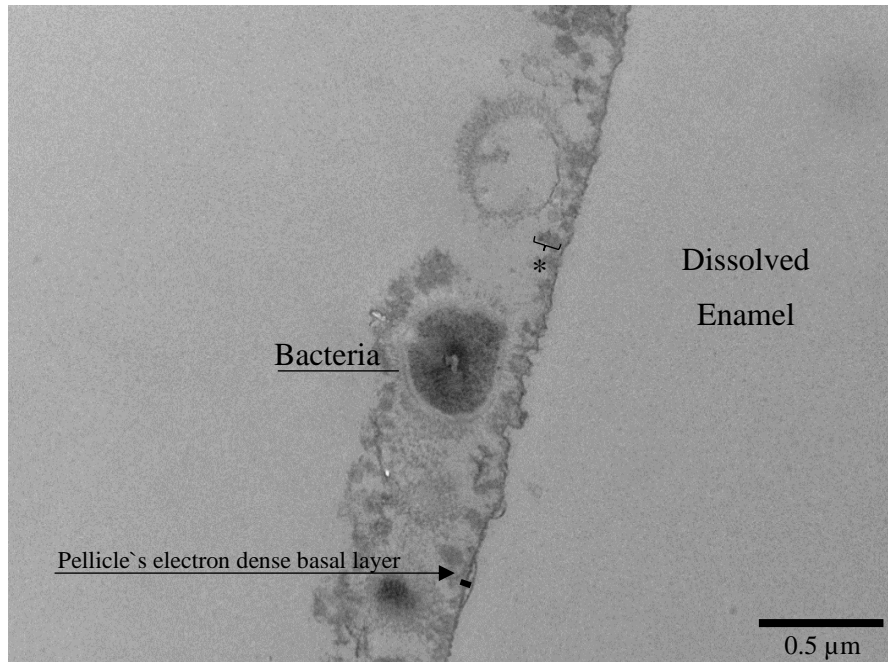
Figure 58 TEM micrographs at 23,000-fold (Ti) and 30,000-fold (enamel and ceramic) magnifications of a 24-h biofilm formed on enamel, titanium and ceramic surfaces after rinsing with HAP II. Attached bacteria are visible on all surfaces. The asterisks represent the pellicle`s outer layer. Some small black spots scattered randomly on the sample were detected. They may represent single particles and clusters of hydroxyapatite nanoparticles that were not dissolved during the TEM processing steps.
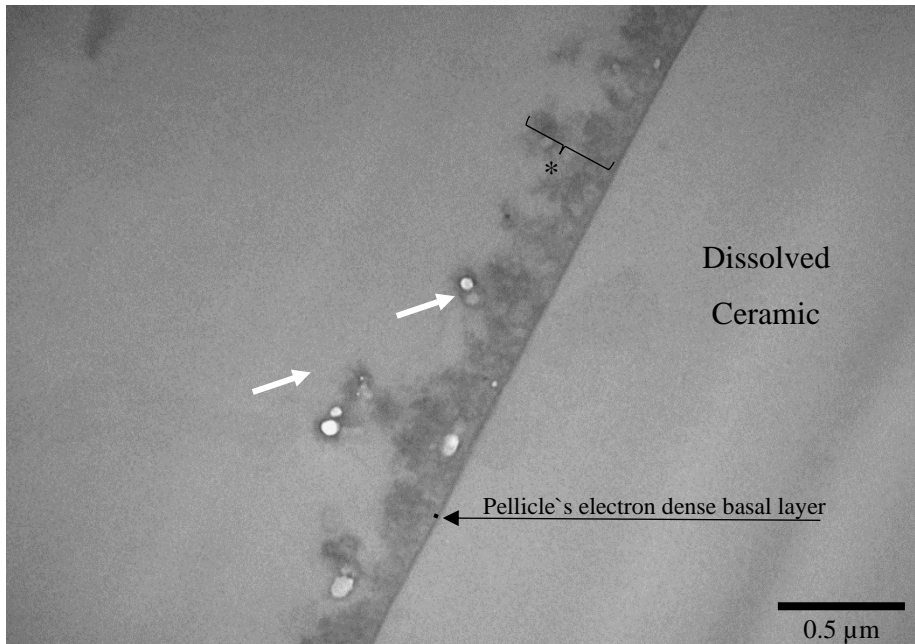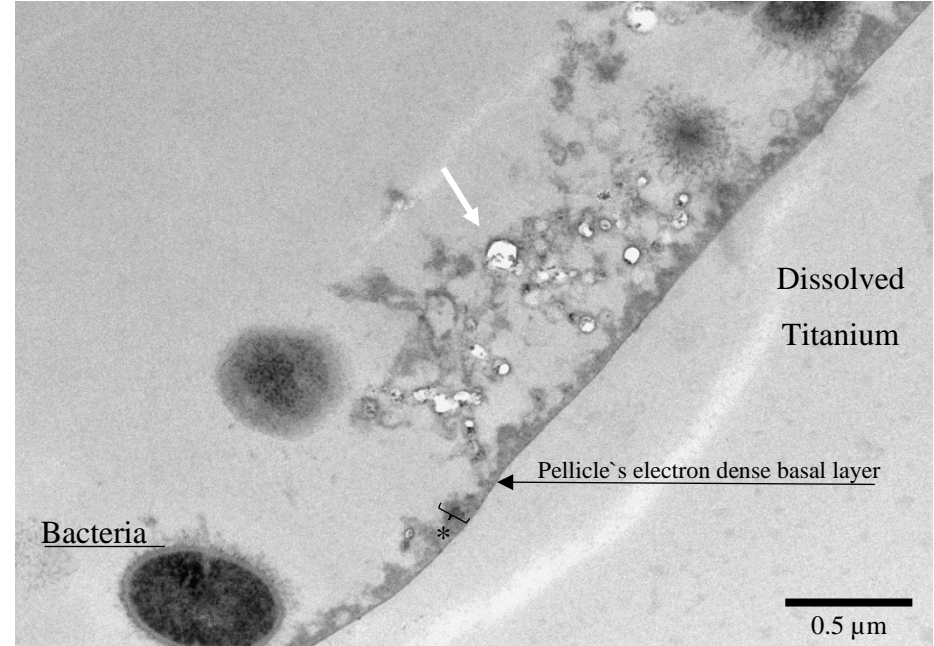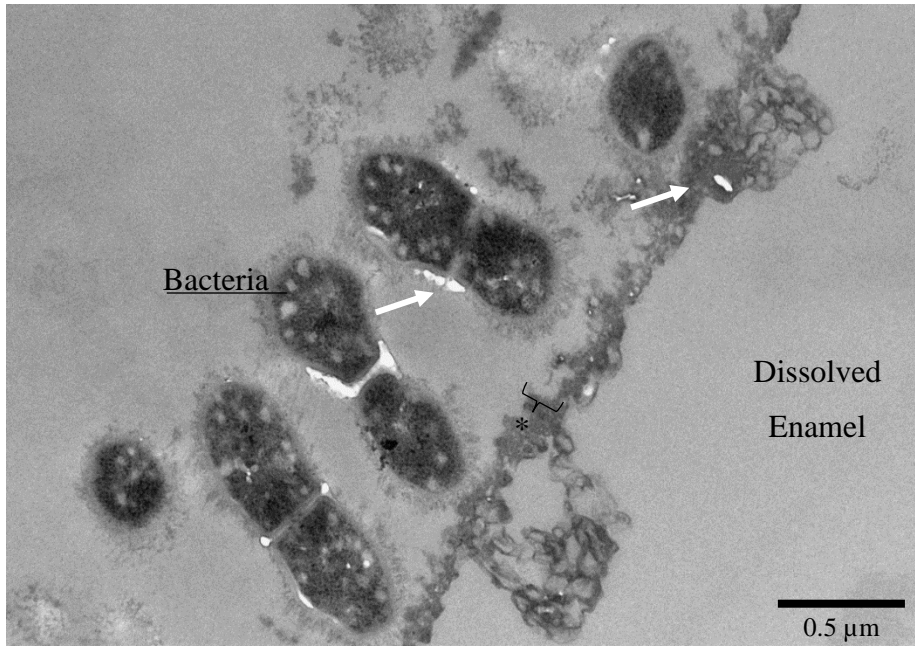
Figure 59 TEM micrographs at 30,000-fold (enamel and Ti) and 49,000-fold (ceramic) magnifications of a 24-h biofilm formed on enamel, titanium and ceramic surfaces after rinsing with HAP III. It is possible to visualize round-shaped structures of low electron density (white arrows). They might represent HAP particles that were dissolved during the TEM processing steps. The asterisks represent the pellicle`s outer layer.
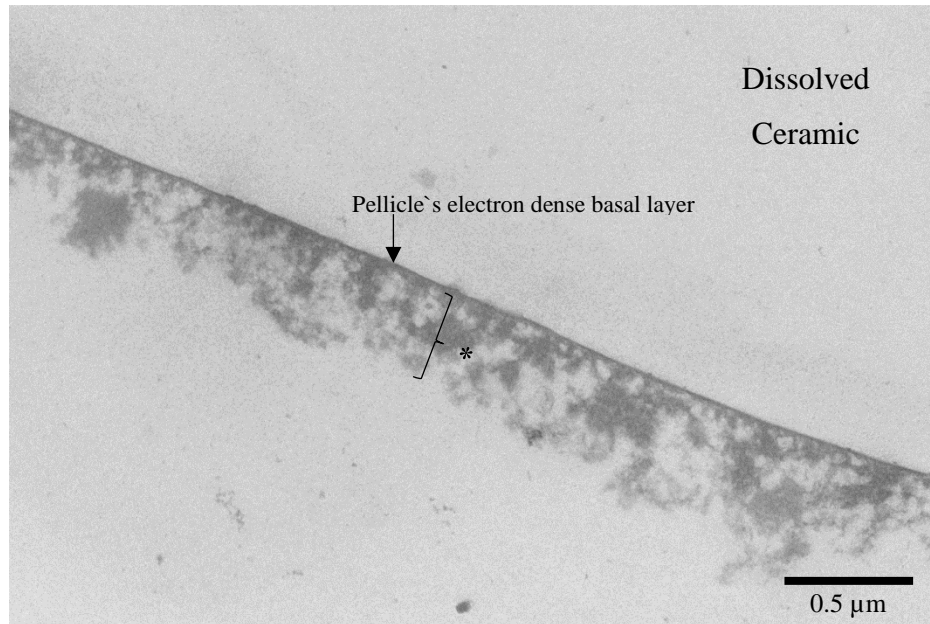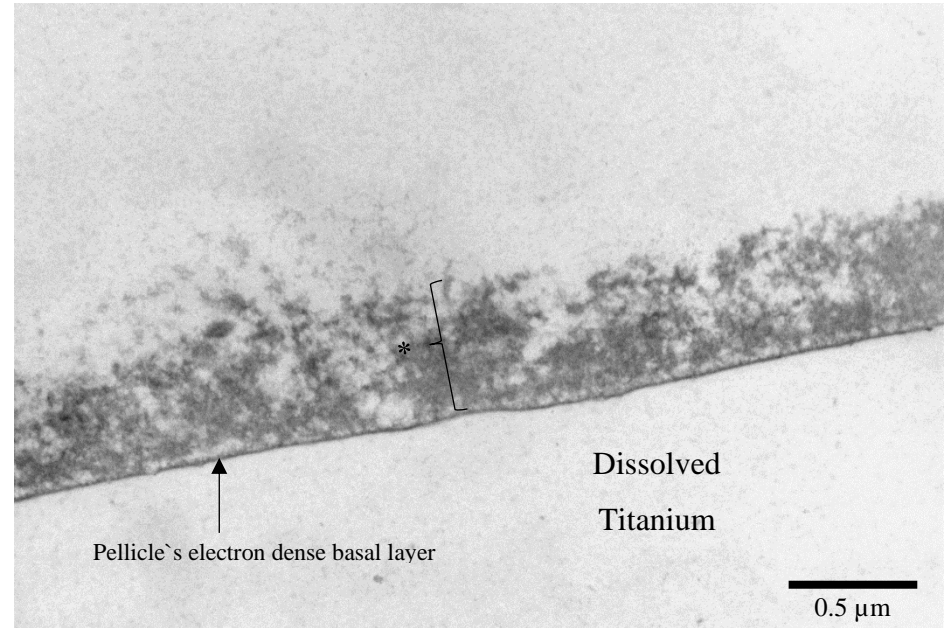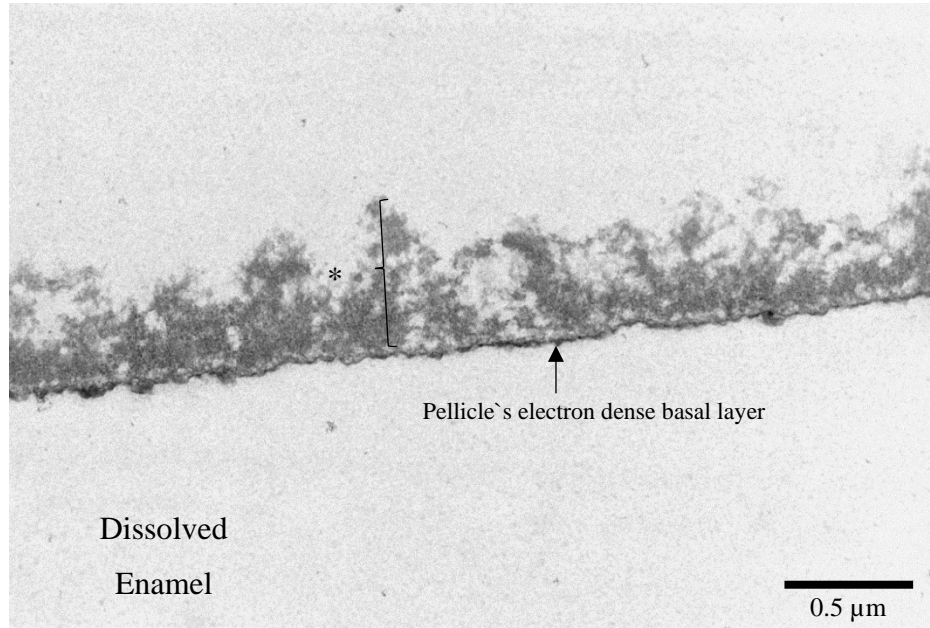
Figure 60 TEM micrographs at 30,000-fold magnifications of a 24-h pellicle formed on enamel, titanium and ceramic surfaces after rinsing with CHX according to protocol 2. Pellicle on all three materials present a thick basal and outer layer, with no visible adherent bacteria. The asterisks represent the pellicle`s outer layer.

4.5 Effects of HAP solutions on the 48-h biofilm formation on polished and non-polished Ti

Protocol 3 was applied only on titanium specimens. Microbial biofilm was formed in situ within 48 h on all samples, regardless of the solution used (HAP II, water or CHX). However, there were variations concerning the quantity of bacteria adherent to the Ti surfaces as well as with regard to the bacterial viability.

4.5.1 BacLight assay: biofilm coverage

As shown in Figure 61 and Figure 62, samples rinsed with water presented a thick biofilm layer, covering the majority of the Ti surfaces after 48 h. There was no significant difference between polished and non-polished surfaces when rinsed with water ($p = 0.1587$) or with CHX ($p = 0.3413$). However, differences were significant between P and NP samples with HAP II ($p = 0.0079$) rinsing, with NP samples presenting a thicker coverage.

Furthermore, another predictable result was the significantly lower bacterial coverage after treatment with CHX (0.2%), when compared with the water rinse ($p = 0.0215$) on polished samples. Interestingly, similar results were achieved comparing the HAP II test solution and water ($p = 0.0485$), but with no significant difference between HAP II and CHX rinsed samples ($p > 0.9999$), with samples rinsed with both solutions presenting lower biofilm coverage.

4.5.2 BacLight assay: biofilm viability

ImageJ was used to analyze the biofilm viability (Figure 61, Table 3). As we can see on Figure 63, there was no significant difference between polished and non-polished samples rinsed with water ($p = 0.5317$) or HAP II ($p = 0.5317$) concerning the bacteria viability, presenting a majority of live bacteria. However, significantly more live bacteria could be observed on non-polished samples rinsed with CHX than on polished samples rinsed with the same solution ($p = 0.0317$). Regarding the polished samples, significantly more live bacteria could be seen after water rinsing, when compared with CHX ($p = 0.0012$). However, no significant difference between polished samples rinsed with water and with HAP II could be detected ($p = 0.2307$). Samples rinsed with CHX showed a significant reduction in the number of vital bacteria compared with HAP II rinsed samples ($p = 0.0079$) (Figure 61 and Figure 63).
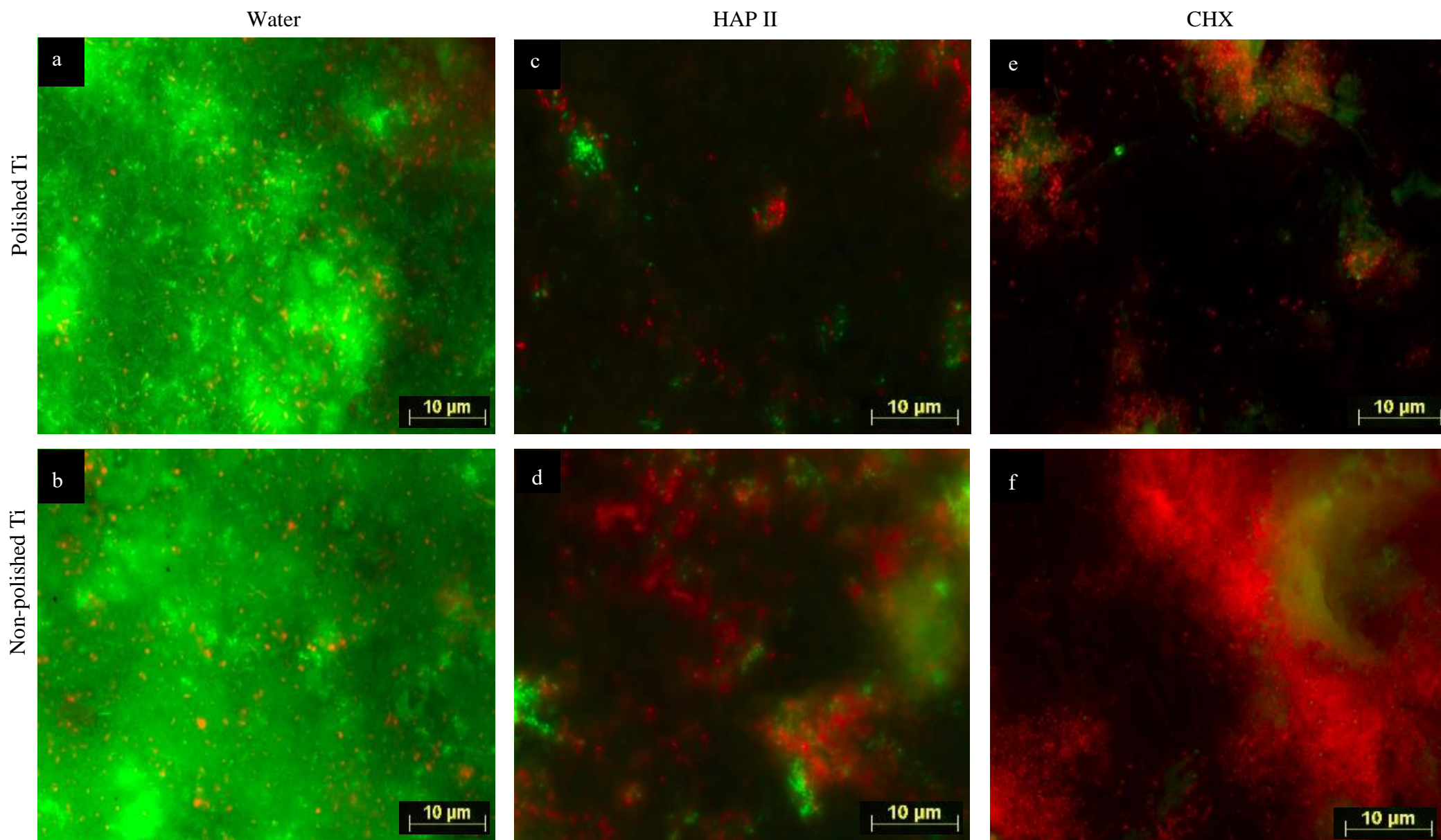
Figure 61 Fluorescence microscopic investigation of Live/Dead stained biofilm allows bacterial coverage visualization and differentiation between live (green) and dead (red) bacteria. After 48 h, non-polished samples (b,d,f) presented significantly higher amounts of adherent bacteria than polished samples (a,c,e). While the water rinsed negative controls appeared densely covered with live bacteria (a,b), samples rinsed with HAP II (c,d) and CHX 0.2% (e,f) presented less bacterial colonies.
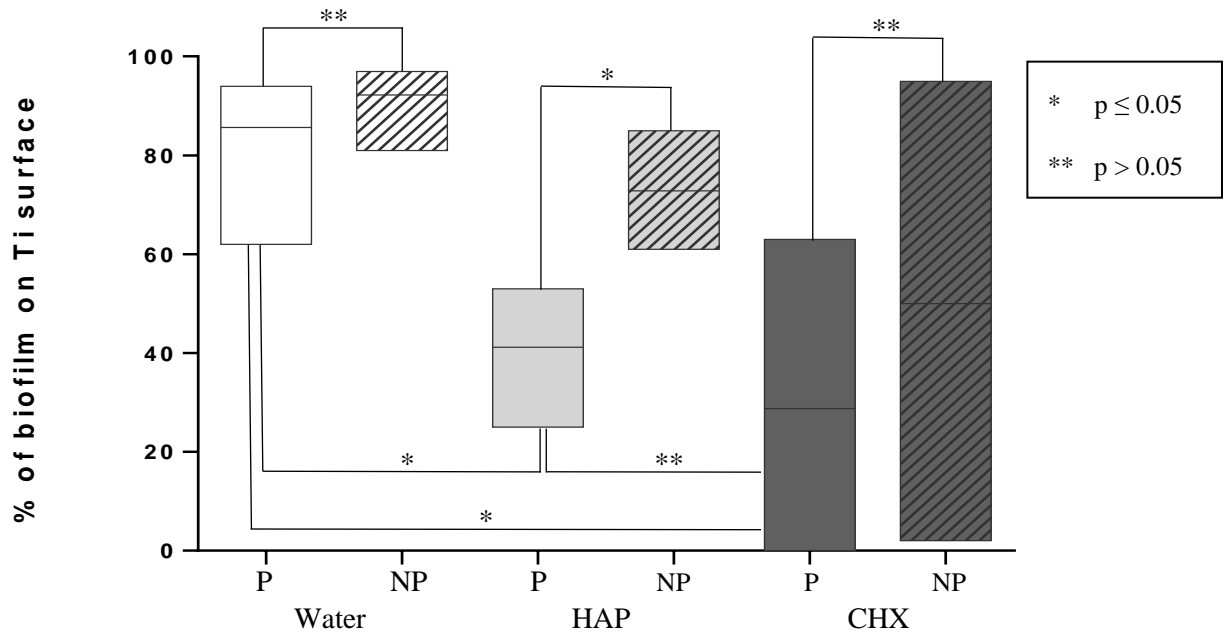
Figure 62 Biofilm coverage: on the polished Ti samples (P), CHX 0.2% and HA reduced the bacterial adherence compared to water. There was no significant difference between the gold standard 0.2% CHX and the test solution of HAP II. Comparing polished (P) and non-polished samples (NP), the only significant difference was between samples rinsed with HAP II solution.
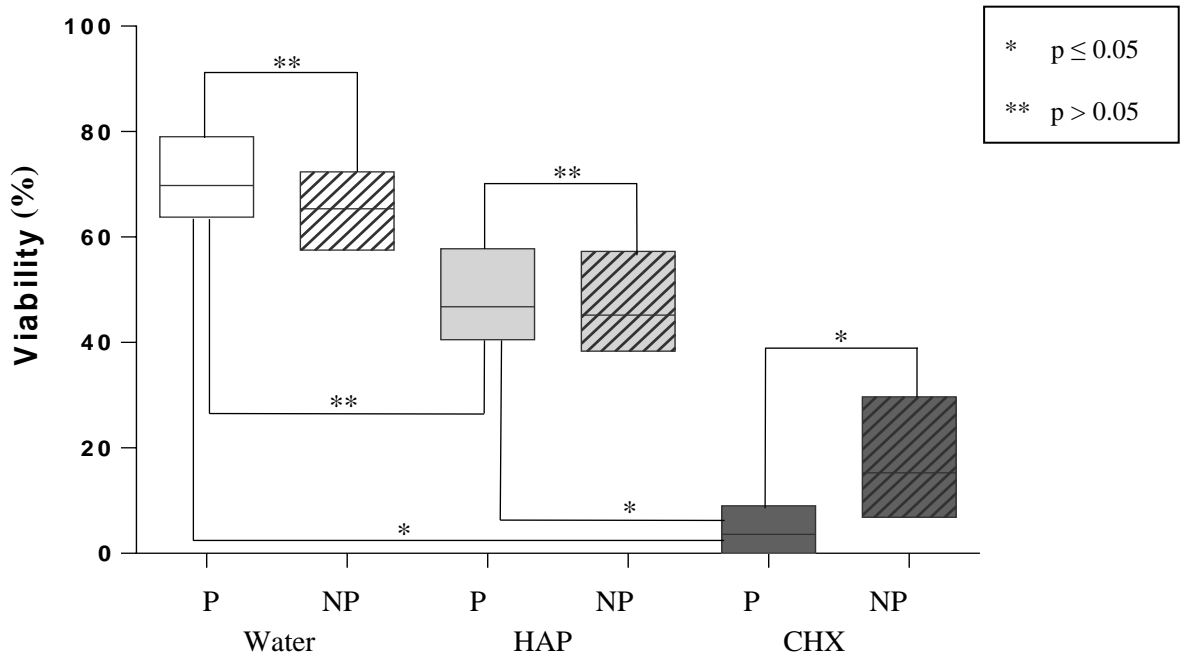
Figure 63 Biofilm viability: CHX rinsing significantly reduced the number of live bacteria compared to the negative control (water rinsing) on polished (P, $p = 0.0012$) and on non-polished (NP, $p = 0.0079$) samples. Non-significant reduction of viability between HAP II and water rinsed samples was present on P ($p = 0.2307$) titanium discs.

93

4.5.3 Scanning electron microscopy

SEM analyses were performed on two types of surfaces: polished and non-polished titanium (Figure 64). The 48-h biofilm formed on titanium surfaces was associated predominantly with coccoid and rod-shaped bacteria (Figure 65). These bacteria were distributed randomly on the titanium surfaces as individual bacteria or colonies (Figure 65). These observations were independent of the surface type (polished, non-polished samples).
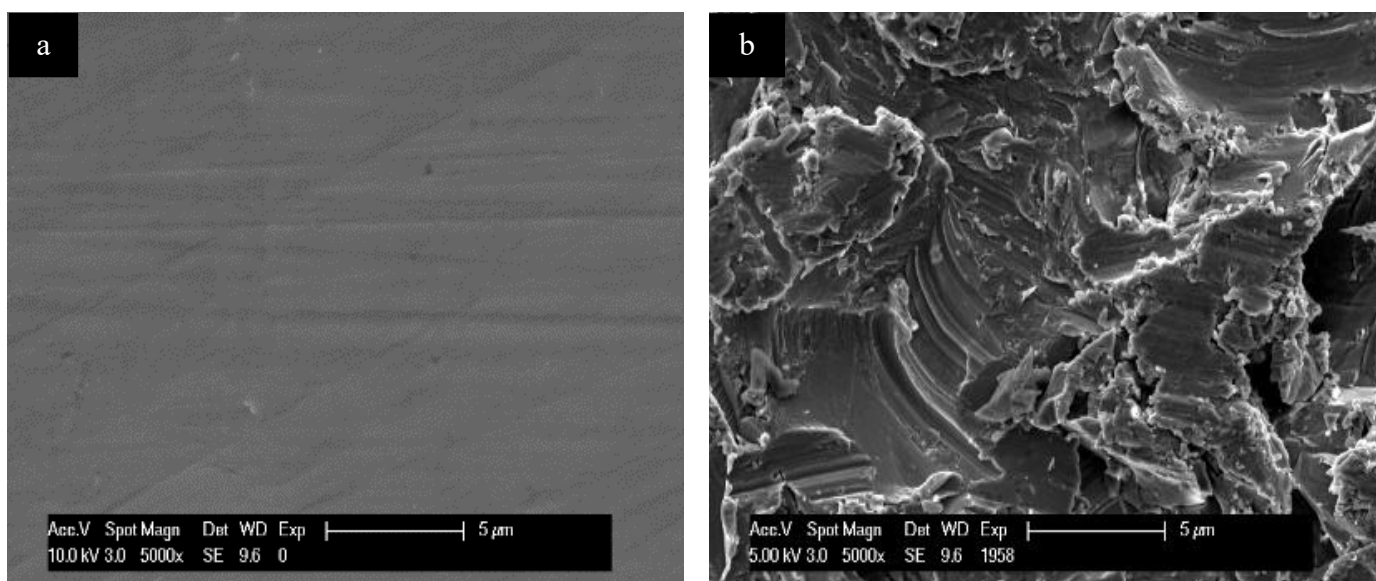
Figure 64 SEM figures at 5,000-fold magnification from polished titanium discs by wet grinding with abrasive paper from 800 to 4000 grit (a) and from original titanium specimens without polishing (b). Samples were not exposed to the oral cavity.
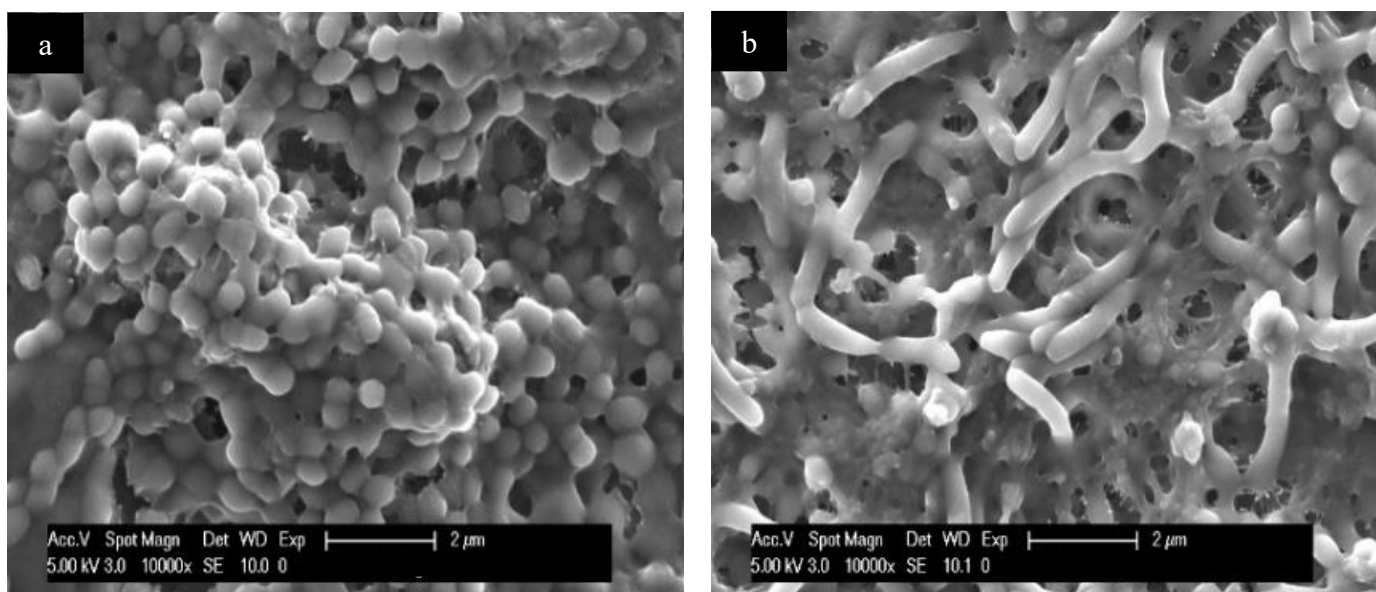
Figure 65 SEM at 10,000-fold magnification of non-polished samples rinsed with water shows a mature biofilm with cocci and rod-shaped bacteria species after 48 h of *in situ* intraoral exposure in two different volunteers.

The SEM investigation showed that some volunteers presented a slightly thinner biofilm coverage on polished samples rinsed with water, compared to the biofilm on non-polished samples rinsed with the same solution (Figure 66). In both cases, coccoid and rod-shaped bacteria were agglomerated and overlapped over each other, forming a multilayered bacterial coverage.

Additionally, most Ti specimens rinsed with the water control solution presented a thicker and multilayered biofilm coverage, independent of the surface topography (Figure 66 and Figure 67).
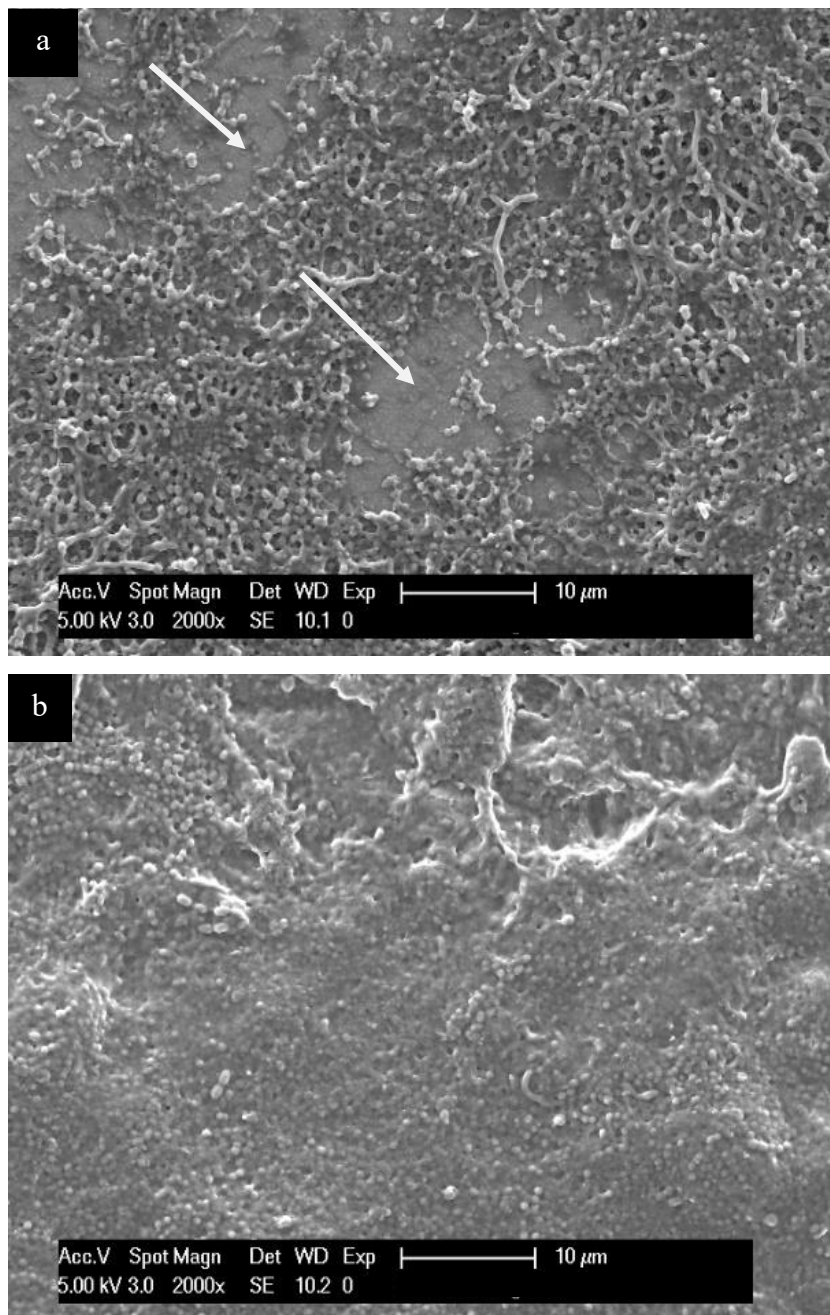
Figure 66 SEM images at 2,000-fold magnification of polished (a) and non-polished (b) Ti surfaces after 48 h intraoral exposure and rinsed with water. White arrows point to areas free of microorganisms on polished Ti samples.

This pattern changed when analyzing the polished titanium samples treated with hydroxyapatite or chlorhexidine solutions. The titanium surface rinsed with the HAP II solution presented areas without biofilm and a thin biofilm with bacteria cells arranged in small colonies on top of a thick pellicle. Single cells were also detected over the titanium surface (Figure 67c). When rinsed with CHX, the titanium surface was covered by globular structures, which may represent a thick 48-h pellicle with damaged bacterial cells on top (Figure 67e). Very few single bacterial cells were detected. Therefore, SEM analysis corroborated the FM results, indicating that the HAP II rinsing solution reduced the amount of mature biofilm formed on polished Ti surfaces.

Finally, Figure 67 also shows that regardless of the solution applied, the non-polished samples presented higher numbers of bacterial colonies compared to the respective polished sample. However, there are differences concerning the distribution of the bacteria. The samples rinsed with HAP II or water presented a highly dense and compact bacterial layer. On the other hand, samples rinsed with CHX present a monolayer of small bacterial colonies and single bacteria scattered over the surface. They were mainly present on retentive areas, such as pits from the non-polished titanium surface structure (Figure 67).

Water HAP II CHX
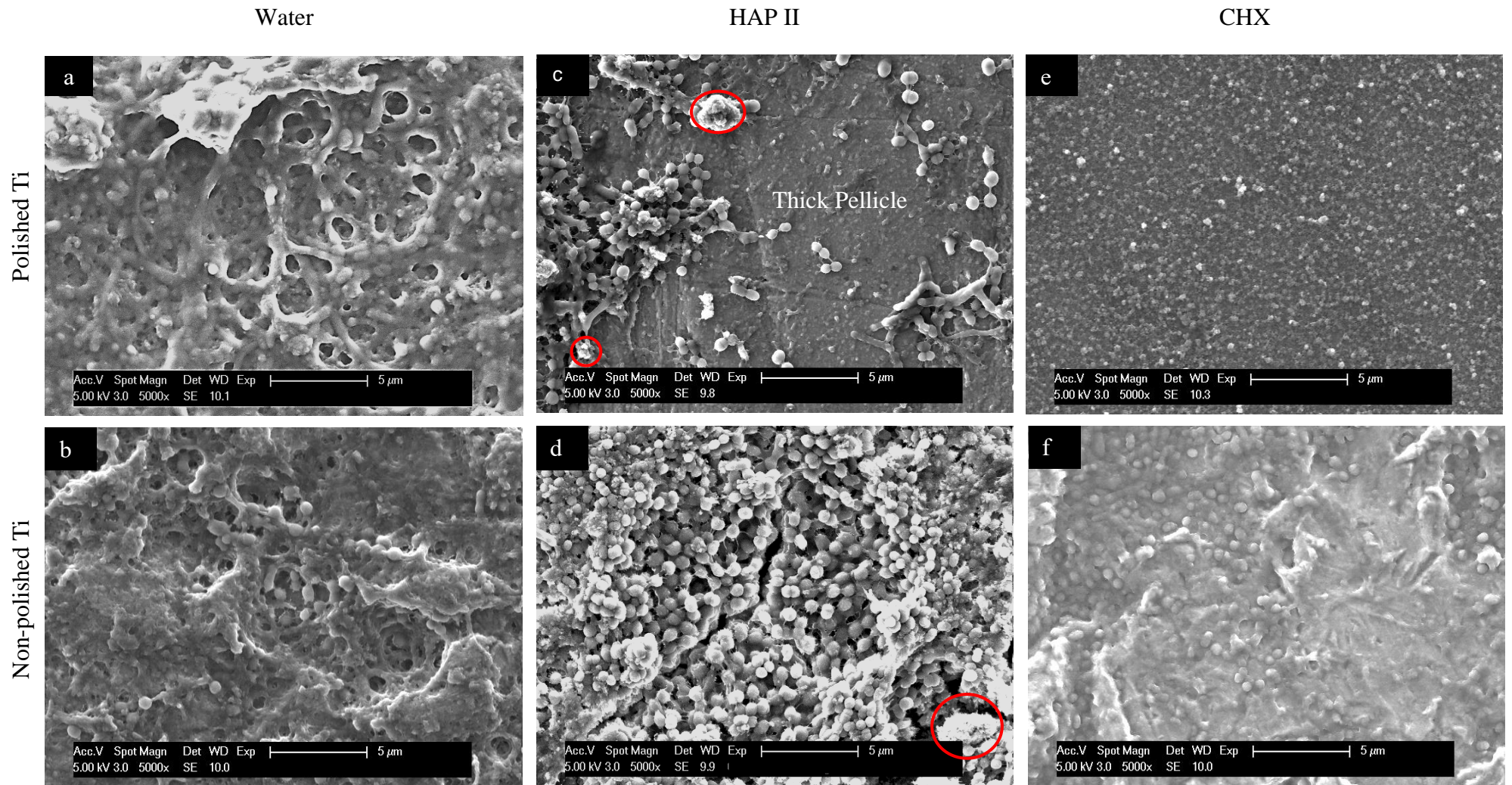
Figure 67 SEM images at 5,000-fold magnification of polished (a,c,e) and non-polished (b,d,f) Ti surfaces after 48 h intraoral exposure and rinsing with water (a,b), HAP II (c,d) and CHX 0.2% (e,f). The red circles delimitate the hydroxyapatite clusters.

4.5.4 Transmission electron microscopy

TEM micrographs at 30,000-fold also show a higher number of bacteria in samples rinsed with water (69). In Figure 68 and Figure 69d, some small black spots scattered randomly on the sample were detected. They may represent single particles and clusters of hydroxyapatite nanoparticles that were not dissolved during the TEM processing steps.

At 68,000-fold, results show a similarity between HAP II and CHX rinsed samples concerning the thickness of the biofilm layer (Figure 69). However, on micrograph "e" a denser pellicle layer is visible after chlorhexidine treatment, while a more disperse layer is present on picture "c" after HAP II rinsing (Figure 69).
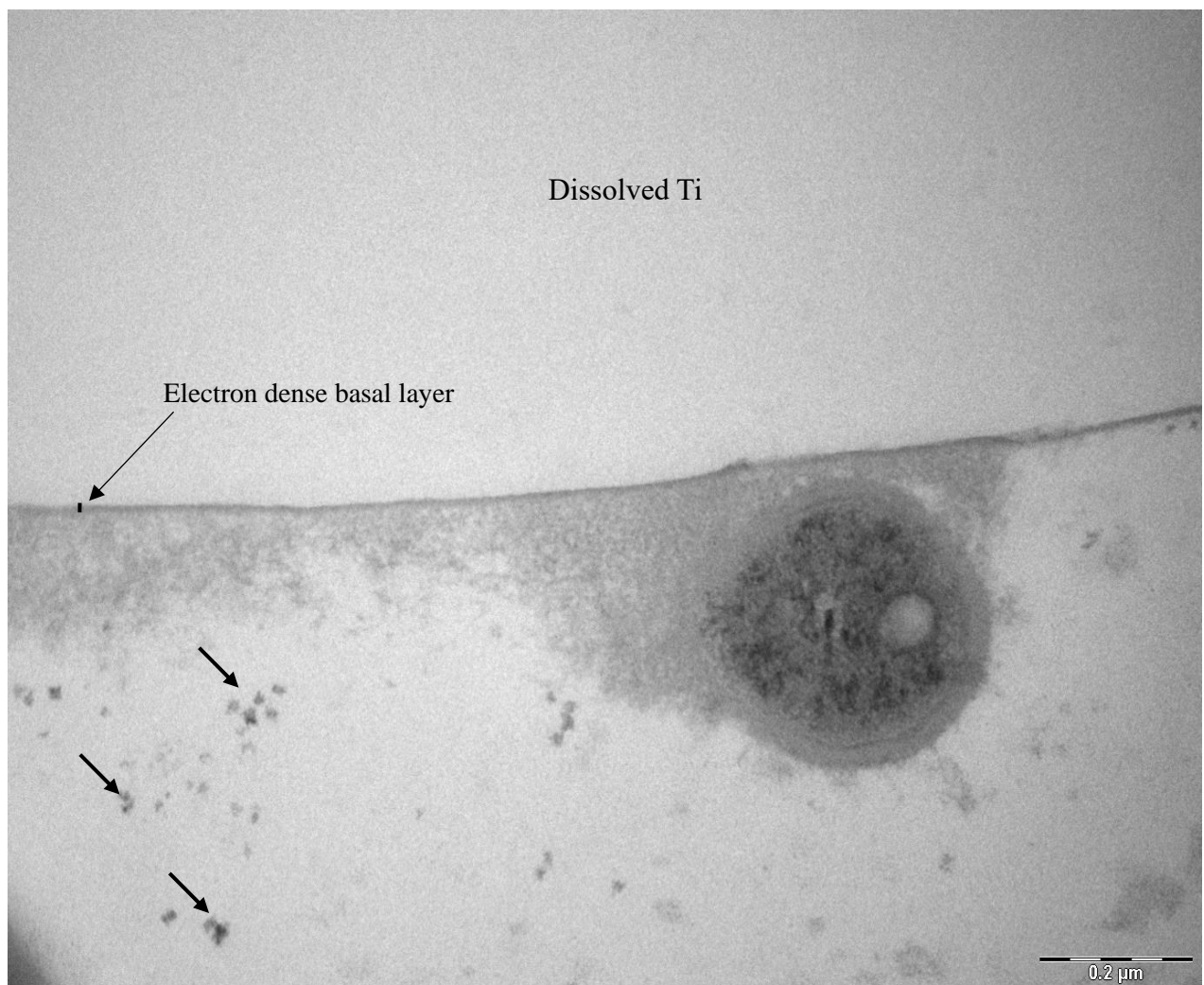
Figure 68 TEM micrograph at 68,000-fold magnification of polished titanium sample after rinse with HAP II according to protocol 3. The pellicle ultrastructure presents an electron dense and linear basal layer, and a disperse and granular outer layer. There are a few black particles on top of the pellicle outer layer, which may represent the non-dissolved HAP II nanoparticles (Black arrows).
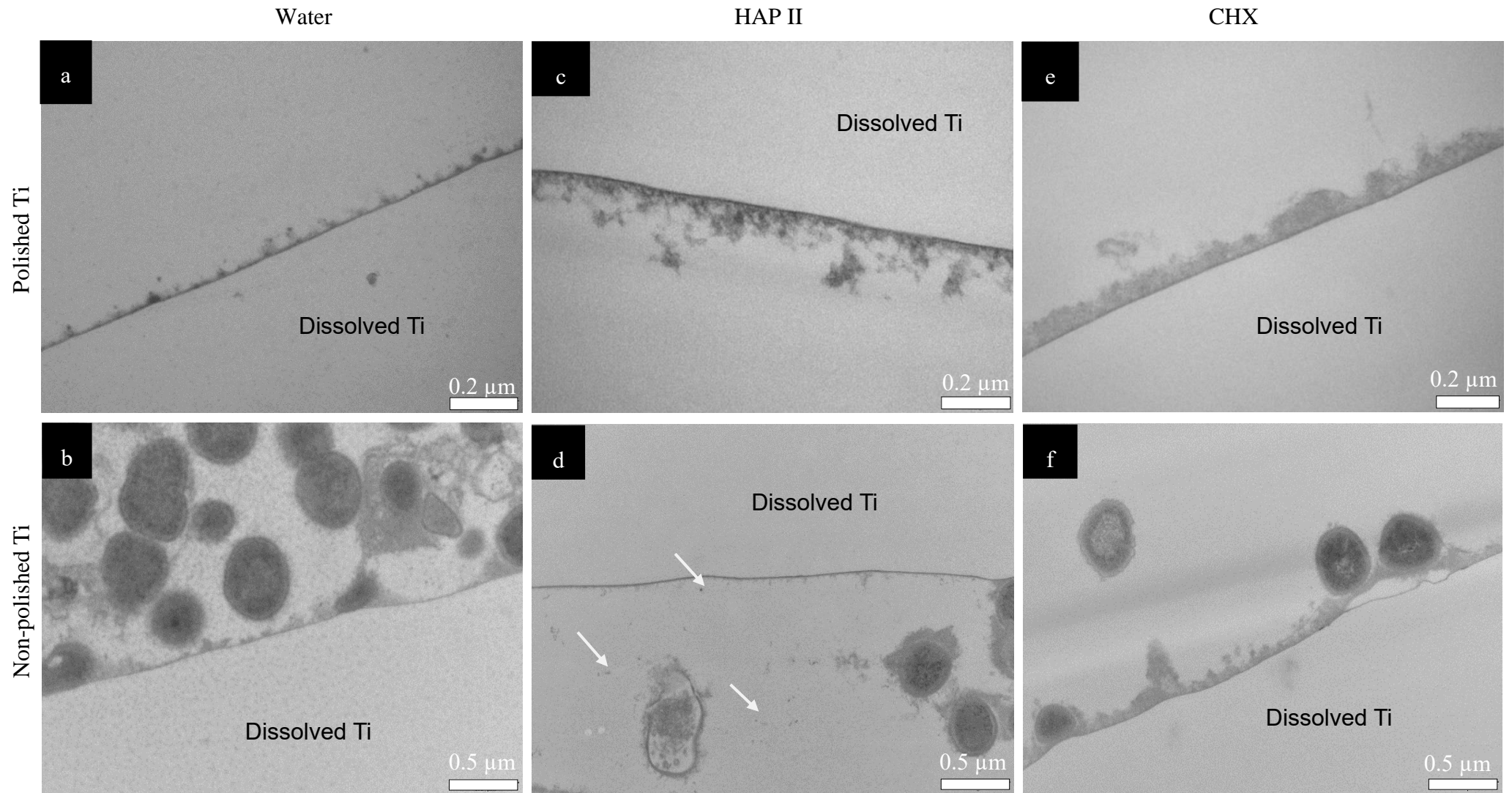
Figure 69 TEM micrographs of 48-h biofilm at 68,000-fold (a,c,e) and 30,000-fold (b,d,f) magnifications of polished Ti samples after rinsing with water (a,b), HAP II (c,d) and CHX (e,f). White arrows on micrograph "d" point to probable hydroxyapatite nanoparticles. The sample rinsed with water on micrograph b present several bacteria layers, while samples rinsed with HAP II (d) and CHX (f) have a lower amount of bacteria cells.

5 Discussion

5.1 Discussion of Material and Methods

5.1.1 Use of tested specimens

SLA grade 2 titanium discs with micro-structured topography used in the current study represent a common type of implant surface applied in day-by-day dental surgical procedures. It has various desirable properties, such as good wettability, strength, ductility, formability, excellent corrosion resistance, and high impact toughness. A mean roughness of 2 μm present in its surface structure is important to enhance the osseointegration between bone and implant surfaces (LI, MAI, 2017; PERRIN et al., 2002; WENNERBERG et al., 1998). However, such roughness can contribute to bacteria adhesion, leading to periodontal inflammation and periimplantitis complications (BOLLEN et al., 1996; QUIRYNEN et al., 1996).

Feldspathic ceramic and Poly(methyl methacrylate) (PMMA) are well-consolidated dental materials and used by many professionals worldwide until nowadays (RASHID, 2014; BERTOLINI et al., 2014). Furthermore, both have essential applications in dentistry: ceramics can be used to manufacture crowns, bridges, and abutments; while PMMA is the most used resin to build a denture base and it is also used for provisional prostheses and removable partial dentures (BABU et al., 2015; FANG et al., 2016). Therefore, many patients may have ceramic restorations or prostheses with a PMMA base. Thus, it is important to investigate new methods to inhibit biofilm on these material surfaces.

Enamel was also used to compare how the hydroxyapatite solution behaves on the natural component of the tooth in comparison to the manufactured dental materials included. In this study, bovine enamel was applied. The use of human teeth for research has decreased over the last decades due to several factors, such as difficult standardization, difficulty to obtain sufficient amount and mostly due to ethical issues (MELO et al., 2015; YASSEN et al., 2011). Hence, the use of animal teeth came as an alternative. Bovine enamel has similarities with human enamel regarding mineral composition, density, and structure. Despite these similarities, bovine teeth can be easily obtained in large scale, and they have more uniform characteristics. Additionally, because of their bigger size and flatter surface, they are also easy to handle (AL-AHMAD et al., 2013; FABRITIUS-VILPOUX et al., 2019; YASSEN et al., 2011).

5.1.2 Adoption of intraoral removable splints

The *in situ* experimental model was applied in this study due to its capacity to reproduce the intraoral *in vivo* situation. According to Hannig and Hannig (2009), the biofilm adhesion processes occur differently under *in vitro* and *in vivo* conditions (HANNIG, HANNIG, 2009). Moreover, the literature states that the *in vitro* pellicle is significantly different from *in vivo* or *in situ* pellicles due to a complex intraoral environment with a diverse oral bacterial community, presence of shearing forces and saliva properties (AL-AHMAD et al., 2013; VAN DER MEI et al., 2008; YAO et al., 2001). Another advantage of an *in situ* approach is that it is possible to analyze the bacteria in their adherent state by fluorescence microscopy (HANNIG et al., 2007). Therefore, the *in situ* model is recommended to understand the bioadhesion process properly.

Sectioned intraoral removable splints were applied to proceed with the in situ investigation. This methodology has been used in many previous studies with good results (HANNIG et al., 2007; HANNIG, 1997; HERTEL et al., 2016; HERTEL et al., 2017; KENSCHE et al., 2017). The use of splints has the advantage of stability and reproducibility, and do not block the saliva flow. Additionally, the acrylic appliance is a convenient method for subjects, due to be easily removable during mealtime or for oral hygiene purposes, not affecting the biofilm formation on the samples' surfaces (AL-AHMAD et al., 2013; HANNIG, 1999a).

The considerable small number of subjects was a limitation of this investigation. The materials involved and the complexity of in situ methodologies were reasons to select such small number of volunteers, such as in previous studies with similar methods (AL-AHMAD et al., 2009; HERTEL et al., 2016; HERTEL et al., 2017; JUNG et al., 2010; KENSCHE et al., 2017).

5.1.3 Selection of rinsing agents

In the present investigation, HAP as 5% watery suspension was chosen as a test solution, while chlorhexidine 0.2% and water were positive and negative controls, respectively.

Hydroxyapatite is a calcium phosphate ceramic that has structural and functional similarities to the principal mineral component in teeth. As a bioinspired material, HAP is non-toxic and non-immunogenic (EPPLE, 2018). Kensche et al. observed that a pure hydroxyapatite containing mouthwash could reduce the number of adherent bacteria on enamel specimens exposed to the oral cavity, having comparable effects to chlorhexidine (KENSCHE et al., 2017). Thus, HAP may have preventive properties against bacterial adhesion. For this reason, the HAP

solution was chosen to test its anti-adhesive properties on enamel, titanium, ceramics, and PMMA samples.

According to the literature, the size and shape of the particles and aggregates may affect the hydroxyapatite properties and their applications, and, additionally, the size of the HAP particle represents a critical factor for adhesion efficiency on enamel (ELIAZ, METOKI, 2017; FABRITIUS-VILPOUX et al., 2019; HU et al., 2007; JIN et al., 2013). In an *in vitro* study, Li et al. proposed that crystallites of HAP with a 20 nm diameter would be the best size for nano-HAP applications (LI et al., 2008). Kensche et al. suppose that as smaller the particle size was, better would be their incorporation to the pellicle and more efficient would be the anti-adhesive effect on the bacteria (KENSCHE et al., 2017). In the present study, three different HAP particles with a median size in the nanoscale were evaluated, hypothesizing that smaller nanoparticles would have better anti-adhesion effects. It was decided to test the hydroxyapatite powder that was already mentioned by Kensche et al., which contains particles with approximately 100 nm (HAP II) and another two powders with larger (HAP III) and smaller sized (HAP I) particles (Table 1) (KENSCHE et al., 2017).

Nowadays, chlorhexidine is still the first-choice solution for prevention of dental biofilm formation, widely used as a broad-spectrum antiseptic. For this reason, chlorhexidine 0.2% was chosen to be the positive control in this investigation to compare the antimicrobial ability of the HAP tested solution (EMILSON, 1977; JONES, 1997; VARONI et al., 2012). However, the long-term use of this solution is not recommended, due to adverse effects such as teeth staining, oral mucosal erosion, and transient taste disturbance (FLOTRA et al., 1971; LANG, LINDHE, 2015; QUIRYNEN et al., 2001; VARONI et al., 2012). Therefore, to achieve reasonable biofilm control and less adverse effects as possible, the search for new biomimetic materials is of utmost importance.

5.1.4 Methods of analysis

Biofilm coverage and viability assay

The samples were visualized under the fluorescence microscopy (FM), scanning electron microscopy (SEM) and transmission electron microscopy (TEM) to characterize the hydroxyapatite nanoparticles and the biofilm formation on all the surfaces after oral rinsing with the tested solutions. Fluorescence microscopy analysis, in association with the BacLight viability kit assay, is a well-established method used in many studies not only to assess biofilm

coverage but also to distinguish vital from non-vital bacteria within the biofilm (HANNIG et al., 2013a; HANNIG, HANNIG, 2009; KENSCHE et al., 2017; STIEFEL et al., 2015). The use of this kit provides a rapid procedure for quantitative analyses that can be measured with the fluorescence microscope (LEUKO et al., 2004; STIEFEL et al., 2015). Moreover, with FM, it is possible to visualize bacteria in the state of adherence (HANNIG et al., 2007).

The Sefexa free image segmentation tool is an open-source software, and it was adopted in this study to evaluate the coverage results obtained from the fluorescence microscopic analysis and to semi-quantify the bacterial cells on the surface of the analyzed materials. The software allows splitting the images from FM into two parts: bacteria cells and background. In this way, it is simple to evaluate the total area corresponding to the bacterial coverage and have an accurate and reproducible result. This method presents a small individual bias since the examiner must define a threshold that will determine the area occupied by the bacterial cells.

Two different methods evaluated the biofilm viability: scoring system and ImageJ. The scoring system is a practical method created for biofilm viability assessment (RUPF et al., 2012). However, this methodology presents two negative points. One is the presence of individual bias, which can be reduced with a blind evaluation from two calibrated examiners. The second and foremost issue is that the images from FM are two dimensions images (2D); therefore, the dead cell layer might be overlapped by the layer of living cells, giving a misleading result. To overcome this problem, an open-source and image processing software called ImageJ was used to evaluate the vitality of the bacterial cells. The ImageJ makes it possible to calculate the integrated density from each channel (red and green), giving a more accurate measure concerning the amount of living and dead cells. There is still some individual bias because a threshold also needs to be set to quantify the integrated density. After statistical analysis, the two methods presented similar results. However, it was chosen to use the results obtained with ImageJ, since it offers more reliable results.

SEM is the preferred tool for visualizing the material surface characteristics and the biofilm structure, morphology, distribution and also to evaluate the process of biofilm formation (GOMES et al., 2017; HUNG et al., 2013). In association with TEM, it is possible to analyze not only the surface but also the subsurface of each material. Besides, TEM microscopy allows the characterization of the pellicle ultrastructure and the initial biofilm matrix structure (DENKHAUS et al., 2007).

5.2   Discussion of Results

5.2.1 Qualitative results

This study evaluated the differences of the oral pellicle and of the biofilm formation under the influence of water, chlorhexidine and three different hydroxyapatite-based watery solutions (HAP I, HAP II, HAP III) on enamel and on three different dental materials surfaces commonly used for oral rehabilitation: ceramics, poly(methyl methacrylate) and titanium (polished and non-polished). In general, the three HAP-based solutions were able to adhere to the pellicle and to reduce the biofilm coverage on all tested polished samples without compromising the bacterial vitality. Detailed information will be discussed in this and in the following section.

First, according to the scarce literature in this matter, the size and shape of the hydroxyapatite particles may affect the HAP properties and effects (ELIAZ, METOKI, 2017; FABRITIUS-VILPOUX et al., 2019; HU et al., 2007; JIN et al., 2013; LI et al., 2008). According to Kensche et al., smaller particles would be better incorporated to the pellicle, thus better interfering with the bacteria adhesion (KENSCHE et al., 2017). In this study, the influence of the particles' size of the selected hydroxyapatite powders could not be evaluated as considered when designing the study protocol. In discordance with the manufacturer's data provided in Table 1, there were discrepancies in the range of the particle' size within each powder, leading to a small range of size variation in-between the powders. Thus, it is important the search for better synthetization methodologies to standardize the size of the HAP particles.

With respect to the shape of the hydroxyapatite particles, results showed that rounded and a few needle particles compose HAP III. Curiously, in the present experiment, the round particles adhered to all surfaces as the needle particles from HAP I and HAP II. *In vitro* experiments revealed that needle-like HAP crystallites would have better adhesion to enamel because they have a morphology similar to the natural enamel building units (FABRITIUS-VILPOUX et al., 2019; LI et al., 2008). Although, another *in vitro* study showed that spherical nano-HAP particles had a great potential to remineralize the enamel (SHAFFIEY, SHAFFIEY, 2016). To our knowledge, this is the first *in situ* study comparing the effects between spherical and crystallite-like HAP particles, and it showed that both could adhere to the pellicle formed on different dental materials. Regardless of the type or size, all of the three different hydroxyapatite SEM results showed that the particles used in this experiment tended to form

clusters in aqueous solution (Figure 16, 18, 20; Table 1). This tendency to aggregate might be related to hydroxyapatite being a dipole molecule, and consequently to the Van der Waals and electrostatic forces in between the particles (KENSCHE et al., 2017).

Protocol 1 evaluated the adherence efficacy of the different HAP particles to the acquired pellicle on different materials. The SEM images from the control samples (Figure 25, Figure 29, Figure 33, Figure 37) demonstrate the pellicle formation over time. According to Hannig and Joiner (2006), the adsorption of proteins and the salivary pellicle formation starts right after the material is exposed to the intraoral cavity (HANNIG, JOINER, 2006). In the present experiment, it is already possible to see a thin pellicle film 3 minutes after intraoral exposure on all tested surfaces. The protein-protein interactions continue, and a thicker and more homogeneous proteinaceous film is visible after 30 and 120 minutes (Figure 25, Figure 29, Figure 33, Figure 37). Thus, the number of absorbed proteins increased over time in all tested samples. According to Hannig and Joiner (2006), the acquired pellicle growth reaches a plateau after 30-90 min, reaching its full thickness around one or two hours after oral exposure (HANNIG, JOINER, 2006).

In general, after application of the HAP solutions according to protocol 1, a typical result was observed for all four tested samples: immediately after the rinse, big aggregates were present and after 30- and 120-minutes smaller clusters and individual particles in lower quantity were dispersed on the surfaces. This pattern can be explained by the continuous process of adsorption and desorption that happens in the oral cavity (HANNIG, JOINER, 2006). After rinsing with the HAP solutions, the particles of each powder are deposited on the material surface. Over time, as hydroxyapatite is soluble in the saliva, those particles are dissolved by the saliva, where individual intraoral shearing forces help to disrupt them into small aggregates and single particles, some of them are re-adsorbed by the pellicle and others are swallowed (Figure 70). The continuous dissolution of hydroxyapatite nanoparticles also happens.

Additionally, bigger clusters have a larger contact area, which makes them more susceptible to shearing forces, and removal from the material surface. According to the literature, some proteins from saliva, such as histatins, have a high affinity to hydroxyapatite crystals present on natural teeth, starting the acquired pellicle formation process (VUKOSAVLJEVIC et al., 2014). We hypothesized that the same interactions might attract the HA particles absorbed by the saliva, initiating their attachment onto the pellicle. Further experiments with saliva analysis are essential to elucidate this topic.
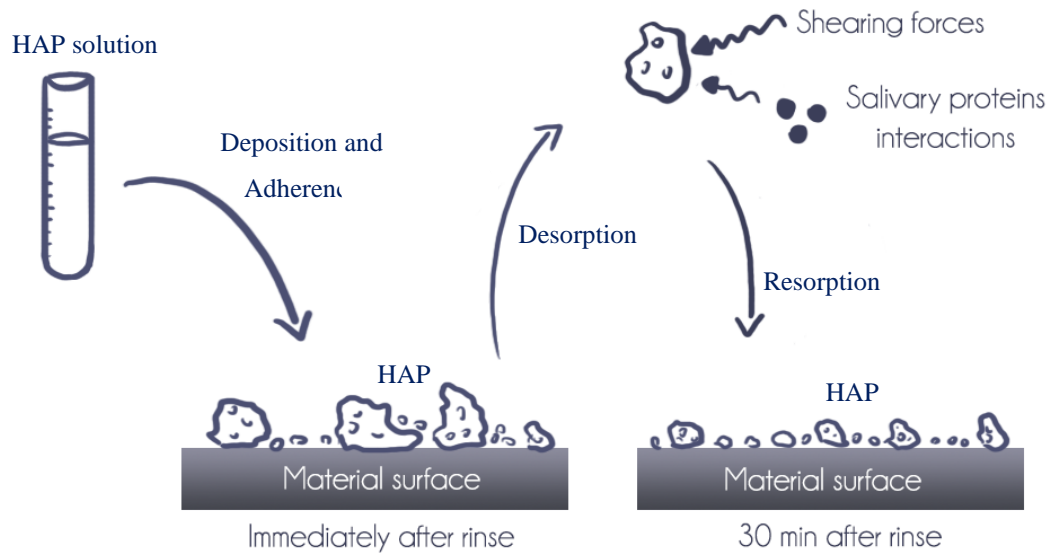
Figure 70 Illustrative scheme of hydroxyapatite particles breakdown due to absorption and resorption process.

Interestingly, hydroxyapatite particles could be detected on all surfaces, even 12 h after the last rinse in protocols 2 and 3. Experiments with a longer time interval should be performed to evaluate the limit for this HAP accumulation related to the intraoral continuous adsorption and desorption processes.

Furthermore, SEM results from protocol 1 show that ceramic samples (Figure 34 - 35) had slightly lower deposition of HAP after 2 h, when compared to the other materials, while the PMMA samples presented a higher amount of particles and clusters after the same time (Figure 38 - 39). The porosities and retentions areas on the PMMA surfaces explain the association with higher HAP deposition and adsorption (CHEN et al., 2017; SPASOJEVIC et al., 2015). Also, HAP tends to accumulate in regions presenting more profound surface defects and irregularities, which is also visible on titanium (Figure 32b) and ceramic surfaces (Figure 36c).

After 2 h of oral exposure to the HAP solutions, connective structures in-between the particles and between the particles and the pellicle were visible under SEM on enamel, titanium and PMMA surfaces. These connective structures were not visible on the ceramics samples, maybe due to the reduced quantity of hydroxyapatite particles on this surface after 2 h. Pepla et al. reported that nano-HAP could bind to proteins, biofilm, and bacteria due to their nanosized and consequently increased surface area (PEPLA et al., 2014). According to Vukosavljevic et al., pellicle precursors proteins, such as histatins or statherins have high affinity to

hydroxyapatite crystals present on natural teeth, starting the acquired pellicle formation process (VUKOSAVLJEVIC et al., 2014). Therefore, one reason behind the adhesion of the synthetic nano hydroxyapatite particles to the pellicle could be the bonding properties of these pellicle components. However, detailed *in vivo/ in situ* studies are needed to clarify these relationships.

After 2h of intraoral exposure, almost all samples presented scattered simple nano-HAP particles in contact with the pellicle outer layer. At the present date, the scarce *in situ* literature on this topic reported the presence of adhesion between the HAP particles and the enamel surface (HANNIG et al., 2013a; KENSCHE et al., 2017). But now it is possible to state that the adhesion of hydroxyapatite nanoparticles also occurs on other dental surfaces as well, such as titanium, ceramics and polymethyl methacrylate resin, opening a promising research field in preventive dentistry.

Considering the protocols 2 and 3, all the volunteers presented a similar pattern for bacteria adherence on all samples (Figures 51-54 and Figure 65). Cocci shaped bacteria were present in a higher proportion, but rods could also be seen, mainly in the 48-h experiment. This result agrees with the literature since gram-positive facultative cocci, rods, and *Actinomyces* are the main early colonizers on titanium surfaces and some filamentous rods can be found after one day of biofilm growth (STEINBERG et al., 1995; ZIJNGE et al., 2010). Furthermore, the morphological appearance of the bacteria found on ceramics, titanium, and PMMA samples was not different from the enamel samples. This is also in accordance with previous research being an indication that biofilm formation is similar on different surfaces (AL-AHMAD et al., 2013; Hannig, 1999b). Observing the rough and smooth titanium surfaces used in protocol 3 (Figure 64), there was no difference between rods and cocci proportions, but a difference in thickness and biofilm density was visible. Thus, the surface roughness had a significant influence on biofilm adhesion on titanium, which was also observed in previous studies (AL-AHMAD et al., 2010; FOSTER, KOLENBRANDER, 2004).

In protocols 2 and 3, volunteers used the intraoral splint for 24- and 48-hours, consecutively. The mature and complete acquired pellicle acted as a link between the material surface and the bacteria present in the intraoral environment due to specific adhesins receptors present on its proteins (HANNIG, JOINER, 2006). After this one-day period, a multilayered biofilm could be seen in SEM and TEM figures on most parts of the samples rinsed with water due to this pellicle-bacteria interaction (Figures 51-54 and Figure 56), and an even thicker biofilm was present after the 48 hours experiment on polished titanium samples (Figure 67 and

Figure 69a). On the other hand, SEM micrographs show that the polished materials surfaces applied in this study were covered with a similar hydroxyapatite nanoparticles distribution and a smaller number of single bacteria and bacterial colonies was present (Figures 51-54 and Figure 56).

One hypothesis is that the particle deposition would restrain the adhesion of bacteria to the acquired pellicle (Figure 71). Kensche et al. also proposed that the hydroxyapatite nanoparticles accumulated on the enamel surface could hamper the bacterial attachment to pellicle receptors by blocking cell wall adhesins from bacteria (KENSCHE et al., 2017). On Figures 51-54 and, more detailed, on Figure 55, it is possible to see that HAP interacts not only with the pellicle but also with the bacteria (PEPLA et al., 2014). The exact way of how these interaction works are not yet well documented. More studies on this relationship should be made in this concern.
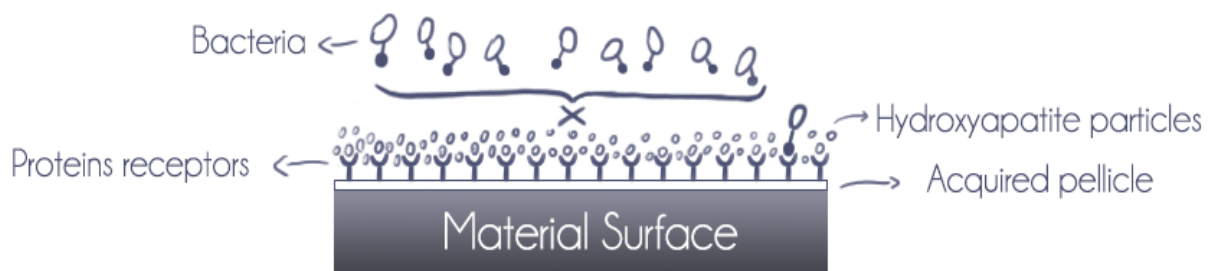
Figure 71 Illustrative scheme of hydroxyapatite particles blocking the pellicle–bacteria interaction.

Findings from the TEM analysis of the 24-h biofilm indicate that the three HAP solutions did not affect the pellicle's ultrastructure, showing similar characteristics as the regular pellicle formed on samples rinsed with water. These results are in accordance with the SEM and FM results since living bacteria were present in all samples from HAP solutions, but in an inferior amount than in water control samples. Thus, these findings suggest that HAP is rather anti-adhesive than an antibacterial, in accordance with the findings from Kensche et al. (KENSCHE et al., 2017). On the other hand, TEM micrographs (Figure 56-60) indicated that the materials might have some influence on the pellicle ultrastructural characteristics, showing some differences in the basal and outer layer structure.

Additionally, control samples from protocol 2 rinsed with 0.2% chlorhexidine presented a thin biofilm layer and areas without or with dead microorganisms, endorsing the well-consolidated antibacterial properties of the gold standard chlorhexidine (JAMES et al., 2017).

According to the SEM results of protocol 3, no visible difference in biofilm density was detected when comparing polished and non-polished samples rinsed with water. Some subjects had a slightly lower biofilm amount on polished samples; however, most Ti discs presented a complex and multilayer biofilm for both surfaces (Figure 66). These small variations in biofilm formation may be due to personal factors, such as salivary flow rate, saliva composition, or nutritional habits (MARSH, 2012). The biofilm could develop to advanced stages with bacterial coaggregation and co-adherence, because there were neither external factors like antibacterial or antiadhesive agents nor mechanical shear forces to disturb it (KRETH et al., 2009).

SEM results (Figure 67) show a denser multilayer biofilm on non-polished samples rinsed with the HAP solution. Thus, HAP could not control the biofilm adhesion and accumulation on rough titanium surfaces. Even non-polished samples rinsed with CHX presented a significant number of bacterial colonies. Other *in vivo* studies have already reported this relationship between surface roughness and biofilm formation (AL-AHMAD et al., 2010; BOLLEN et al., 1997; BURGERS et al., 2010; NAKAZATO et al., 1989; QUIRYNEN et al., 1990; QUIRYNEN, VAN STEENBERGHE, 1989; RIMONDINI et al., 1997). Reasons behind these results are directly related to the titanium topography. The increase of titanium surface roughness is directly related not only to a higher rate of biofilm formation but also to better osseointegration (DO NASCIMENTO et al., 2008; TEUGHELS et al., 2006).

Increased roughness on titanium surface provides better adhesion of fibroblasts to the titanium substrate, establishing better osseointegration with substantial epithelial soft tissue seal around the implant (BOLLEN et al., 1996; QUIRYNEN et al., 1996). However, this irregular topography facilitates bacterial accumulation and colonization due to a larger surface for bacterial adhesion and retention areas (DHIR, 2013). In an *in vivo* split-mouth and double-blinded clinical trial, Quirynen et al. (1990) evaluated the titanium roughness effects on biofilm formation. After the 6-days experiment, a positive relationship between surface roughness and biofilm accumulation was detected (QUIRYNEN et al., 1990). Wu-Yuan et al. (1995) examined, by an *in vitro* study, the oral bacteria attachment to Ti discs with different types of surfaces (smooth, grooved, or rough). Their results also pointed to a higher amount of biofilm on rough surfaces (WU-YUAN et al., 1995). To solve this problem, previous studies suggested a surface arithmetic mean roughness (Ra) threshold value of 0.2 μ. When Ra > 0.2 μ, the biofilm formation and accumulation rate is increased, whereas a Ra < 0.2 μ does not influence the bacterial adhesion but still supply an irregular surface proper to fibroblast adhesion (BOLLEN et al., 1996; BUSER et al., 1991; QUIRYNEN et al., 1996; RUPP et

al., 2018). Therefore, to avoid or reduce initial bacterial adhesion and still ensure the osseointegration process, the implant systems should present specific surface characteristics for each interface. The implant area exposed to the saliva should be polished and smooth, whereas, on the implant-bone interface, a microroughness is required (AL-AHMAD et al., 2013; RUPP et al., 2018).

With SEM and TEM, it was also possible to confirm that hydroxyapatite particles are randomly distributed over the titanium surface (Figure 54 and Figure 68). HAP crystallites measuring 90 nm to 500 nm could be identified even 12 h after the last rinse. Previous studies had also observed the hydroxyapatite accumulation, but on enamel surfaces and not for so long observative periods (HANNIG et al., 2013a; KENSCHE et al., 2017).

Therefore, according to the SEM and TEM qualitative analysis, all three HAP rinsing solutions reduced the amount of mature biofilm on polished enamel, titanium, ceramic, and PMMA. In contrast, on non-polished Ti surfaces rinsing with the HAP solution has no effect on the process of biofilm formation. Additionally, low surface roughness can minimize biofilm formation *in vivo.*

5.2.2 Quantitative results

Fluorescence microscopic results in this study demonstrated that application of CHX as a mouthwash presented the most effective bactericidal effects for both protocol 2 (Figure 50) and protocol 3 (Figure 63), significantly reducing biofilm vital cells on all tested surfaces compared to water and hydroxyapatite solutions, which is in accordance with previous literature (HANNIG et al., 2013a; HANNIG et al., 2013b; KENSCHE et al., 2017). This result is related to the chlorhexidine properties, such as bacteriostatic and bactericidal action, broad-spectrum activity and substantivity, which makes it the gold standard solution on reducing bacterial vitality and biofilm formation (HANNIG et al., 2013b; JONES, 1997; RIBEIRO et al., 2007). Comparing HAP solutions with water, common outcomes for protocol 2 and 3 were also found: there was no significant difference in viability between HAP solutions and water. Also, no difference in viability between each HAP solution in protocol 2 was found. Thus, both the water solution and the HAP solutions presented a majority of living cells in the FM micrographs. These data show that 5% hydroxyapatite watery solution had no anti-bactericidal effect, regardless of their size or configuration (KENSCHE et al., 2017).

When the biofilm coverage was analyzed on polished samples (Figure 49 and Figure 62), FM confirmed a considerable reduction of biofilm formation even 12 h after the last CHX rinsing due

to the substantivity of CHX (VARONI et al., 2012). A significant difference between water and CHX was detected in both protocols 2 and 3, which was an expected result between negative and positive controls. On the other hand, interesting results with regard to biofilm coverage are present when comparing the HAP solutions with CHX. In the 48-h protocol, HAP II was as effective as the CHX solution in reducing biofilm formation on polished titanium discs, with no significant difference between them (p > 0.9999). In the 24-h protocol, these same results were demonstrated for most of the HAP solutions and material samples. This indicates that oral rinsing with 5% HAP solution significantly reduces the number of bacteria adhered on enamel and on artificial dental surfaces. Similar results were already shown by Kensche et al. for enamel surfaces (KENSCHE et al., 2017).

Therefore, the presence of a significantly small number but alive bacteria observed in FM investigations suggests that HAP has a rather anti-adhesive than an antibacterial effect, which is in accordance with the findings from Kensche et al. (KENSCHE et al., 2017). According to the scarce literature in this matter, the anti-adherent effect is related to the hydroxyapatite particles sizes. The size effect would facilitate the direct interaction with the bacteria, meaning that nano and micro hydroxyapatite particles can interact with adhesins on the bacterial membrane, reducing the bacterial adherence (PEPLA et al., 2014; VENEGAS et al., 2006). However, the three hydroxyapatite solutions used in this study had similar effects in reducing bacterial coverage. All of them were on the nanometer scale, presenting similarities on their particles' size range. The other mechanism of action for HAP's anti-adhesive properties suggested by Kensche et al. was already mentioned in the section above. The pellicle-bacterial interaction blockage by the HAP would reduce the amount of adhered bacterial and subsequent biofilm formation, as shown in this study results (KENSCHE et al., 2017). Furthermore, both mechanisms of particles accumulation and receptor sites inhibition could also be the reason for the slightly higher number of dead bacteria observed by FM after HAP solutions rinsing when compared with the water control.

Another discussion point concerns the surface topography of the applied materials. The graph in Figure 49 shows that PMMA samples have a higher percentage of biofilm coverage than titanium, enamel, or ceramic specimens tested in protocol 2. This result is associated with the intrinsic porous structure of PMMA (Figure 54), which creates retention sites, providing bacterial accumulation (CHEN et al., 2017; SPASOJEVIC et al., 2015). In addition, because of its increased roughness, non-polished titanium discs applied in protocol 3 presented higher numbers of bacteria than polished samples, when rinsed with HAP or CHX (Figure 62 and Figure 67). This is in

accordance with the literature, and the roughness factor was already discussed in the section above (DHIR, 2013).

Despite being the gold standard solution for biofilm control, long-term use of CHX is not indicated due to its well-known side effects such as teeth staining, oral mucosal erosion, and transient taste disturbance (FLOTRA et al., 1971; LANG, LINDHE, 2015; QUIRYNEN et al., 2001). On the other hand, after rinsing with the hydroxyapatite solutions, volunteers reported an acceptable taste and no side effects during the study. Furthermore, HAP mimics the dental enamel structure, and for being a biocompatible solution, side effects are unlikely to occur. Additionally, results suggested that HAP had anti-adherent but not anti-bactericidal effects, therefore, the tested solution is less likely to impact on the oral cavity homeostasis. Finally, the literature states that HAP particles are dissolved in the gastric fluid in case of ingestion, not being harmful to the human body (EPPLE, 2018). The results of this investigation point to pure hydroxyapatite mouthrinse as a promising adjunct solution for biofilm management.

5.3 Conclusions

The pure 5% hydroxyapatite nanoparticles solution alone yielded a significant impact on biofilm formation under oral conditions on polished surfaces of enamel, titanium, ceramic and PMMA, representing a bioinspired approach for biofilm control. Due to anti-adherent properties, the HAP efficacy to reduce the biofilm coverage was comparable to 0.2% chlorhexidine on polished surfaces. In summary, the following conclusions:

- HAP adhered to the pellicle formed on enamel, titanium, ceramics, and PMMA.

- HAP may interact with proteins in saliva and with the acquired pellicle.

- 5% HAP watery solution reduced the biofilm coverage on all tested, polished materials.

- The different HAP sizes and morphology used in these experiments had no significant influence on its anti-adherent effects on titanium, enamel, PMMA, or ceramics.

- 5% HAP watery solutions did not alter bacterial viability.

- Surface topography influences the biofilm formation.

Accordingly, the results of this investigation suggest the pure hydroxyapatite mouthrinse as a promising adjunct solution for biofilm management. However, the small number of

subjects was a limitation of this study. Long term clinical trials with more volunteers, as well as patients with gingivitis should be conducted to confirm the properties of pure HAP solution.

6 References

1. Ajaj-Alkordy NM, Alsaadi MH (2014) Elastic modulus and flexural strength comparisons of high-impact and traditional denture base acrylic resins. Saudi Dent J 26:15-18

2. Al-Ahmad A, Follo M, Selzer A-C, Hellwig E, Hannig M, Hannig C (2009) Bacterial colonization of enamel in situ investigated using fluorescence in situ hybridization. Journal of medical microbiology 58:1359-1366

3. Al-Ahmad A, Wiedmann-Al-Ahmad M, Faust J, Bachle M, Follo M, Wolkewitz M, Hannig C, Hellwig E, Carvalho C, Kohal R (2010) Biofilm formation and composition on different implant materials in vivo. J Biomed Mater Res B Appl Biomater 95:101-109

4. Al-Ahmad A, Wiedmann-Al-Ahmad M, Fackler A, Follo M, Hellwig E, Bachle M, Hannig C, Han JS, Wolkewitz M, Kohal R (2013) In vivo study of the initial bacterial adhesion on different implant materials. Arch Oral Biol 58:1139-1147

5. Albrektsson T, Branemark PI, Hansson HA, Lindstrom J (1981) Osseointegrated titanium implants. Requirements for ensuring a long-lasting, direct bone-to-implant anchorage in man. Acta orthopaedica Scandinavica 52:155-170

6. Albrektsson T, Wennerberg A (2004) Oral implant surfaces: Part 1--review focusing on topographic and chemical properties of different surfaces and in vivo responses to them. The International journal of prosthodontics 17:536-543

7. Allen PF, McMillan AS, Walshaw D (2001) A patient-based assessment of implant-stabilized and conventional complete dentures. J Prosthet Dent 85:141-147

8. Arweiler NB, Netuschil L (2016) The Oral Microbiota. Adv Exp Med Biol 902:45-60

9. Arweiler NB, Auschill TM, Sculean A (2018) Patient self-care of periodontal pocket infections. Periodontol 2000 76:164-179

10. Auschill TM, Arweiler NB, Brecx M, Reich E, Sculean A, Netuschil L (2002) The effect of dental restorative materials on dental biofilm. Eur J Oral Sci 110:48-53

11. Babu PJ, Alla RK, Alluri VR, Datla SR, Konakanchi A (2015) Dental Ceramics: Part I An Overview of Composition, Structure and Properties. American Journal of Materials Engineering and Technology 3:13-18

12. Ballo AM, Omar O, Xia W, Palmquist A (2011). Dental implant surfaces–physicochemical properties, biological performance, and trends. In Implant Dentistry-A Rapidly Evolving Practice (IntechOpen).

13. Belibasakis GN, Charalampakis G, Bostanci N, Stadlinger B (2015) Peri-implant infections of oral biofilm etiology. Adv Exp Med Biol 830:69-84

14. Berger D, Rakhamimova A, Pollack A, Loewy Z (2018) Oral Biofilms: Development, Control, and Analysis. High Throughput 7

15. Berglundh T, Armitage G, Araujo MG, Avila-Ortiz G, Blanco J, Camargo PM, Chen S, Cochran D, Derks J, Figuero E (2018) Peri-implant diseases and conditions: Consensus report of workgroup 4 of the 2017 World Workshop on the Classification of Periodontal and Peri-Implant Diseases and Conditions. Journal of clinical periodontology 45:S286-S291

16. Berkovitz BK, Holland GR, Moxham BJ (2017) Oral Anatomy, Histology and Embryology E-Book, Elsevier Health Sciences).

17. Bertolini MM, Portela MB, Curvelo JA, Soares RM, Lourenco EJ, Telles DM (2014) Resins-based denture soft lining materials modified by chlorhexidine salt incorporation: an in vitro analysis of antifungal activity, drug release and hardness. Dent Mater 30:793-798

18. Bhardwaj G, Yazici H, Webster TJ (2015) Reducing bacteria and macrophage density on nanophase hydroxyapatite coated onto titanium surfaces without releasing pharmaceutical agents. Nanoscale 7:8416-8427

19. Blanc V, Isabal S, Sanchez MC, Llama-Palacios A, Herrera D, Sanz M, Leon R (2014) Characterization and application of a flow system for in vitro multispecies oral biofilm formation. J Periodontal Res 49:323-332

20. Bollen CM, Papaioanno W, Van Eldere J, Schepers E, Quirynen M, van Steenberghe D (1996) The influence of abutment surface roughness on plaque accumulation and peri-implant mucositis. Clin Oral Implants Res 7:201-211

21. Bollen CM, Lambrechts P, Quirynen M (1997) Comparison of surface roughness of oral hard materials to the threshold surface roughness for bacterial plaque retention: a review of the literature. Dent Mater 13:258-269

22. Bonesvoll P (1977) Oral pharmacology of chlorhexidine. Journal of clinical periodontology 4:49-65

23. Brånemark P-I, Chien S (2005) The osseointegration book: from calvarium to calcaneus, Quintessence Publishing Company).

24. Branemark PI, Hansson BO, Adell R, Breine U, Lindstrom J, Hallen O, Ohman A (1977) Osseointegrated implants in the treatment of the edentulous jaw. Experience from a 10-year period. Scand J Plast Reconstr Surg Suppl 16:1-132

25. Branemark PI (1983) Osseointegration and its experimental background. J Prosthet Dent 50:399-410

26. Burgers R, Gerlach T, Hahnel S, Schwarz F, Handel G, Gosau M (2010) In vivo and in vitro biofilm formation on two different titanium implant surfaces. Clin Oral Implants Res 21:156-164

27. Busenlechner D, Furhauser R, Haas R, Watzek G, Mailath G, Pommer B (2014) Long-term implant success at the Academy for Oral Implantology: 8-year follow-up and risk factor analysis. J Periodontal Implant Sci 44:102-108

28. Buser D, Schenk RK, Steinemann S, Fiorellini JP, Fox CH, Stich H (1991) Influence of surface characteristics on bone integration of titanium implants. A histomorphometric study in miniature pigs. J Biomed Mater Res 25:889-902

29. Camilo CC, de Souza EC, Di Lorenzo PL, de Almeida Rollo JMD (2011) Measurement of the grain boundary energy of commercially-pure grade 2 titanium at high temperature. Rev Bras Eng Biom 27:175-181

30. Chapple ILC, Mealey BL, Van Dyke TE, Bartold PM, Dommisch H, Eickholz P, Geisinger ML, Genco RJ, Glogauer M, Goldstein M, Griffin TJ, Holmstrup P, Johnson GK, Kapila Y, Lang NP, Meyle J, Murakami S, Plemons J, Romito GA, Shapira L, Tatakis DN, Teughels W, Trombelli L, Walter C, Wimmer G, Xenoudi P, Yoshie H (2018) Periodontal health and gingival diseases and conditions on an intact and a reduced periodontium: Consensus report of workgroup 1 of the 2017 World Workshop on the

Classification of Periodontal and Peri-Implant Diseases and Conditions. J Periodontol 89 Suppl 1:S74-S84

31. Chen R, Han Z, Huang Z, Karki J, Wang C, Zhu B, Zhang X (2017) Antibacterial activity, cytotoxicity and mechanical behavior of nano-enhanced denture base resin with different kinds of inorganic antibacterial agents. Dent Mater J 36:693-699

32. Costerton JW, Montanaro L, Arciola CR (2005) Biofilm in implant infections: its production and regulation. Int J Artif Organs 28:1062-1068

33. Darvell BW (2018) Materials science for dentistry, Woodhead publishing).

34. Denkhaus E, Meisen S, Telgheder U, Wingender J (2007) Chemical and physical methods for characterisation of biofilms. Microchimica Acta 158:1-27

35. Dhir S (2013) Biofilm and dental implant: The microbial link. J Indian Soc Periodontol 17:5-11

36. do Nascimento C, Barbosa RE, Issa JP, Watanabe E, Ito IY, Albuquerque RF, Jr. (2008) Bacterial leakage along the implant-abutment interface of premachined or cast components. Int J Oral Maxillofac Surg 37:177-180

37. Duckworth RM (2006) The teeth and their environment: physical, chemical and biochemical influences, Vol 19, Karger Medical and Scientific Publishers).

38. Eick S, Glockmann E, Brandl B, Pfister W (2004) Adherence of Streptococcus mutans to various restorative materials in a continuous flow system. Journal of oral rehabilitation 31:278-285

39. Eliaz N, Metoki N (2017) Calcium Phosphate Bioceramics: A Review of Their History, Structure, Properties, Coating Technologies and Biomedical Applications. Materials 10

40. Elkassas D, Arafa A (2017) The innovative applications of therapeutic nanostructures in dentistry. Nanomedicine-Nanotechnology Biology and Medicine 13:1543-1562

41. Emilson CG (1977) Susceptibility of various microorganisms to chlorhexidine. Scand J Dent Res 85:255-265

42. Enax J, Epple M (2018) Synthetic Hydroxyapatite as a Biomimetic Oral Care Agent. Oral Health Prev Dent 16:7-19

43. Epple M (2018) Review of potential health risks associated with nanoscopic calcium phosphate. Acta Biomater 77:1-14

44. Fabritius-Vilpoux K, Enax J, Herbig M, Raabe D, Fabritius H-O (2019) Quantitative affinity parameters of synthetic hydroxyapatite and enamel surfaces in vitro. Bioinspired, Biomimetic and Nanobiomaterials:1-13

45. Fang J, Wang C, Li Y, Zhao Z, Mei L (2016) Comparison of bacterial adhesion to dental materials of polyethylene terephthalate (PET) and polymethyl methacrylate (PMMA) using atomic force microscopy and scanning electron microscopy. Scanning 38:665-670

46. Figueiredo M, Henriques J, Martins G, Guerra F, Judas F, Figueiredo H (2010) Physicochemical Characterization of Biomaterials Commonly Used in Dentistry as Bone Substitutes-Comparison with Human Bone. Journal of Biomedical Materials Research Part B-Applied Biomaterials 92B:409-419

47. Filoche S, Wong L, Sissons CH (2010) Oral biofilms: emerging concepts in microbial ecology. J Dent Res 89:8-18

48. Flotra L, Gjermo P, Rolla G, Waerhaug J (1971) Side effects of chlorhexidine mouth washes. Scand J Dent Res 79:119-125

49. Foster JS, Kolenbrander PE (2004) Development of a multispecies oral bacterial community in a saliva-conditioned flow cell. Appl Environ Microbiol 70:4340-4348

50. Frazer RQ, Byron RT, Osborne PB, West KP (2005) PMMA: an essential material in medicine and dentistry. J Long Term Eff Med Implants 15:629-639

51. Furst MM, Salvi GE, Lang NP, Persson GR (2007) Bacterial colonization immediately after installation on oral titanium implants. Clin Oral Implants Res 18:501-508

52. Gomes LC, Mergulh, #xe3, o FJ, #xe9 (2017) SEM Analysis of Surface Impact on Biofilm Antibiotic Treatment. Scanning 2017:7

53. Gonçalves S, Bresciani E (2017). Reconstructions using alloys and ceramics. In Material-Tissue Interfacial Phenomena (Elsevier), pp. 23-66.

54. Grenho L, Manso MC, Monteiro FJ, Ferraz MP (2012) Adhesion of Staphylococcus aureus, Staphylococcus epidermidis, and Pseudomonas aeruginosa onto

nanohydroxyapatite as a bone regeneration material. Journal of Biomedical Materials Research Part A 100A:1823-1830

55. Hannig C, Hannig M, Rehmer O, Braun G, Hellwig E, Al-Ahmad A (2007) Fluorescence microscopic visualization and quantification of initial bacterial colonization on enamel in situ. Arch Oral Biol 52:1048-1056

56. Hannig C, Hannig M (2009) The oral cavity--a key system to understand substratum-dependent bioadhesion on solid surfaces in man. Clin Oral Investig 13:123-139

57. Hannig C, Basche S, Burghardt T, Al-Ahmad A, Hannig M (2013a) Influence of a mouthwash containing hydroxyapatite microclusters on bacterial adherence in situ. Clin Oral Investig 17:805-814

58. Hannig C, Gaeding A, Basche S, Richter G, Helbig R, Hannig M (2013b) Effect of conventional mouthrinses on initial bioadhesion to enamel and dentin in situ. Caries Res 47:150-161

59. Hannig M (1997) Transmission electron microscopic study of in vivo pellicle formation on dental restorative materials. Eur J Oral Sci 105:422-433

60. Hannig M (1999a) Ultrastructural investigation of pellicle morphogenesis at two different intraoral sites during a 24-h period. Clinical oral investigations 3:88-95

61. Hannig, M. (1999b). Transmission electron microscopy of early plaque formation on dental materials in vivo. European Journal of Oral Sciences, 107(1), 55.

62. Hannig M, Joiner A (2006) The structure, function and properties of the acquired pellicle. Monographs in oral science 19:29-64

63. Hao Y, Huang X, Zhou X, Li M, Ren B, Peng X, Cheng L (2018) Influence of Dental Prosthesis and Restorative Materials Interface on Oral Biofilms. International journal of molecular sciences 19

64. Hertel S, Graffy L, Potschke S, Basche S, Al-Ahmad A, Hoth-Hannig W, Hannig M, Hannig C (2016) Effect of Inula viscosa on the pellicle's protective properties and initial bioadhesion in-situ. Archives of Oral Biology 71:87-96

65. Hertel S, Potschke S, Basche S, Delius J, Hoth-Hannig W, Hannig M, Hannig C (2017) Effect of Tannic Acid on the Protective Properties of the in situ Formed Pellicle. Caries Research 51:34-45

66. Hu Q, Tan Z, Liu Y, Tao J, Cai Y, Zhang M, Pan H, Xu X, Tang R (2007) Effect of crystallinity of calcium phosphate nanoparticles on adhesion, proliferation, and differentiation of bone marrow mesenchymal stem cells. Journal of Materials Chemistry 17:4690-4698

67. Huang S, Gao S, Cheng L, Yu H (2011) Remineralization potential of nano-hydroxyapatite on initial enamel lesions: an in vitro study. Caries research 45:460-468

68. Hung C, Zhou YZ, Pinkner JS, Dodson KW, Crowley JR, Heuser J, Chapman MR, Hadjifrangiskou M, Henderson JP, Hultgren SJ (2013) Escherichia coli Biofilms Have an Organized and Complex Extracellular Matrix Structure. Mbio 4

69. Invernici MM, Salvador SL, Silva PHF, Soares MSM, Casarin R, Palioto DB, Souza SLS, Taba M, Jr., Novaes AB, Jr., Furlaneto FAC, Messora MR (2018) Effects of Bifidobacterium probiotic on the treatment of chronic periodontitis: A randomized clinical trial. J Clin Periodontol 45:1198-1210

70. James P, Worthington HV, Parnell C, Harding M, Lamont T, Cheung A, Whelton H, Riley P (2017) Chlorhexidine mouthrinse as an adjunctive treatment for gingival health. The Cochrane database of systematic reviews 3:CD008676

71. Jayesh RS, Dhinakarsamy V (2015) Osseointegration. Journal of Pharmacy and Bioallied Sciences 7:S226-S229

72. Jemt T (2016) Single-Implant Survival: More Than 30 Years of Clinical Experience. International Journal of Prosthodontics 29:551-558

73. Jin J, Xu X, Lai G, Kunzelmann K-H (2013) Efficacy of tooth whitening with different calcium phosphate-based formulations. European journal of oral sciences 121:382-388

74. John J, Gangadhar SA, Shah I (2001) Flexural strength of heat-polymerized polymethyl methacrylate denture resin reinforced with glass, aramid, or nylon fibers. J Prosthet Dent 86:424-427

75. Jones CG (1997) Chlorhexidine: is it still the gold standard? Periodontol 2000 15:55-62

76. Jung DJ, Al-Ahmad A, Follo M, Spitzmuller B, Hoth-Hannig W, Hannig M, Hannig C (2010) Visualization of initial bacterial colonization on dentine and enamel in situ. Journal of Microbiological Methods 81:166-174

77. Kalykakis G, Mojon P, Nisengard R, Spiekermann H, Zafiropoulos G (1998) Clinical and microbial findings on osseo-integrated implants; comparisons between partially dentate and edentulous subjects. The European journal of prosthodontics and restorative dentistry 6:155-159

78. Kensche A, Holder C, Basche S, Tahan N, Hannig C, Hannig M (2017) Efficacy of a mouthrinse based on hydroxyapatite to reduce initial bacterial colonisation in situ. Arch Oral Biol 80:18-26

79. Kim KH, Loch C, Waddell JN, Tompkins G, Schwass D (2017) Surface Characteristics and Biofilm Development on Selected Dental Ceramic Materials. Int J Dent 2017:7627945

80. Klinge B, Hultin M, Berglundh T (2005) Peri-implantitis. Dental clinics of North America 49:661-676, vii-viii

81. Koblischka-Veneva A, Koblischka MR, Schmauch J, Hannig M (2018) Human dental enamel: A natural nanotechnology masterpiece investigated by TEM and t-EBSD. Nano Research 11:3911-3921

82. Kolenbrander PE, Palmer RJ, Jr., Rickard AH, Jakubovics NS, Chalmers NI, Diaz PI (2006) Bacterial interactions and successions during plaque development. Periodontol 2000 42:47-79

83. Koseki Y, Tanaka R, Murata H (2018) Development of antibacterial denture cleaner for brushing containing tea tree and lemongrass essential oils. Dental Materials Journal 37:659-666

84. Kreth J, Merritt J, Qi FX (2009) Bacterial and Host Interactions of Oral Streptococci. DNA and Cell Biology 28:397-403

85. Lang NP, Lindhe J (2015) Clinical periodontology and implant dentistry, 2 Volume Set, John Wiley & Sons).

86. Leuko S, Legat A, Fendrihan S, Stan-Lotter H (2004) Evaluation of the LIVE/DEAD BacLight kit for detection of extremophilic archaea and visualization of microorganisms

in environmental hypersaline samples. Applied and Environmental Microbiology 70:6884-6886

87. Li L, Pan H, Tao J, Xu X, Mao C, Gu X, Tang R (2008) Repair of enamel by using hydroxyapatite nanoparticles as the building blocks. Journal of Materials Chemistry 18:4079-4084

88. Li Q, Mai Y-W (2017) Biomaterials for Implants and Scaffolds, Springer).

89. Locker D, Matear D, Lawrence H (2002) General health status and changes in chewing ability in older Canadians over seven years. J Public Health Dent 62:70-77

90. Marsh PD (2006) Dental plaque as a biofilm and a microbial community - implications for health and disease. BMC oral health 6 Suppl 1:S14

91. Marsh PD (2012) Contemporary perspective on plaque control. British Dental Journal 212:601-606

92. Melo TA, Grundling GS, Montagner F, Scarparo RK, Figueiredo JA, Vier-Pelisser FV (2015) Are bovine teeth a suitable substitute for human teeth in in vitro studies to assess endotoxin load in root canals? Braz Oral Res 29

93. Misch CE (2007) Contemporary implant dentistry-E-Book, Elsevier Health Sciences).

94. Mombelli A, van Oosten MA, Schurch E, Jr., Land NP (1987) The microbiota associated with successful or failing osseointegrated titanium implants. Oral microbiology and immunology 2:145-151

95. Mombelli A (1993) Microbiology of the dental implant. Advances in dental research 7:202-206

96. Mombelli A, Lang NP (1994) Microbial aspects of implant dentistry. Periodontol 2000 4:74-80

97. Mombelli A (2018) Microbial colonization of the periodontal pocket and its significance for periodontal therapy. Periodontol 2000 76:85-96

98. Moy PK, Medina D, Shetty V, Aghaloo TL (2005) Dental implant failure rates and associated risk factors. Int J Oral Maxillofac Implants 20:569-577

99. Muddugangadhar BC, Amarnath GS, Sonika R, Chheda PS, Garg A (2015) Meta-analysis of Failure and Survival Rate of Implant-supported Single Crowns, Fixed Partial Denture, and Implant Tooth-supported Prostheses. J Int Oral Health 7:11-17

100. Nakazato G, Tsuchiya H, Sato M, Yamauchi M (1989) In vivo plaque formation on implant materials. Int J Oral Maxillofac Implants 4:321-326

101. Nicolini AC, Grisa TA, Muniz FWMG, Rosing CK, Cavagni J (2019) Effect of adjuvant use of metformin on periodontal treatment: a systematic review and meta-analysis. Clinical oral investigations 23:2659-2666

102. Nobre CMG, Pütz N, Hannig M (2020) Adhesion of Hydroxyapatite Nanoparticles to Dental Materials under Oral Conditions. Scanning 2020

103. Norowski PA, Jr., Bumgardner JD (2009) Biomaterial and antibiotic strategies for peri-implantitis: a review. J Biomed Mater Res B Appl Biomater 88:530-543

104. Oh SH, Kim Y, Park JY, Jung YJ, Kim SK, Park SY (2016) Comparison of fixed implant-supported prostheses, removable implant-supported prostheses, and complete dentures: patient satisfaction and oral health-related quality of life. Clin Oral Implants Res 27:e31-37

105. Okada M, Furuzono T (2012) Hydroxylapatite nanoparticles: fabrication methods and medical applications. Science and Technology of Advanced Materials 13

106. Oshida Y, Tuna EB, Aktoren O, Gencay K (2010) Dental implant systems. Int J Mol Sci 11:1580-1678

107. Padovani GC, Fucio SB, Ambrosano GM, Correr-Sobrinho L, Puppin-Rontani RM (2015) In situ bacterial accumulation on dental restorative materials. CLSM/COMSTAT analysis. Am J Dent 28:3-8

108. Pelgrift RY, Friedman AJ (2013) Nanotechnology as a therapeutic tool to combat microbial resistance. Advanced Drug Delivery Reviews 65:1803-1815

109. Pepla E, Besharat LK, Palaia G, Tenore G, Migliau G (2014) Nano-hydroxyapatite and its applications in preventive, restorative and regenerative dentistry: a review of literature. Ann Stomatol (Roma) 5:108-114

110. Perrin D, Szmukler-Moncler S, Echikou C, Pointaire P, Bernard JP (2002) Bone response to alteration of surface topography and surface composition of sandblasted and acid etched (SLA) implants. Clin Oral Implants Res 13:465-469

111. Pjetursson BE, Bragger U, Lang NP, Zwahlen M (2007) Comparison of survival and complication rates of tooth-supported fixed dental prostheses (FDPs) and implant-supported FDPs and single crowns (SCs). Clin Oral Implants Res 18 Suppl 3:97-113

112. Puckett SD, Taylor E, Raimondo T, Webster TJ (2010) The relationship between the nanostructure of titanium surfaces and bacterial attachment. Biomaterials 31:706-713

113. Quirynen M, van Steenberghe D (1989) Is early plaque growth rate constant with time? Journal of clinical periodontology 16:278-283

114. Quirynen M, Marechal M, Busscher HJ, Weerkamp AH, Darius PL, van Steenberghe D (1990) The influence of surface free energy and surface roughness on early plaque formation. An in vivo study in man. J Clin Periodontol 17:138-144

115. Quirynen M, Bollen CM, Papaioannou W, Van Eldere J, van Steenberghe D (1996) The influence of titanium abutment surface roughness on plaque accumulation and gingivitis: short-term observations. The International journal of oral & maxillofacial implants 11:169-178

116. Quirynen M, Avontroodt P, Peeters W, Pauwels M, Coucke W, van Steenberghe D (2001) Effect of different chlorhexidine formulations in mouthrinses on de novo plaque formation. J Clin Periodontol 28:1127-1136

117. Raghavan RN (2012). Ceramics in dentistry. In Sintering of Ceramics-New Emerging Techniques (IntechOpen).

118. Ramesh N, Moratti SC, Dias GJ (2018) Hydroxyapatite-polymer biocomposites for bone regeneration: A review of current trends. Journal of Biomedical Materials Research Part B-Applied Biomaterials 106:2046-2057

119. Rashid H (2014) The effect of surface roughness on ceramics used in dentistry: A review of literature. Eur J Dent 8:571-579

120. Ribeiro LGM, Hashizume LN, Maltz M (2007) The effect of different formulations of chlorhexidine in reducing levels of mutans streptococci in the oral cavity: A systematic review of the literature. Journal of dentistry 35:359-370

121. Richmond S, Chestnutt I, Shennan J, Brown R (2007) The relationship of medical and dental factors to perceived general and dental health. Community Dent Oral Epidemiol 35:89-97

122. Rimondini L, Fare S, Brambilla E, Felloni A, Consonni C, Brossa F, Carrassi A (1997) The effect of surface roughness on early in vivo plaque colonization on titanium. J Periodontol 68:556-562

123. Rupf S, Balkenhol M, Sahrhage TO, Baum A, Chromik JN, Ruppert K, Wissenbach DK, Maurer HH, Hannig M (2012) Biofilm inhibition by an experimental dental resin composite containing octenidine dihydrochloride. Dental materials : official publication of the Academy of Dental Materials 28:974-984

124. Rupp F, Liang L, Geis-Gerstorfer J, Scheideler L, Huttig F (2018) Surface characteristics of dental implants: A review. Dent Mater 34:40-57

125. Ruse ND, Sadoun MJ (2014) Resin-composite blocks for dental CAD/CAM applications. J Dent Res 93:1232-1234

126. Sakae T, Hirayama K, Yamamoto H, Suzuki K, Hayakawa Y, Takahashi Y, Kuwada T, Nakao K, Nogami K, Inagaki M, Tanaka T, Hayakawa K, Sato I, Kakei M (2011) Three-dimensional Orientation Analysis of Human Enamel Crystallites Using X-ray Diffraction. Journal of Hard Tissue Biology 20:7-10

127. Sakaguchi RL, Powers JM (2012) Craig's restorative dental materials-e-book, Elsevier Health Sciences).

128. Sargozaie N, Moeintaghavi A, Shojaie H (2017) Comparing the Quality of Life of Patients Requesting Dental Implants Before and After Implant. Open Dent J 11:485-491

129. Schwarz F, Derks J, Monje A, Wang HL (2018) Peri-implantitis. J Clin Periodontol 45 Suppl 20:S246-S266

130. Shaffiey SR, Shaffiey SF (2016) Surface enamel remineralization by biomimetic nano hydroxyapatite crystals and fluoride ions effects. Journal of Ceramic Processing Research 17:109-112

131. Shahmoradi M, Bertassoni LE, Elfallah HM, Swain M (2014). Fundamental structure and properties of enamel, dentin and cementum. In Advances in calcium phosphate biomaterials (Springer), pp. 511-547.

132. Shenoy A, Shenoy N (2010) Dental ceramics: An update. J Conserv Dent 13:195-203

133. Silverstein LH, Kurtzman D, Garnick JJ, Schuster GS, Steflik DE, Moskowitz ME (1994) The microbiota of the peri-implant region in health and disease. Implant dentistry 3:170-174

134. Skjorland KK, Rykke M, Sonju T (1995) Rate of pellicle formation in vivo. Acta odontologica Scandinavica 53:358-362

135. Smeets R, Henningsen A, Jung O, Heiland M, Hammacher C, Stein JM (2014) Definition, etiology, prevention and treatment of peri-implantitis--a review. Head Face Med 10:34

136. Socransky SS, Haffajee AD, Cugini MA, Smith C, Kent RL, Jr. (1998) Microbial complexes in subgingival plaque. Journal of clinical periodontology 25:134-144

137. Solderer A, Kaufmann M, Hofer D, Wiedemeier D, Attin T, Schmidlin PR (2019) Efficacy of chlorhexidine rinses after periodontal or implant surgery: a systematic review. Clinical oral investigations 23:21-32

138. Souza JC, Mota RR, Sordi MB, Passoni BB, Benfatti CA, Magini RS (2016) Biofilm Formation on Different Materials Used in Oral Rehabilitation. Braz Dent J 27:141-147

139. Spasojevic P, Zrilic M, Panic V, Stamenkovic D, Seslija S, Velickovic S (2015) The Mechanical Properties of a Poly(methyl methacrylate) Denture Base Material Modified with Dimethyl Itaconate and Di-n-butyl Itaconate. International Journal of Polymer Science

140. Staines M, Robinson WH, Hood JAA (1981) Spherical Indentation of Tooth Enamel. Journal of Materials Science 16:2551-2556

141. Steinberg D, Klinger A, Kohavi D, Sela MN (1995) Adsorption of human salivary proteins to titanium powder. I. Adsorption of human salivary albumin. Biomaterials 16:1339-1343

142. Stiefel P, Schmidt-Emrich S, Maniura-Weber K, Ren Q (2015) Critical aspects of using bacterial cell viability assays with the fluorophores SYTO9 and propidium iodide. BMC microbiology 15:36

143. Tanner A, Maiden MF, Lee K, Shulman LB, Weber HP (1997) Dental implant infections. Clinical infectious diseases : an official publication of the Infectious Diseases Society of America 25 Suppl 2:S213-217

144. Teughels W, Van Assche N, Sliepen I, Quirynen M (2006) Effect of material characteristics and/or surface topography on biofilm development. Clin Oral Implants Res 17 Suppl 2:68-81

145. Vallittu P, Shinya A (2017). Structural properties of dental FRC structures. In A Clinical Guide to Fibre Reinforced Composites (FRCs) in Dentistry (Elsevier), pp. 35-56.

146. van der Mei HC, Engels E, de Vries J, Busscher HJ (2008) Effects of amine fluoride on biofilm growth and salivary pellicles. Caries Res 42:19-27

147. Varoni E, Tarce M, Lodi G, Carrassi A (2012) Chlorhexidine (CHX) in dentistry: state of the art. Minerva Stomatol 61:399-419

148. Veerachamy S, Yarlagadda T, Manivasagam G, Yarlagadda PK (2014) Bacterial adherence and biofilm formation on medical implants: a review. Proc Inst Mech Eng H 228:1083-1099

149. Venegas C, Palacios JM, Apella MC, Morando PJ, Blesa MA (2006) Calcium modulates interactions between bacteria and hydroxyapatite. Journal of Dental Research 85:1124-1128

150. Vukosavljevic D, Hutter JL, Helmerhorst EJ, Xiao Y, Custodio W, Zaidan FC, Oppenheim FG, Siqueira WL (2014) Nanoscale Adhesion Forces between Enamel Pellicle Proteins and Hydroxyapatite. Journal of Dental Research 93:514-519

151. Wennerberg A, Hallgren C, Johansson C, Danelli S (1998) A histomorphometric evaluation of screw-shaped implants each prepared with two surface roughnesses. Clinical oral implants research 9:11-19

152. Westas E, Gillstedt M, Lonn-Stensrud J, Bruzell E, Andersson M (2014) Biofilm formation on nanostructured hydroxyapatite-coated titanium. Journal of biomedical materials research Part A 102:1063-1070

153. Williams DF (1977) Titanium as a metal for implantation. Part 2: biological properties and clinical applications. Journal of medical engineering & technology 1:266-270

154. Wittneben JG, Wismeijer D, Bragger U, Joda T, Abou-Ayash S (2018) Patient-reported outcome measures focusing on aesthetics of implant- and tooth-supported fixed dental prostheses: A systematic review and meta-analysis. Clin Oral Implants Res 29 Suppl 16:224-240

155. Wu-Yuan CD, Eganhouse KJ, Keller JC, Walters KS (1995) Oral bacterial attachment to titanium surfaces: a scanning electron microscopy study. The Journal of oral implantology 21:207-213

156. Ximenez-Fyvie LA, Haffajee AD, Socransky SS (2000) Comparison of the microbiota of supra- and subgingival plaque in health and periodontitis. Journal of clinical periodontology 27:648-657

157. Yao Y, Grogan J, Zehnder M, Lendenmann U, Nam B, Wu Z, Costello CE, Oppenheim FG (2001) Compositional analysis of human acquired enamel pellicle by mass spectrometry. Arch Oral Biol 46:293-303

158. Yassen GH, Platt JA, Hara AT (2011) Bovine teeth as substitute for human teeth in dental research: a review of literature. Journal of oral science 53:273-282

159. Zijnge V, van Leeuwen MB, Degener JE, Abbas F, Thurnheer T, Gmur R, Harmsen HJ (2010) Oral biofilm architecture on natural teeth. PLoS One 5:e9321

160. American Academy of Implant Dentistry (AAID), 1951, United States of America, accessed 12 February 2019 <www.aaid.com/about/press_room/dental_implants_faq.html>

161. Deutsche Gesellschaft für Implantologie im Zahn-, Mund- und Kieferbereich e. V (DGI) 2019, Germany, accessed 12 February 2019 <https://www.dginet.de/web/dgi/warum>

7 Publication / Acknowledgements

7.1 Publications

Published Papers:

Nobre CMG, Pütz N, Hannig M (2020) Adhesion of Hydroxyapatite Nanoparticles to Dental Materials under Oral Conditions. Scanning, 2020.

Nobre CMG, Pütz N, König B, Rupf S, Hannig M (2020) Modification of in situ biofilm formation on titanium by a hydroxyapatite nanoparticle-based solution. Frontiers in Bioengineering and Biotechnology – Biomaterials.

Abstracts on Conferences

Nobre CMG, Hannig M (2019) Hydroxyapatite based mouthrinse for biofilm control. 51 Jahrestagung der Arbeitsgemeinschaft für Grundlagenforschung (AfG). Mainz, Germany.

Nobre CMG, Reda B, Hannig M (2018) PR689: Hydroxyapatite based mouthrinse against initial biofilm adhesion on titanium. Europerio9. J Clin Periodontol, 45:357-357.

Nobre CMG, Reda B, Hannig M (2018) Hydroxyapatite based mouthwash effects on bacterial adhesion on titanium surface. 50 Jahrestagung der Arbeitsgemeinschaft für Grundlagenforschung (AfG). Mainz, Germany.

7.2   Acknowledgements

8 Curriculum Vitae

The curriculum vitae was removed from the electronic version of the doctoral thesis for reasons of data protection.

9 APPENDIX

9.1 List of Figures

9.2 List of Tables